University of Alberta

Mathematical Modelling of HTLV-I Infection: A Study of Viral Persistence *in vivo*

by

Aaron Guanliang Lim

A thesis submitted to the Faculty of Graduate Studies and Research
in partial fulfillment of the requirements for the degree of

Master of Science

in

Applied Mathematics

Department of Mathematical and Statistical Sciences

Fall 2010
Edmonton, Alberta

Examining Committee

Michael Y. Li, Mathematical and Statistical Sciences

James S. Muldowney, Mathematical and Statistical Sciences

Hao Wang, Mathematical and Statistical Sciences

Jutta Preiksaitis, Medicine, Division of Infectious Diseases

Abstract

Human T-lymphotropic virus type I (HTLV-I) is a persistent human retrovirus characterized by life-long infection and risk of developing HAM/TSP, a progressive neurological and inflammatory disease. Despite extensive studies of HTLV-I, a complete understanding of the viral dynamics has been elusive. Previous mathematical models are unable to fully explain experimental observations.

Motivated by a new hypothesis for the mechanism of HTLV-I infection, a three dimensional compartmental model of ordinary differential equations is constructed that focusses on the highly dynamic interactions among populations of healthy, latently infected, and actively infected target cells. Results from mathematical and numerical investigations give rise to relevant biological interpretations. Comparisons of these results with experimental observations allow us to assess the validity of the original hypothesis. Our findings provide valuable insights to the infection and persistence of HTLV-I *in vivo* and motivate future mathematical and experimental work.

I would like to thank my family and friends for their continued support and advice throughout the years. I would also like to thank Dr. Michael Li, my supervisor, mentor, and friend, for his guidance during my studies (B. Sc., M. Sc.) at the University of Alberta. I acknowledge the financial support from the Natural Sciences and Engineering Research Council of Canada (NSERC), the University of Alberta, the Department of Mathematical and Statistical Sciences (U of A), and the Government of Alberta.

Table of Contents

List of Tables

List of Figures

Chapter 1

Introduction

1.1 Objectives

The objective of this thesis is to develop a more realistic mathematical model for the *in vivo* infection dynamics of human T-lymphotropic virus type I (HTLV-I), the first-discovered human retrovirus. Since its isolation and identification three decades ago, the virus has been studied extensively using both mathematical and experimental methods. These works have contributed greatly to our understanding of the infection, yet a complete picture of the way in which HTLV-I persists has thus far been elusive; previous models cannot fully explain experimental observations and even observed phenomena are not entirely understood [3, 4, 11, 12, 22]. Moreover, a definitive risk factor involved in the acquisition of HTLV-I-associated pathologies has been difficult to pinpoint; current hypotheses are frequently challenged by conflicting evidence [2, 10, 25, 26, 39]. A mathematical model based on a new hypothesis for the infection of HTLV-I will be constructed. Results from mathematical and numerical investigations give rise to relevant biological interpretations. By comparing our main findings with experimental observations, we are not only able to assess the validity of the original hypothesis, but also to make important inferences from the model that motivate future mathematical and experimental work.

The key issue we address is that of HTLV-I persistence *in vivo* by examining how HTLV-I-infected target cells manage to survive and propagate in chronically infected individuals despite strong positive selection by the human immune system. One well-established line of thinking suggests that the virus is completely passive and evades the human immune response simply by hiding in a latent pool of host cells throughout its lifetime. However, such a strategy cannot explain the widely reproduced experimental observations of on-going viral replication and the presence of persistent HTLV-I-specific immune responses. A recent alternative hypothesis,

proposed by Asquith and Bangham [4] and Asquith et al. [7], suggests that not complete passivity but rather a dynamic interplay between passivity and viral activation is key to describing the outcome of the infection. Based on this new proposed mechanism of HTLV-I infection, we build a mathematical model that captures the interactions that occur, focussing in particular on the role of spontaneous expression of viral proteins accompanied by infected target cell activation not previously considered in mathematical models for HTLV-I infection. Our results, utilizing both mathematical and numerical analysis, elucidate the infection and persistence of HTLV-I, and provide insights to the pathogenesis of HTLV-I-associated diseases.

1.2 Overview

Principal immunological features incorporated in the model are (i) both horizontal and vertical transmission of the virus, (ii) the presence of a latent reservoir of infected target cells that contains a predominant proportion of the viral burden, (iii) the dynamic interaction between infected target cell activation and latency, and (iv) the effect of human immune responses to infected cells. The mathematical model that arises is a three-dimensional compartmental system of ordinary differential equations, which is formulated as model (2.3) in Section 2.7.

The outline of the thesis is as follows. In Chapter 2, we provide some background to the virus and formulate a mathematical model from the proposed mechanism of infection. Chapters 3 and 4 deal primarily with the mathematical analysis and theoretical considerations of the model. In Chapter 3, we define important quantities, including the *basic reproduction number for viral infection*, obtain a feasible region on which the dynamics of the infection may be analyzed, and state mild conditions under which the infection-free and up to two endemic equilibria may exist in the feasible region. The local stability of each respective equilibrium is examined, leading to the existence of a backward bifurcation and a resulting region of bi-stability: there is an open range of parameter values for which the infection-free equilibrium and an endemic equilibrium co-exist and are both stable. In Chapter 4, we resolve the mathematical issue of characterizing the global behaviour of solutions to our system, which is complicated and non-trivial due to the high dimension of our model coupled with the presence of bi-stability. In Chapter 5, we investigate our model for HTLV-I numerically by selecting parameters in biologically reasonable ranges. Focussing on new aspects of the model, we present and discuss relevant biological implications of our findings. In Chapter 6, we conclude the thesis and raise questions for future considerations.

Chapter 2

HTLV-I

2.1 Epidemiology

Human T-lymphotropic virus type I (HTLV-I) is the first discovered exogenous human retrovirus and it infects an estimated 10 to 20 million individuals worldwide [10, 11, 21, 45, 51]. The infection is endemic in southern Japan, the Carribean, and the equatorial regions of South America, Africa, the Middle East, and Melanesia [3, 10, 11, 45, 51]. There is currently no cure nor preventative vaccine for HTLV-I, and neither is there satisfactory treatment for HTLV-I-associated pathologies; infection is life-long [10, 45]. HTLV-I has been identified as the aetiological agent of two major, clinically independent diseases: adult T-cell leukaemia/lymphoma (ATL), an aggressive T-cell malignancy which usually kills the host within 12 months, and HTLV-I-associated myelopathy, more commonly known as tropical spastic paraparesis (HAM/TSP), a slowly progressive neurological and inflammatory disease whose symptoms include spasticity, hyper-reflexia, weakening of the legs, and urinary and bowel dysfunction; in addition, HTLV-I infection is often accompanied by a wide range of chronic inflammatory afflictions, such as arthritis, uveitis, myositis, alveolitis, and infectious dermatitis [4, 9, 11, 39, 45, 51]. While the majority of HTLV-I-infected individuals, over 90%, remains as lifelong asymptomatic carriers (ACs), i.e. individuals who are infected with the virus but display no symptoms, between 5% and 10% will fall victim to one of the two major diseases after a long asymptomatic phase, with fewer than 3% exhibiting neurological dysfunction and developing HAM/TSP [3, 4, 9, 10, 23, 39, 45]. In this thesis, we will discuss chronic HTLV-I infection as a precursor to HAM/TSP development.

2.2 Viral Dynamics: Infection and Persistence

Unlike other human retroviruses, HTLV-I is not particularly infectious: cell-free virions are typically undetectable *in vivo* in the peripheral blood and are unable to efficiently infect $CD4^+$ helper T-cells, its primary targets. The transfer of infected cells either through breast milk, semen, or blood is necessary for infection to occur between individuals [10, 12, 45]. As a result, the proportion of peripheral blood mononuclear cells (PBMCs) that carry an integrated copy of the viral genome in an HTLV-I-infected individual, called the *proviral load*, is an accurate measure of the viral burden. An infected cell containing viral DNA is called a *proviral cell*, and the integrated viral DNA within an infected cell is called the *provirus*. An interesting characteristic of HTLV-I infection is that infected individuals, both ACs and HAM/TSP patients, may harbour extraordinarily high proviral loads: upwards of 70% or higher of $CD4^+$ helper T-cells may carry copies of the viral DNA, and may infect 10 - 20% of peripheral blood mononuclear cells (PBMCs) [10, 37, 53]. Even with such high proviral loads, the infection does not cause severe immunosuppression, although a degree of immune impairment in normal $CD4^+$ helper T-cell functionality has been observed, including an increased risk of *opportunistic infections* — infectious pathogens that are normally unable to cause disease in an individual with a healthy immune system but thrive against one with a weakened immune system — such as *Strongyloides stercoralis*, *Staphylococcus aureus*, and *Mycobacterium tuberculosis* [3, 45].

There are two primary routes of transmission for HTLV-I: vertical or 'mitotic' transmission, and horizontal or 'infectious' transmission. Infectious transmission of the provirus must occur by direct cell-to-cell contact [46]. Rearrangement of the proviral cell's cytoskeleton forms an organized structure called the virological synapse that is tightly bound to the uninfected target cell, and enveloped HTLV-I virions are transmitted from one cell into the other across the virological synapse without escaping into the periphery [12]. Once inside the cytoplasm, the viral genome integrates itself into the target cell's DNA using the enzyme reverse transcriptase [12, 23]. This process, known as reverse transcription, is highly error-prone as with other retroviruses such as HIV-1, resulting in high mutability in the genetic structure of the viral DNA and a wide variation among horizontally infected target cells [37, 53]. Mitotic transmission of the virus occurs when a provirus-containing parent cell undergoes cellular division, passing on identical copies of the provirus to each of it two daughter cells. It is known that the HTLV-I genome has remarkable genetic stability and exhibits very few sequence variations; as infectious transmission is error-prone, this observation suggests that persistent HTLV-I replication via the mitotic route is a significant contributing factor to infection by HTLV-I and may

even play a more important role than direct cell-to-cell transmission [3, 4, 37, 51, 53].

2.3 The HTLV-I-specific CTL Response

As with most pathogenic invasions, HTLV-I infection induces innate and adaptive immune responses, including recruitment and activation of macrophages, dendritic cells, B-cells, and T-cells. Adaptive immune responses specific to HTLV-I are largely mediated by cellular immunity and is associated with the activation and clonal expansion of anti-HTLV-I $CD8^+$ cytotoxic T-lymphocytes (CTLs), or so-called 'killer T-cells'. The primary antigen recognized by circulating HTLV-I-specific CTLs is the viral protein *Tax*, and it is known that chronically activated CTLs targeting Tax are typically abundant in the peripheral blood of infected hosts [3, 9, 10, 12]. As Tax-specific CTL-mediated lysis of HTLV-I-infected cells has been shown to be highly efficient, persistent CTL activity suggests the presence of on-going viral replication that provides a source of antigenic stimulation for CTL proliferation [5, 7, 12]. It is clear that any meaningful discussion of HTLV-I infection *in vivo* must consider, either implicitly or explicitly, the role of cellular immunity in the course of HTLV-I infection.

2.4 Previous Models

The basic understanding of HTLV-I infection outlined above has prompted mathematical and numerical investigations by several authors. In this section, we briefly describe some previous work in mathematical modelling of HTLV-I.

2.4.1 Gómez-Acevedo and Li (2005)

A mathematical model for HTLV-I infection taking into account both routes of viral transmission, infectious and mitotic, was developed by Gómez-Acevedo and Li in [22]. A key feature of the model is an implicit incorporation of adaptive immune responses targeting newly infected cells from horizontal transmission. Denote by $x(t)$ and $y(t)$ the respective populations of healthy and infected $CD4^+$ helper T-cells. It is assumed that production of new target cells occurs at a constant rate λ and does not depend on the $CD4^+$ helper T-cell carrying capacity, K. Mitotic division, however, is subject to restriction with respect to the total number of target cells. The density-dependent rate of homeostatic proliferation of healthy cells is given by $\nu_1 x\big(1 - \frac{x+y}{K}\big)$, and that of provirus-containing target cell proliferation is $\nu_2 y\big(1 - \frac{x+y}{K}\big)$. Infectious transmission via direct cell-to-cell contact occurs at a rate βxy, and newly infected cells risk destruction by strong adaptive immune responses.

The result is that only a fraction $\sigma\beta xy$, where $0 \leq \sigma \leq 1$, survive the immune system attack and enter the infected cell compartment. Natural death rates of healthy and infected target cells are $\mu_1 x$ and $\mu_2 y$, respectively. This leads to the following pair of differential equations:

$$\begin{aligned} x' &= \lambda + \nu_1 x\left(1 - \frac{x+y}{K}\right) - \mu_1 x - \beta xy \\ y' &= \sigma\beta xy + \nu_2 y\left(1 - \frac{x+y}{K}\right) - \mu_2 y. \end{aligned} \tag{2.1}$$

Mathematical analysis of system (2.1) has revealed complicated dynamical behaviour of solutions, most notably the existence of a backward bifurcation with respect to the parameter σ for small values of σ. There may exist up to three distinct equilibria: an infection-free equilibrium as well as two endemic, or chronic infection, equilibria. A quantity called the basic reproductive ratio of the virus R_0, defined as the average number of secondarily infected cells produced by each infected cell at the beginning of the infection, is given by

$$R_0 = \frac{1}{\mu_2}\left[\sigma\beta x_0 + \nu_2\Big(1 - \frac{x_0}{K}\Big)\right].$$

Both infectious and mitotic transmission are seen to contribute additively to the value of R_0. In this model R_0, which depends on σ, does not act as a sharp threshold parameter determining the outcome of the infection as is commonly the case in the literature of compartmental models. Rather, it is possible for bi-stability to occur: a stable infection-free equilibrium and a stable endemic equilibrium co-exist. The low dimension of the model allows for thorough mathematical analysis of the global behaviour of solutions to be performed, and following the mathematical investigation one is able to deduce interesting biological consequences that greatly enhance our understanding of HTLV-I persistence. In particular, the presence of a backward bifurcation and bi-stability helps explain why HTLV-I infection is so difficult to clear and raises challenges faced by treatment regimes. As we will see in the analysis of our proposed mathematical model, backward bifurcation appears to be an inherent characteristic of HTLV-I infection that plays an important role in the survival of the virus. The work of Gómez-Acevedo and Li [22] illustrates the importance of incorporating the human immune response for studying the dynamics of HTLV-I infection and simultaneously highlights the necessity for mathematical rigour to make solid inferences from the theoretical results.

Although the model by Gómez-Acevedo and Li [22] sheds light on the complicated dynamics of HTLV-I infection, it still does not explain how chronically infected individuals are able to accumulate and maintain high proviral loads, even

in the presence of a highly efficient Tax-specific CTL response. Another aspect that remains unanswered by the model is the identification of risk factors associated with the pathogenesis of HAM/TSP. Further investigation is required to gain a more detailed understanding of HTLV-I persistence *in vivo*.

2.4.2 Wodarz, Nowak, and Bangham (1999)

Wodarz, Nowak, and Bangham [54] developed a mathematical model for HTLV-I infection that explicitly incorporates the Tax-specific CTL response. In this model, both horizontal and vertical transmission of the provirus are also considered. Denote healthy $CD4^+$ helper T-cells by $x(t)$, proviral $CD4^+$ helper T-cells by $y(t)$, and HTLV-I-specific $CD8^+$ CTLs by $z(t)$. It is assumed that new target cells are produced at a rate λ, and proliferation of healthy and infected target cells have density-dependent proliferation constants r and s, respectively. The rate r represents homeostatic proliferation of the $CD4^+$ helper T-cell population while the rate s represents mitotic transmission of the provirus in infected $CD4^+$ T-cells. The total number of target cells, including both healthy and infected, cannot exceed a certain carrying capacity, k. Infectious transmission between a healthy target cell and an infected target cell occurs at a rate β and is assumed to have bi-linear incidence. Meanwhile, anti-HTLV-I CTLs encounter and lyse infected cells at a bi-linear incidence rate p. The proliferation constant of CTLs is designated by c, and CTL proliferation at high densities is assumed to be proportional simply to the number of infected target cells. Lastly, the respective natural death rates of healthy and infected $CD4^+$ helper T-cells are dx and ay, and that of $CD8^+$ CTLs is bz. The system of equations is given below:

$$\begin{aligned} x' &= (\lambda + rx)\left(1 - \frac{x+y}{k}\right) - dx - \beta xy \\ y' &= \beta xy + sy\left(1 - \frac{x+y}{k}\right) \pm ay \pm pyz \\ z' &= \frac{cyz}{z+1} - bz. \end{aligned} \tag{2.2}$$

Preliminary mathematical study of system (2.2) indicates that the model is characterized by two possible equilibria: the disease-free equilibrium, $E_0 = (x_0, 0, 0)$, where $x_0 > 0$, and an equilibrium corresponding to target cell-limited viral growth with CTL response, $E_1 = (x_1, y_1, z_1)$, where $x_1, y_1, z_1 > 0$. The basic reproductive ratio for system (2.2) is

$$R_0 = \frac{1}{a}\left[\beta x_0 + s\Big(1 - \frac{x_0}{k}\Big)\right],$$

and displays a similar form as the R_0 in Gómez-Acevedo and Li [22], namely, they are both constructed from two terms, one describing infectious transmission and the other describing mitotic transmission. Wodarz, Nowak, and Bangham [54] observe that in the absence of a lytic CTL response, i.e. no z equation, R_0 is a sharp threshold parameter that completely determines the outcome of the infection: when $R_0 < 1$, the virus is unable to establish itself in the host and the system moves to E_0, whereas when $R_0 > 1$, infection is persistent and the system may instead settle at E_1.

Incorporation of the virus-specific CTL response, however, complicates the dynamics. Although analytical techniques are not utilized, Wodarz, Nowak, and Bangham [54] investigate numerically the behaviour of solutions of their system (2.2), and elucidate several aspects regarding HTLV-I. One significant finding is the proof of principle that horizontal transmission is important to maintain viral infection, despite the relative invariance of the HTLV-I genome sequence, thus both routes of viral transmission, infectious and mitotic, are integral parts of the infection and persistence of HTLV-I. The model also reinforces the need to include the role of HTLV-I-specific immune responses to fully understand the interactions that take place during infection, and suggests that low CTL responsiveness may be associated with an increased pre-disposition to development of the debilitating disease HAM/TSP. Unfortunately, like the model by Gómez-Acevedo and Li [22], the work of Wodarz, Nowak, and Bangham [54] does not resolve the conflicting observations that CTLs efficiently lyse infected cells *in vivo* yet infected individuals, both ACs and HAM/TSP patients, often display high proviral loads [5, 13]. It has become increasingly clear that a thorough exploration of this issue must be performed in the quest to create a complete picture of HTLV-I infection.

2.5 Risk of HAM/TSP

The reason why some HTLV-I-infected individuals develop inflammatory disease while most remain asymptomatic is still not known. It is widely accepted that a high proviral load is an important risk factor to the development of HAM/TSP and ACs harbour generally lower proviral loads; however, the level of proviral loads between ACs and HAM/TSP patients have a broad overlapping range, and there exist ACs that display a high proviral load (characterized as greater than 3% PBMCs infected) along with HAM/TSP patients that exhibit a low proviral load (characterized as less than 1% PBMCs infected) [3, 6, 11, 39]. This shows that a high proviral load cannot be the sole factor in determining disease outcome.

Next, it is believed that cellular immunity plays an important role in the determi-

nation of proviral load and pathogenesis of HAM/TSP, although there is conflicting evidence as to whether CTL activity is beneficial or detrimental to the host [2, 5, 11]. On the one hand, an immunogenetics study conducted in southern Japan has shown that certain human leukocyte antigen (HLA) class I-restricted CTL responses are significantly associated with a reduced proviral load as well as a lower prevalence of HAM/TSP, thus indicating that the effect of CTLs is protective [25, 26]. On the other hand, it has been suggested that the chronic activation and high frequencies of CTLs have a deleterious impact on infected individuals, being the main underlying cause of the inflammation and damage to the nervous system seen in HAM/TSP patients [9, 10, 39]. From these observations, it is apparent that the magnitude of the proviral load and the role of CTL-mediated lysis do not adequately assess an infected individual's chance of developing HTLV-I-associated diseases. We conclude that there must be an additional factor influencing the outcome of HTLV-I infection and identification of this risk factor requires a more detailed look into the interactions that occur between HTLV-I-infected target cells and the immune system.

2.6 A Dynamic Interaction Between Viral Expression, Latency, and Immune Responses: A New Hypothesis

The question remains as to how some HTLV-I-infected individuals display elevated proviral loads whilst maintaining a persistently activated Tax-specific CTL response. To explain this phenomenon, several authors have suggested that infected cells are almost exclusively latent, harbouring transcriptionally silent viral genes thereby escaping CTL-induced lysis by effectively remaining 'invisible' to the human immune system, and maintenance of the proviral load occurs principally by normal homeostatic mitotic division of $CD4^+$ helper T-cells [37, 53]. However, such a mechanism does not adequately justify the high frequencies of circulating anti-HTLV-I $CD8^+$ CTLs found in the peripheral blood, which require antigenic stimulation from transcriptionally active proviral cells in order to proliferate. At the same time, in the presence of efficient CTL-mediated lysis, the high proviral loads often observed cannot be maintained solely by normal homeostatic mitosis of $CD4^+$ helper T-cells; selective proliferation of provirus-containing cells must be involved. These objections have motivated the development of a new hypothesis proposed by Asquith and Bangham [4] and Asquith et al. [7] that focus on the dynamic interaction between transcriptional latency of proviral cells and infected target cell activation corresponding to either suppression or expression of viral antigens.

The viral Tax protein, encoded by the HTLV-I genome, is the principle antigen

characteristic of all HTLV-I infected cells and is involved in activating the transcription of HTLV-I genes and triggering infected T-cell proliferation [10, 37]. Proviral cells are separated into two types, which may be distinguished by the absence or presence of Tax on the cell surface due to T-cell latency or T-cell activation: (i) latently infected, or Tax^-, target cells are resting $CD4^+$ helper T-cells that contain a provirus and do not display Tax, and (ii) actively infected, or Tax^+, target cells are activated provirus-carrying $CD4^+$ helper T-cells that do display Tax. Latently infected cells that suppress Tax are transcriptionally silent and do not make copies of the provirus, whereas actively infected cells that express the viral protein undergo persistent Tax-induced replication of its provirus through rapid selective mitotic division. Experimental evidence has suggested that at any given time, latently infected target cells make up the vast majority of all provirus-containing cells; up to 99% of proviral cells may be transcriptionally latent [3, 4].

Tax expression is both beneficial and detrimental to the HTLV-I proviral cell. On the one hand, displaying the viral protein is required for infectious transmission and drives rapid selective clonal expansion of actively infected cells, which is significantly faster than the rate of normal homeostatic T-cell proliferation, via up-regulation of cellular genes involved in mitosis and down-regulation of cell-cycle checkpoints [6, 7, 37, 53]. On the other hand, Tax expression simultaneously exposes the proviral cell to immune surveillance as the Tax protein is the dominant antigen recognized by the anti-HTLV-I human immune response, both humoral and cell-mediated [9, 10, 12, 53]. Indeed, lysis of HTLV-I-infected cells by $CD8^+$ CTLs is known to be highly efficient, but is only able to target actively infected $CD4^+$ T-cells that express Tax; latently infected $CD4^+$ T-cells that do not express Tax are rendered 'invisible' to the anti-HTLV-I CTL response and avoid destruction [3, 5, 6, 12, 13]. Blood samples taken from most HTLV-I-infected individuals consistently show the presence of chronic HTLV-I-specific immune responses, both CTL and antibody, suggesting that Tax is continuously being expressed [4, 9, 39]. Thus, it appears that HTLV-I persists in-host not by complete viral latency, but rather by balancing latency with activation.

An illustration of the proposed mechanism of HTLV-I infection *in vivo* describing a dynamic interaction between infected T-cell activation leading to expression of viral proteins, target cell latency, and anti-HTLV-I immune responses is shown in Figure 2.1.

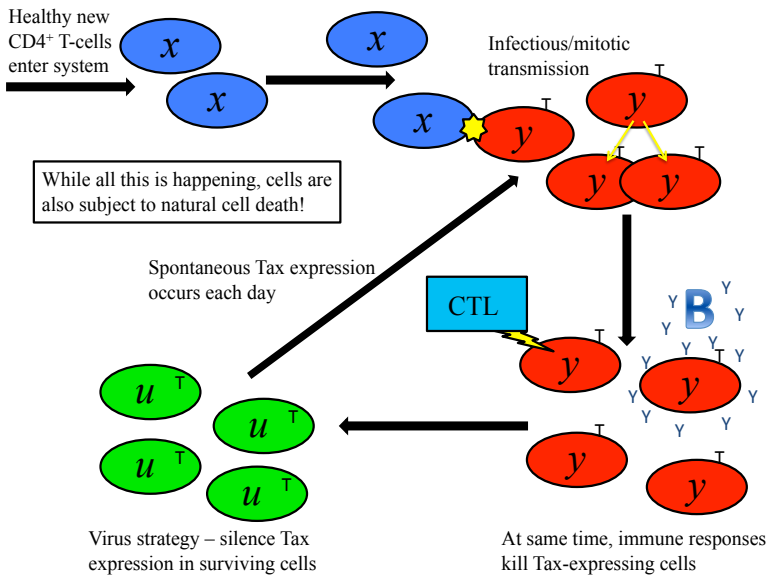

Figure 2.1: Biological mechanism of HTLV-I infection *in vivo*. Ovals represent $CD4^+$ T-cells, the target cells of HTLV-I infection. Healthy (x), latently infected (u), and actively infected (y) target cells are represented by the colours blue, green, and red, respectively.

2.7 Formulation of Mathematical Model

In this section, we formulate a mathematical model that explores the dynamic interaction between transcriptional latency and viral activation represented by the suppression or expression of Tax whilst maintaining the essential characteristics of HTLV-I infection *in vivo*. It should be noted that although an explicit incorporation of the HTLV-I-specific cytotoxic T-cell response via a compartment of $CD8^+$ CTLs may be done as in Wodarz, Nowak, and Bangham [54], the resulting four-dimensional system of differential equations would unnecessarily complicate the mathematical analysis and make it difficult to draw solid inferences from the investigations. As our primary focus is to illuminate the holistic mechanism of HTLV-I infection, including the roles of viral latency and activation on the infection dynamics, rather than solely on the particular role of Tax-specific $CD8^+$ CTLs, we instead follow the approach of Gómez-Acevedo and Li [22] by incorporating anti-HTLV-I immune responses implicitly, rather than explicitly, by including parameters representing fractions of infected target cells either through horizontal or vertical transmission that survive elimination by Tax-specific immune responses. Hence, a three-dimensional compartmental system of ordinary differential equations that describes the mechanism of HTLV-I infection *in vivo* will be derived.

We begin by compartmentalizing the $CD4^+$ T-cell population into three distinct

classes. Denote

$x(t)$: number of uninfected (healthy) CD4$^+$ helper T-cells at time t,
$u(t)$: number of latently infected (Tax$^-$) CD4$^+$ helper T-cells at time t,
$y(t)$: number of actively infected (Tax$^+$) CD4$^+$ helper T-cells at time t.

It is common to assume that CD4$^+$ helper T-cells are produced in the bone marrow at a constant rate λ, and that all of these new cells are healthy. These cells enter the bloodstream, where they may encounter actively infected cells. To describe the infectious transmission of HTLV-I via direct cell-to-cell contact between an actively infected (Tax-expressing) and uninfected CD4$^+$ T-cell, a bilinear incidence term is assumed, βxy, where the coefficient of infectious transmissibility β is indicative of the rate at which horizontal transmission occurs. That is, at time t, $\beta x(t)y(t)$ cells exit the uninfected cell class. Within 7-10 days after the initial infection, strong adaptive immune responses, both humoral and cellular, are established in an attempt to counter-act the infection [7, 9, 10, 12, 53]. The humoral immune response involves the activation of B-lymphocytes and the subsequent release of anti-HTLV-I antibodies, while the cellular immune response involves CTL-mediated lysis of infected CD4$^+$ T-cells expressing the viral Tax protein. Coupled with the low mutation rate and genetic stability of the HTLV-I genome mentioned in Section 2.2, the result is that only a fraction σ, where $\sigma \in [0, 1]$, of newly infected cells via infectious transmission, which at this point are actively infected, will survive the immune response and subsequently silence Tax expression, by mechanisms that are not yet understood [4]. Thus $\sigma\beta xy$ CD4$^+$ T-cells enter the latently infected cell class, while the remaining $(1 - \sigma)\beta xy$ die off.

Next, as pointed out in Section 2.6, latency does not offer benefits to viral transmission, both through infectious and mitotic routes, and it has been observed that each day, a small proportion τ of latently infected (Tax$^-$) CD4$^+$ T-cells spontaneously express the viral Tax protein and become actively infected (Tax$^+$) [4, 7]. Selective clonal expansion of these Tax-expressing proviral CD4$^+$ T-cells, which divide more rapidly than either healthy or latently infected target cells, occurs at a rate r and is assumed to follow a logistic growth pattern. The full form of such a term is given by $ry\big(1 - \frac{x+u+y}{k}\big)$, where k is the CD4$^+$ T-cell carrying capacity. However, since the vast majority of the infected target cell population is latent (see Section 2.6), then at any given time t, $y(t) \ll u(t)$, and it is justified to instead use the slightly simplified form $ry\big(1 - \frac{x+u}{k}\big)$ to describe the vertical transmission of HTLV-I in actively infected target cells. Expression of the Tax protein in a newly divided proviral cell exposes the cell to immune surveillance and increases its risk of elimination by CTL-mediated lysis. It is assumed that a fraction ϵ, where $\epsilon \in [0, 1]$,

of newly infected cells via mitotic transmission, survives destruction and hides Tax expression, thereby contributing to the latently infected target cell compartment. The remaining fraction $(1 - \epsilon)$ is immediately eliminated by anti-HTLV-I immune responses. Although mitosis is a natural process that occurs in all $CD4^+$ T-cells, normal homeostatic proliferation occurs at a much slower rate than that of selective mitotic division of Tax-expressing infected target cells and to avoid complicating the mathematical analysis of the model unnecessarily, we do not consider here the effects of passive proliferation of the healthy nor latently infected target cell populations.

Lastly, it is assumed that all $CD4^+$ T-cell populations under consideration are removed from the system by natural cell death at a rate proportional to their numbers. In particular, the removal rates of uninfected, latently infected, and actively infected $CD4^+$ helper T-cells are given by μ_1, μ_2, μ_3, respectively. All parameters are assumed to be positive with the exception of σ and ϵ, which may be zero.

A transfer diagram for the described interactions is shown in Figure 2.2.

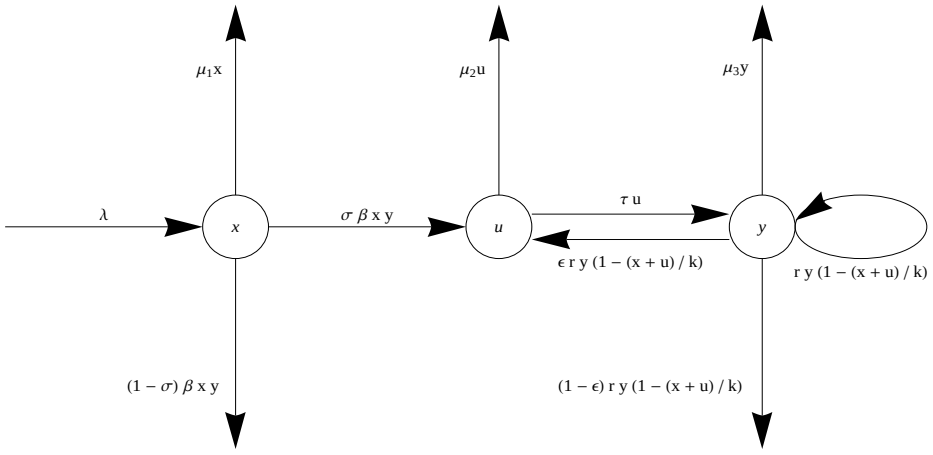

Figure 2.2: Transfer diagram describing the infection dynamics of HTLV-I *in vivo*.

This leads to the following system of ordinary differential equations:

$$\begin{aligned} x' &= \lambda - \beta xy - \mu_1 x \\ u' &= \sigma\beta xy + \epsilon ry\left(1 - \frac{x+u}{k}\right) - (\tau + \mu_2)u \\ y' &= \tau u - \mu_3 y. \end{aligned} \tag{2.3}$$

Remark 2.7.1. The *proviral load* at any time t is $v(t) = u(t) + y(t)$. It measures the total number of provirus-containing target cells at time t, regardless of Tax expression.

2.8 Main Findings

Significant mathematical results and biological insights arise from the study of our three-dimensional model for HTLV-I infection. Most notably is the possible existence of a backward bifurcation and bi-stability. It is seen that together with the complicated phenomenon of a backward bifurcation, compartmentalization of two distinct pools of infected cells, while allowing us to investigate the role of latency in HTLV-I infection, raises non-trivial mathematical issues due to the high dimension of the model. Characterization of the global dynamics of our model, both in the absence and presence of bi-stability, forms our main theoretical result and is summarized in Theorem 4.5.1 and Theorem 4.5.2, respectively. The key to the establishing the global dynamics when bi-stability occurs lies in Theorem 4.4.3, which precludes the existence of non-constant periodic orbits and allows us to demonstrate the convergence of each trajectory to a single equilibrium. The establishment of the global behaviour of solutions, especially in the presence of bi-stability, requires the use of advanced mathematical concepts including the theory of monotone dynamical systems, the theory of compound differential systems, and the Butler-McGehee Lemma. A complete understanding of the dynamical behaviour of solutions is needed in order to examine unambiguously the finer aspects of our system, such as the role played by parameters on equilibrium points.

Next, we turn our attention to the specific impact of viral latency and rate of Tax expression, the new aspects of our model, on the persistence of HTLV-I. We discover that when parameter values are chosen from biologically reasonable ranges, numerical investigations yield interesting and at times unexpected results and provide useful biological insights to realistic HTLV-I infection. Our model verifies the experimental observation that the proviral load may be quite high during chronic HTLV-I infection: greater than 70% of target cells may carry a copy of the provirus. Moreover, it is demonstrated that a substantial proportion of proviral cells are transcriptionally silent at any given time, suggesting latency is a survival strategy allowing the provirus to escape elimination by the immune system. Our most noteworthy finding is the identification of the rate of spontaneous Tax expression as an essential component of HTLV-I infection. It is revealed that Tax expression, which has not been before considered in mathematical models of HTLV-I, drives chronic infection and promotes bi-stability, affects the time to reach steady state, and has a substantial impact not only on the proviral load, but may also be a significant risk factor to the development of HAM/TSP. Our investigations suggest that treatment regimes that help to reduce Tax expression may be pivotal on the road to controlling chronic HTLV-I infection.

Chapter 3

Equilibria, Local Stability, and Backward Bifurcation

In this chapter, several important quantities are defined and a feasible region on which the dynamics of our mathematical model (2.3) may be studied is obtained. Under appropriate assumptions, it will be shown that an infection-free equilibrium always exists in such a feasible region. Sufficient conditions will be given for the existence of up to two endemic equilibria. The local stability of each equilibrium will be examined. It will be shown that it is possible for both a stable infection-free equilibrium and a stable endemic equilibrium to co-exist, leading to the phenomenon of a backward bifurcation and bi-stability.

3.1 Defined Quantities and Assumptions

3.1.1 Defined Quantities

We define the following important quantities.

Definition 3.1.1 (Important Quantities)**.**

$$\begin{aligned} R_0 &= \frac{\tau}{\mu_3(\tau+\mu_2)}\Big(\sigma\beta x_0 + \epsilon r\Big(1-\frac{x_0}{k}\Big)\Big) > 0, \quad \text{where } x_0 = \frac{\lambda}{\mu_1}, \\ \sigma_0 &= \frac{\epsilon r}{k\beta} - \frac{\epsilon r - \frac{\mu_3}{\tau}(\tau+\mu_2)}{2\beta x_0}\left[\frac{k\beta\tau\big(\epsilon r - \frac{\mu_3}{\tau}(\tau+\mu_2)\big)}{2\epsilon r\mu_1\mu_3} + 1\right], \\ \bar{\sigma} &= \frac{\epsilon r}{k\beta} - \frac{1}{\beta x_0}\Big(\epsilon r - \frac{\mu_3}{\tau}(\tau+\mu_2)\Big) > 0, \\ \tilde{x}(\sigma) &= \frac{\epsilon r - \frac{\mu_3}{\tau}(\tau+\mu_2)}{2\big(\frac{\epsilon r}{k} - \sigma\beta\big)}. \end{aligned} \tag{3.1}$$

Remark 3.1.1. R_0 is called the *basic reproduction number* or *basic reproductive ratio* for viral infection. Biologically, it represents the average number of secondary

infected cells produced from a single actively infected cell over its lifetime. For a full derivation of R_0, see Appendix A.1.

3.1.2 Assumptions

Throughout this thesis we make the following mild mathematical assumptions:

$$\triangleright\ \epsilon r - \frac{\mu_3}{\tau}(\tau + \mu_2) > 0, \tag{A1}$$

$$\triangleright\ \sigma\beta < \frac{\epsilon r}{k}, \tag{A2}$$

$$\triangleright\ \left[\frac{\beta\tau}{\mu_1\mu_3}\tilde{x}_{\sigma=0} + 1\right]\tilde{x}(\sigma) > x_0, \quad \text{for some } \sigma > 0, \tag{A3(i)}$$

$$\triangleright\ \left[\frac{\beta\tau}{\mu_1\mu_3}\tilde{x}_{\sigma=0} + 1\right]\tilde{x}_{\sigma=0} < x_0, \tag{A3(ii)}$$

$$\triangleright\ \sigma_0 < \bar{\sigma}. \tag{A4}$$

Remark 3.1.2.

- If we consider $R_0 = R_0(\sigma)$ as a function of the parameter σ, then $R_0(\bar{\sigma}) = 1$.
- Assumptions (A3(i)) and (A3(ii)) are equivalent to the conditions $\sigma > \sigma_0$ for some $\sigma > 0$ and $\sigma_0 > 0$, respectively. For the full derivation of Assumption (A3(i)) and a discussion of Assumption (A3(ii)), we refer the reader to Appendix A.2. Note that $R_0(\sigma)$ is an increasing function of σ, hence Assumption (A4) is equivalent to $R_0(\sigma_0) < 1$.

3.1.3 Biological Motivations of Assumptions

Assumptions (A1)–(A4) have reasonable biological interpretations. In particular, Assumption (A1) indicates that the net effect of infected T-cell activation and subsequent expression of viral antigens that is accompanied by selective mitotic transmission is more beneficial to the virus than transcriptional latency. Assumption (A2) implies that the contribution from horizontal transmission has slightly less of an impact than that from vertical transmission in maintaining the proviral load. Assumptions (A3(i)) and (A3(ii)) are especially important in the initial stages of the infection. Assumption (A3(i)) states that chronic infection is possible if a large enough proportion of newly infected target cells manage to survive immune responses and successfully hide Tax expression, creating a pool of latently infected cells. Assumption (A3(ii)) states the intuitive idea that such a pool cannot be established in individuals with a strong enough immune system, and the infection will always be cleared. Finally, Assumption (A4) is a technical condition with a

corresponding interpretation that there are individuals whose anti-HTLV-I immune responses are neither strong nor weak, rather they constitute being moderate.

3.2 Feasible Region

Before we begin the mathematical analysis, we first derive upper bounds for the T-cell populations to find a biologically relevant region for which our model is well-posed. Denote by $\mathbb{R}^3_+$ the closed positive orthant of $\mathbb{R}^3$, and let

$$\Gamma := \left\{ (x,u,y) \in \mathbb{R}^3_+ : x \leq \frac{\lambda}{\mu_1},\ x+u \leq N,\ y \leq \frac{\tau}{\mu_3} N \right\}, \tag{3.2}$$

where $N = \dfrac{\lambda + \epsilon r k}{\epsilon r + \tilde{\mu}} > 0$ and $\tilde{\mu} = \min\{\mu_1, \mu_2\}$.

Our first result, Theorem 3.2.1, shows that all solutions of model (2.3) are bounded in the positively invariant set Γ as $t \to \infty$. Thus, the set Γ is a feasible region on which the dynamics may be analyzed.

Theorem 3.2.1 (Feasible Region)**.** *The set Γ is defines a bounded feasible region for model (2.3).*

Proof. From the first equation of model (2.3), we obtain

$$x' \leq \lambda - \mu_1 x,$$

and this implies that

$$\limsup_{t\to\infty} x(t) \leq \frac{\lambda}{\mu_1}.$$

Adding the first two equations of our model yields

$$\begin{aligned}
(x+u)' &= \lambda \underline{-(1-\sigma)\beta x y} + \epsilon r \underline{y} \left(1 - \frac{x+u}{k}\right) \underline{-\tau u} - \mu_1 x - \mu_2 u \\
&\leq \lambda + \epsilon r k \left(1 - \frac{x+u}{k}\right) - \tilde{\mu}(x+u), \quad \text{where } \tilde{\mu} = \min\{\mu_1, \mu_2\}, \\
&= (\lambda + \epsilon r k) - (\epsilon r + \tilde{\mu})(x+u).
\end{aligned}$$

Therefore,

$$\limsup_{t\to\infty} (x+u)(t) \leq \frac{\lambda + \epsilon r k}{\epsilon r + \mu} = N.$$

Finally, if $\big(x(t), u(t), y(t)\big)$ is a solution of model (2.3) with $x(0) + u(0) \leq N$, then

from the third equation of the model, we obtain

$$y' = \tau u - \mu_3 y \leq \tau N - \mu_3 y, \quad \text{and thus} \quad \limsup_{t\to\infty} y(t) \leq \frac{\tau}{\mu_3} N.$$

This allows us to consider the region

$$\Gamma := \left\{ (x,u,y) \in \mathbb{R}^3_+ : x \leq \frac{\lambda}{\mu_1},\ x+u \leq N,\ y \leq \frac{\tau}{\mu_3} N \right\}.$$

It is easy to verify (by considering the differential equations on the boundary of Γ) that Γ is positively invariant in $\mathbb{R}^3$ and that the model is well-posed. Thus, it suffices to analyze the dynamics of model (2.3) in the feasible region Γ. □

3.3 Existence of Equilibria

Equilibria occur when

$$0 = \lambda - \beta x y - \mu_1 x, \tag{3.3}$$

$$0 = \sigma\beta x y + \epsilon r y \left(1 - \frac{x+u}{k}\right) - (\tau + \mu_2) u, \tag{3.4}$$

$$0 = \tau u - \mu_3 y. \tag{3.5}$$

Observe that from Equation (3.5), $u = 0 \iff y = 0$ at equilibrium.

3.3.1 Infection-free Equilibrium

Here we consider the case when $x > 0$ and $u, y = 0$ at equilibrium. Thus, we look for steady state solutions of the form $P_0 = (x_0, 0, 0)$, where $x_0 > 0$. From Equation (3.3),

$$\lambda - \mu_1 x_0 = 0 \quad \Longrightarrow \quad x_0 = \frac{\lambda}{\mu_1}.$$

We find the *infection-free* equilibrium $P_0 = \left(\frac{\lambda}{\mu_1}, 0, 0\right)$ corresponding to a healthy individual. The quantity x_0 is the level of target cells in the absence of an infection and coincides precisely with the normal $CD4^+$ helper T-cell count in a healthy individual.

3.3.2 Endemic Equilibria

Consider the case when chronic infection is present, i.e. $x, u, y > 0$ at equilibrium. That is, we look for steady state solutions of the form $\bar{P} = (\bar{x}, \bar{u}, \bar{y})$, where $\bar{x}, \bar{u}, \bar{y} > 0$.

We will refer to such a steady state as an *endemic*, or *chronic infection*, equilibrium. From Equation (3.5), we find that

$$\boxed{\bar{u} = \frac{\mu_3}{\tau}\bar{y}.} \tag{3.6}$$

Next, look at Equation (3.4):

$$\begin{aligned}
&\sigma\beta\bar{x}\bar{y} + \epsilon r\bar{y}\left(1 - \frac{\bar{x}+\bar{u}}{k}\right) - (\tau+\mu_2)\bar{u} = 0,\\
\Longrightarrow &\left(\sigma\beta - \frac{\epsilon r}{k}\right)\bar{x}\bar{y} + \epsilon r\bar{y}\left(1 - \frac{\bar{u}}{k}\right) - \frac{\mu_3}{\tau}(\tau+\mu_2)\bar{y} = 0,\\
\Longrightarrow &\left(\sigma\beta - \frac{\epsilon r}{k}\right)\bar{x} + \epsilon r - \frac{\mu_3}{\tau}(\tau+\mu_2) = \frac{\epsilon r}{k}\bar{u} = \frac{\epsilon r\mu_3}{k\tau}\bar{y},
\end{aligned}$$

so that

$$\boxed{\bar{y} = \frac{k\tau}{\epsilon r\mu_3}\left[\left(\sigma\beta - \frac{\epsilon r}{k}\right)\bar{x} + \epsilon r - \frac{\mu_3}{\tau}(\tau+\mu_2)\right].} \tag{3.7}$$

Substitution of Equation (3.7) into Equation (3.3) then yields

$$\underbrace{\lambda - \mu_1\bar{x}}_{f_1(x)} = \beta\bar{x}\bar{y} = \underbrace{\frac{k\beta\tau}{\epsilon r\mu_3}\bar{x}\left[\left(\sigma\beta - \frac{\epsilon r}{k}\right)\bar{x} + \epsilon r - \frac{\mu_3}{\tau}(\tau+\mu_2)\right]}_{f_2(x)}.$$

Define

$$\begin{aligned}
f_1(x) &= \lambda - \mu_1 x,\\
f_2(x) &= \frac{k\beta\tau}{\epsilon r\mu_3}x\left[\left(\sigma\beta - \frac{\epsilon r}{k}\right)x + \epsilon r - \frac{\mu_3}{\tau}(\tau+\mu_2)\right].
\end{aligned} \tag{3.8}$$

The x-coordinates of endemic equilibria, if they occur, are the intersection points of the line f_1 with the parabola f_2 (see Figure 3.1). Observe that Assumptions (A1) and (A2) are precisely the requirements that $f_2'(0) > 0$ and $f_2''(x) < 0$, respectively. Both f_1, f_2 have a single positive root:

$$x_0 = \frac{\lambda}{\mu_1} \text{ for } f_1, \quad \hat{x} = 2\tilde{x} = \frac{\epsilon r - \frac{\mu_3}{\tau}(\tau+\mu_2)}{\frac{\epsilon r}{k} - \sigma\beta} \text{ for } f_2.$$

Assumption (A3(i)) ensures that for some positive value of the parameter σ, the height of the vertex of the concave parabola f_2, located at $\tilde{x}$, lies above the height of the corresponding point on the straight line f_1. This condition is equivalent to $\sigma > \sigma_0$, where $\sigma_0 > 0$ is defined as in Section 3.1. Additionally, if we view the quantity $\tilde{x} = \tilde{x}(\sigma)$ as a function of σ, Assumption (A3(ii)), which is equivalent to

$\sigma_0 > 0$, indicates a range for σ where the number of endemic, or chronic infection, equilibria goes from zero to two as σ increases from 0 through σ_0 to $\bar{\sigma}$.

When $R_0 < 1$, equivalently $\sigma < \bar{\sigma}$, it can be easily shown that $\hat{x} < x_0$, leading to the possibility of the graphs of f_1 and f_2 to intersect twice, provided Assumption (A3(i)) holds. However, when $R_0 > 1$, equivalently $\sigma > \bar{\sigma}$, then $\hat{x} > x_0$, and the graphs of f_1 and f_2 must intersect exactly once.

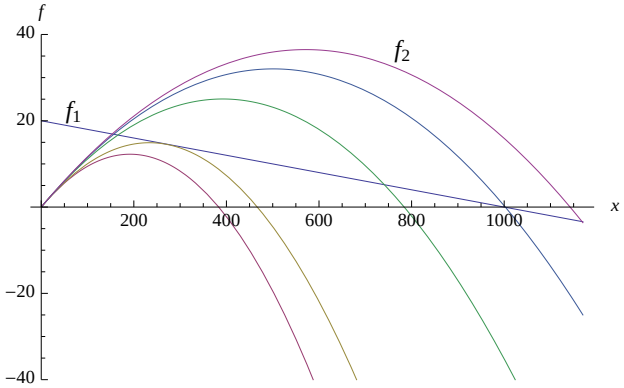

Figure 3.1: Graphs of the straight line f_1 and the concave parabola f_2 for several values of the parameter σ. As σ varies, the two graphs may have zero, one, or two intersection points. All parameter values are selected in the ranges shown in Table 5.1. The five graphs for f_2 correspond to $\sigma = 0, 0.021, 0.06, 0.0725$ and 0.078, while the remaining parameters are fixed: $\lambda = 20$, $\beta = 0.001$, $\epsilon = 0.9$, $\tau = 0.01$, $r = 0.15$, $k = 1150$, $\mu_1 = 0.02$, $\mu_2 = 0.02$, $\mu_3 = 0.03$.

3.3.3 Summary of the Existence of Equilibria

We summarize the results for the existence of equilibria in the following theorem.

Theorem 3.3.1 (Existence of Equilibria)**.** *Assume (A1)–(A4) hold. Then,*

1) *the infection-free equilibrium $P_0 = (x_0, 0, 0)$, where $x_0 = \frac{\lambda}{\mu_1}$, always exists in $\bar{\Gamma}$. Moreover, if $0 < R_0 < R_0(\sigma_0)$ (equivalently, $0 < \sigma < \sigma_0$), then P_0 is the only equilibrium in $\bar{\Gamma}$;*

2) *when $R_0 < 1$ (equivalently, $\sigma < \bar{\sigma}$), then a sufficient condition for the existence of three equilibria, P_0 on the boundary $\partial\Gamma$ along with two distinct endemic, or chronic infection, equilibria $P_1 = (x_1, u_1, y_1)$ and $P_2 = (x_2, u_2, y_2)$ in the interior $\mathring{\Gamma}$ with $x_1 < x_2, u_1 > u_2, y_1 > y_2$, is given by $R_0 > R_0(\sigma_0)$ (equivalently, $\sigma > \sigma_0$). The x-coordinates of P_1 and P_2 satisfy $f_1'(x_1) - f_2'(x_1) < 0$ and $f_1'(x_2) - f_2'(x_2) > 0$, respectively;*

3) when $R_0 > 1$ (equivalently, $\sigma > \bar{\sigma}$), there exist exactly two equilibria, P_0 on $\partial\Gamma$ and a unique endemic, or chronic infection, equilibrium $\bar{P} = P_1 = (\bar{x}, \bar{u}, \bar{y})$ in $\mathring{\Gamma}$, whose x-coordinate satisfies $f_1'(\bar{x}) - f_2'(\bar{x}) < 0$.

3.4 Local Stability

In this section, we determine the local stability of equilibria. The *Jacobian matrix* for model (2.3) is

$$J(x,u,y) = \begin{bmatrix} -\beta y - \mu_1 & 0 & -\beta x \\ \left(\sigma\beta - \frac{\epsilon r}{k}\right) y & -\frac{\epsilon r}{k} y - \tau - \mu_2 & \sigma\beta x + \epsilon r\left(1 - \frac{x+u}{k}\right) \\ 0 & \tau & -\mu_3 \end{bmatrix}. \tag{J}$$

We will also require the use of the *second additive compound matrix* of J, denoted $J^{[2]}$. It is given by

$$J^{[2]}(x,u,y) = \begin{bmatrix} -\beta y - \mu_1 - \frac{\epsilon r}{k} y - \tau - \mu_2 & \sigma\beta x + \epsilon r\left(1 - \frac{x+u}{k}\right) & \beta x \\ \tau & -\beta y - \mu_1 - \mu_3 & 0 \\ 0 & \left(\sigma\beta - \frac{\epsilon r}{k}\right) y & -\frac{\epsilon r}{k} y - \tau - \mu_2 - \mu_3 \end{bmatrix}. \tag{J2}$$

For a discussion of the second additive compound matrix, see Appendix B.1.

3.4.1 Local Stability of the Infection-Free Equilibrium P_0

The local stability of the infection-free equilibrium P_0 is given by the following.

Proposition 3.4.1 (Local Stability of P_0)**.**

i) When $R_0 < 1$ (equivalently, $\sigma < \bar{\sigma}$), the infection-free equilibrium $P_0 = (x_0, 0, 0)$, where $x_0 = \frac{\lambda}{\mu_1}$, is always locally asymptotically stable in the feasible region Γ.

ii) When $R_0 > 1$ (equivalently, $\sigma > \bar{\sigma}$), P_0 is unstable. Specifically, P_0 is a saddle with $\dim W^s_{loc}(P_0) = 2$ and $\dim W^u_{loc}(P_0) = 1$, where $W^s_{loc}(P_0)$, $W^u_{loc}(P_0)$ denote the local stable and unstable manifolds of P_0, respectively.

Proof. At the infection-free equilibrium, the Jacobian matrix is

$$J(P_0) = \begin{bmatrix} -\mu_1 & 0 & -\beta x_0 \\ 0 & -\tau - \mu_2 & \sigma\beta x_0 + \epsilon r\left(1 - \frac{x_0}{k}\right) \\ 0 & \tau & -\mu_3 \end{bmatrix}.$$

We are interested in determining the signs of the real parts of the eigenvalues of $J(P_0)$. Denote by I the 3×3 identity matrix. The characteristic equation is given by

$$\begin{aligned}
&\chi_0(\zeta) = \det\big(\zeta I - J(P_0)\big)\\
&= \det\begin{bmatrix} \zeta+\mu_1 & 0 & \beta x_0 \\ 0 & \zeta+\tau+\mu_2 & -\sigma\beta x_0 - \epsilon r\left(1-\frac{x_0}{k}\right) \\ 0 & -\tau & \zeta+\mu_3 \end{bmatrix}\\
&= (\zeta+\mu_1)\Big[(\zeta+\tau+\mu_2)(\zeta+\mu_3) - \tau\big(\sigma\beta x_0 + \epsilon r\left(1-\tfrac{x_0}{k}\right)\big)\Big] - 0 + \beta x_0(0-0)\\
&= (\zeta+\mu_1)\Big[\zeta^2 + (\tau+\mu_2+\mu_3)\zeta + \mu_3(\tau+\mu_2) - \tau\big(\sigma\beta x_0 + \epsilon r\left(1-\tfrac{x_0}{k}\right)\big)\Big]\\
&= (\zeta+\mu_1)\Big[\zeta^2 + (\tau+\mu_2+\mu_3)\zeta - \mu_3(\tau+\mu_2)\big[\underbrace{\tfrac{\tau}{\mu_3(\tau+\mu_2)}\big(\sigma\beta x_0+\epsilon r\big(1-\tfrac{x_0}{k}\big)\big)}_{R_0} - 1\big]\Big]\\
&= (\zeta+\mu_1)\Big[\zeta^2 + (\tau+\mu_2+\mu_3)\zeta - \mu_3(\tau+\mu_2)\big[R_0-1\big]\Big].
\end{aligned}$$

Let $a_0 = 1$, $b_0 = \tau+\mu_2+\mu_3$, and $c_0 = -\mu_3(\tau+\mu_2)\big[R_0-1\big]$. Then we may write the characteristic polynomial as

$$\chi_0(\zeta) = \ (\zeta+\mu_1)F_0(\zeta), \quad \text{with} \quad F_0(\zeta) = a_0\zeta^2 + b_0\zeta + c_0.$$

Since the discriminant of $F_0(\zeta)$ is

$$b_0^2 - 4a_0c_0 = (\tau+\mu_2+\mu_3)^2 + 4\mu_3(\tau+\mu_2)\big[R_0-1\big],$$

the roots of the characteristic polynomial $\chi_0(\zeta)$, which are precisely the eigenvalues of the Jacobian matrix at P_0, are given by

$$\zeta_1 = -\mu_1 \quad \text{and} \quad \zeta_{2,3} = -\frac{1}{2}(\tau+\mu_2+\mu_3) \pm \frac{1}{2}\sqrt{(\tau+\mu_2+\mu_3)^2 + 4\mu_3(\tau+\mu_2)[R_0-1]}.$$

Clearly, $\mathrm{Re}(\zeta_1) < 0$. Moreover, we observe that if $R_0 < 1$, the remaining two eigenvalues, ζ_2 and ζ_3, will also have negative real parts. Hence, $s\big(J(P_0)\big) < 0$ and we may conclude that P_0 is locally asymptotically stable when $R_0 < 1$. However, if $R_0 > 1$, $\mathrm{Re}(\zeta_2) > 0$, which implies that P_0 is unstable. In this case, P_0 is a saddle whose local stable manifold $W^s_{loc}(P_0)$ is two-dimensional and whose local unstable manifold $W^u_{loc}(P_0)$ is one-dimensional. If $R_0 = 1$, $\zeta_2 = 0$ is a zero eigenvalue of $J(P_0)$ and no immediate conclusions about the local stability of P_0 may be inferred. The preceding observations establish the basic reproduction number for viral infection R_0 as a threshold parameter that characterizes the local stability of the infection-free equilibrium P_0. □

3.4.2 Local Stability of Endemic Equilibria $\bar{P}$

We now examine the local stability properties of any endemic, or chronic infection, equilibrium $\bar{P} = (\bar{x}, \bar{u}, \bar{y})$ whenever it exists. At $\bar{P}$, the Jacobian matrix is

$$J(\bar{P}) = \begin{bmatrix} -\beta\bar{y} - \mu_1 & 0 & -\beta\bar{x} \\ \left(\sigma\beta - \frac{\epsilon r}{k}\right)\bar{y} & -\frac{\epsilon r}{k}\bar{y} - \tau - \mu_2 & \sigma\beta\bar{x} + \epsilon r\left(1 - \frac{\bar{x}+\bar{u}}{k}\right) \\ 0 & \tau & -\mu_3 \end{bmatrix}.$$

For $J(\bar{P})$ to be stable, all three of its eigenvalues must have negative real parts. Commonly, this is shown by verifying the inequalities in the Routh-Hurwitz criterion. However, in this situation, there is no explicit formula for the coordinates of endemic equilibria, rather they are the intersection points of the graphs of two functions of x, namely $f_1(x)$ and $f_2(x)$. The resulting calculations, while possible to compute, lead to technically difficult expressions. An alternative method due to Li and Wang [32] states necessary and sufficient conditions for which all eigenvalues of a given $n \times n$ matrix with real entries have negative real parts. Li et al. [28] applied this alternative method to show the local asymptotic stability of the unique interior equilibrium in an SEIR model with varying total population size. In the special case $n = 3$, McCluskey and van den Driessche [36] observe that when $\det(A) < 0$, the stability of the second compound matrix is equivalent to the conditions $\operatorname{tr}(A) < 0$ and $\det\left(A^{[2]}\right) < 0$. An application of this specialized result to an epidemic model is demonstrated in [1]. We will use this criterion to characterize the stability of the 3×3 matrix $J(\bar{P})$ and thus the local stability of the given endemic, or chronic infection, equilibrium (or equilibria). The statements of the general stability criterion by Li and Wang [32] and the specialized result of McCluskey and van den Driessche [36] are given below.

Theorem 3.4.1 (Theorem 3.1, Li and Wang (1998))**.** *Let A be an $n \times n$ matrix with real entries. For A to be stable, it is necessary and sufficient that*

(i) the second compound matrix $A^{[2]}$ is stable, and

(ii) $(-1)^n \det(A) > 0$.

Lemma 3.4.1 (Lemma 3, McCluskey and van den Driessche (2003))**.** *Let A be a 3×3 matrix with real entries. If $\operatorname{tr}(A)$, $\det(A)$, and $\det\left(A^{[2]}\right)$ are all negative, then all of the eigenvalues of A have negative real part.*

It is straight-forward to see that the converse of Lemma 3.4.1 is also true. Using Lemma 3.4.1, we determine the local stability properties for each endemic equilibrium point $\bar{P}$ by examining the stability of the Jacobian matrix $J(\bar{P})$ at that point.

Theorem 3.4.2 (Local Stability of $\bar{P}$)**.** *Assume (A1)–(A4) hold. Then, the following are true:*

i) When $R_0(\sigma_0) < R_0 < 1$ (equivalently, $\sigma_0 < \sigma < \bar{\sigma}$), there exist two endemic, or chronic infection, equilibria, P_1 and P_2. In this case, P_1 is locally asymptotically stable whereas P_2 is unstable. Moreover, the local stable manifold $W^s_{loc}(P_2)$ of P_2 is two-dimensional.

ii) When $R_0 > 1$ (equivalently, $\sigma > \bar{\sigma}$), the unique endemic, or chronic infection, equilibrium $\bar{P} = P_1$ is locally asymptotically stable.

Proof. At any chronic infection, or endemic, equilibrium $\bar{P} = (\bar{x}, \bar{u}, \bar{y})$, the Jacobian matrix is

$$J(\bar{P}) = \begin{bmatrix} -\beta\bar{y} - \mu_1 & 0 & -\beta\bar{x} \\ \left(\sigma\beta - \frac{\epsilon r}{k}\right)\bar{y} & -\frac{\epsilon r}{k}\bar{y} - \tau - \mu_2 & \sigma\beta\bar{x} + \epsilon r\left(1 - \frac{\bar{x}+\bar{u}}{k}\right) \\ 0 & \tau & -\mu_3 \end{bmatrix},$$

and the second additive compound matrix of J is

$$J^{[2]}(\bar{P}) = \begin{bmatrix} -\beta\bar{y} - \mu_1 - \frac{\epsilon r}{k}\bar{y} - \tau - \mu_2 & \sigma\beta\bar{x} + \epsilon r\left(1 - \frac{\bar{x}+\bar{u}}{k}\right) & \beta\bar{x} \\ \tau & -\beta\bar{y} - \mu_1 - \mu_3 & 0 \\ 0 & \left(\sigma\beta - \frac{\epsilon r}{k}\right)\bar{y} & -\frac{\epsilon r}{k}\bar{y} - \tau - \mu_2 - \mu_3 \end{bmatrix}.$$

From the equilibrium equations (3.3)–(3.5) and Equation (3.7), we observe that

$$\sigma\beta\bar{x} + \epsilon r\left(1 - \frac{\bar{x}+\bar{u}}{k}\right) = \frac{\mu_3}{\tau}(\tau + \mu_2) \quad \text{and} \quad \bar{y} = \frac{k\tau}{\epsilon r \mu_3}\left[\left(\sigma\beta - \frac{\epsilon r}{k}\right)\bar{x} + \epsilon r - \frac{\mu_3}{\tau}(\tau + \mu_2)\right].$$

We first compute

$$\operatorname{tr}\big(J(\bar{P})\big) = -\beta\bar{y} - \mu_1 - \frac{\epsilon r}{k}\bar{y} - \tau - \mu_2 - \mu_3 < 0,$$

and

$$
\begin{aligned}
&\det\Big(J^{[2]}(\bar{P})\Big)\\
&= \det\begin{bmatrix} -\beta\bar{y}-\mu_1-\frac{\epsilon r}{k}\bar{y}-\tau-\mu_2 & \sigma\beta\bar{x}+\epsilon r\left(1-\frac{\bar{x}+\bar{u}}{k}\right) & \beta\bar{x} \\ \tau & -\beta\bar{y}-\mu_1-\mu_3 & 0 \\ 0 & \left(\sigma\beta-\frac{\epsilon r}{k}\right)\bar{y} & -\frac{\epsilon r}{k}\bar{y}-\tau-\mu_2-\mu_3 \end{bmatrix}\\
&= \det\begin{bmatrix} -\beta\bar{y}-\mu_1-\frac{\epsilon r}{k}\bar{y}-\tau-\mu_2 & \frac{\mu_3}{\tau}(\tau+\mu_2) & \beta\bar{x} \\ \tau & -\beta\bar{y}-\mu_1-\mu_3 & 0 \\ 0 & \left(\sigma\beta-\frac{\epsilon r}{k}\right)\bar{y} & -\frac{\epsilon r}{k}\bar{y}-\tau-\mu_2-\mu_3 \end{bmatrix}\\
&= -\Big(\beta\bar{y}+\mu_1+\frac{\epsilon r}{k}\bar{y}+\tau+\mu_2\Big)(\beta\bar{y}+\mu_1+\mu_3)\Big(\frac{\epsilon r}{k}\bar{y}+\tau+\mu_1+\mu_3\Big)\\
&\quad+\mu_3(\tau+\mu_2)\Big(\frac{\epsilon r}{k}\bar{y}+\tau+\mu_1+\mu_3\Big)+\beta\tau\Big(\sigma\beta-\frac{\epsilon r}{k}\Big)\bar{x}\bar{y}\\
&= -\Big(\beta\bar{y}+\mu_1+\frac{\epsilon r}{k}\bar{y}\Big)(\beta\bar{y}+\mu_1+\mu_3)\Big(\frac{\epsilon r}{k}\bar{y}+\tau+\mu_1+\mu_3\Big)\\
&\quad-(\tau+\mu_2)(\beta\bar{y}+\mu_1)\Big(\frac{\epsilon r}{k}\bar{y}+\tau+\mu_1+\mu_3\Big)+\underbrace{\beta\tau\Big(\sigma\beta-\frac{\epsilon r}{k}\Big)\bar{x}\bar{y}}_{<0}\\
&< 0.
\end{aligned}
$$

Lastly, we consider the determinant of $J(\bar{P})$. We compute

$$
\begin{aligned}
&\det\big(J(\bar{P})\big)\\
&= \det\begin{bmatrix} -\beta\bar{y}-\mu_1 & 0 & -\beta\bar{x} \\ \big(\sigma\beta-\frac{\epsilon r}{k}\big)\bar{y} & -\frac{\epsilon r}{k}\bar{y}-\tau-\mu_2 & \sigma\beta\bar{x}+\epsilon r\big(1-\frac{\bar{x}+\bar{u}}{k}\big) \\ 0 & \tau & -\mu_3 \end{bmatrix}\\
&= \det\begin{bmatrix} -\beta\bar{y}-\mu_1 & 0 & -\beta\bar{x} \\ \big(\sigma\beta-\frac{\epsilon r}{k}\big)\bar{y} & -\frac{\epsilon r}{k}\bar{y}-\tau-\mu_2 & \frac{\mu_3}{\tau}(\tau+\mu_2) \\ 0 & \tau & -\mu_3 \end{bmatrix}\\
&= -(\beta\bar{y}+\mu_1)\Big[\tfrac{\epsilon r\mu_3}{k}\bar{y}+\cancel{\mu_3(\tau+\mu_2)}-\cancel{\mu_3(\tau+\mu_2)}\Big]-0-\beta\tau\bar{x}\big(\sigma\beta-\tfrac{\epsilon r}{k}\big)\bar{y}\\
&= -(\beta\bar{y}+\mu_1)\tfrac{\epsilon r\mu_3}{k}\bar{y}-\beta\tau\big(\sigma\beta-\tfrac{\epsilon r}{k}\big)\bar{x}\bar{y}\\
&= \bar{y}\Big[-\tfrac{\epsilon r\beta\mu_3}{k}\bar{y}-\tfrac{\epsilon r\mu_1\mu_3}{k}-\beta\tau\big(\sigma\beta-\tfrac{\epsilon r}{k}\big)\bar{x}\Big], \quad \text{replace } \bar{y} \text{ inside brackets,}\\
&= \bar{y}\Big[-\tfrac{\epsilon r\mu_1\mu_3}{k}-\tfrac{\epsilon r\beta\mu_3}{k}\tfrac{k\tau}{\epsilon r\mu_3}\Big[\big(\sigma\beta-\tfrac{\epsilon r}{k}\big)\bar{x}+\epsilon r-\tfrac{\mu_3}{\tau}(\tau+\mu_2)\Big]-\beta\tau\big(\sigma\beta-\tfrac{\epsilon r}{k}\big)\bar{x}\Big]\\
&= \tfrac{\epsilon r\mu_3}{k}\bar{y}\Big[\underbrace{-\mu_1}_{f_1'(\bar{x})}-\underbrace{\tfrac{k\beta\tau}{\epsilon r\mu_3}\Big[2\big(\sigma\beta-\tfrac{\epsilon r}{k}\big)\bar{x}+\epsilon r-\tfrac{\mu_3}{\tau}(\tau+\mu_2)\Big]}_{f_2'(\bar{x})}\Big]\\
&= \tfrac{\epsilon r\mu_3}{k}\bar{y}\Big[f_1'(\bar{x})-f_2'(\bar{x})\Big]\\
&\quad\begin{cases} <0 & \text{if } f_1'(\bar{x})-f_2'(\bar{x})<0, \text{ i.e. when } \bar{x}=x_1,\\ >0 & \text{if } f_1'(\bar{x})-f_2'(\bar{x})>0, \text{ i.e. when } \bar{x}=x_2. \end{cases}
\end{aligned}
$$

We see that $\det\big(J(\bar{P})\big)$ changes sign depending on the sign of $f_1'(\bar{x})-f_2'(\bar{x})$ and thus may be used to distinguish the stability properties in the case when two distinct endemic, or chronic infection, equilibria exist. When $R_0 > R_0(\sigma_0)$, or equivalently $\sigma > \sigma_0$, the endemic equilibrium P_1 exists in $\mathring{\Gamma}$ and $\det\big(J(P_1)\big) < 0$. Hence, the conditions of Lemma 3.4.1 hold and we may conclude that P_1 is locally asymptotically stable whenever it exists. When $R_0(\sigma_0) < R_0 < 1$, or equivalently $\sigma_0 < \sigma < \bar{\sigma}$, the endemic equilibrium P_2 is also found in $\mathring{\Gamma}$ but, as $\det\big(J(P_2)\big) > 0$, P_2 is unstable.

Next, we take a closer look at the unstable equilibrium P_2 in the case $R_0(\sigma_0) < R_0 < 1$ (i.e. when $\sigma_0 < \sigma < \bar{\sigma}$). Let ζ_1, ζ_2, ζ_3 be the eigenvalues of $J(P_2)$. Since $f_1'(x_2) - f_2'(x_2) > 0$, it has been shown above that

$$\operatorname{tr}(J(P_2)) = \zeta_1+\zeta_2+\zeta_3 < 0 \quad \text{and} \quad \det(J(P_2)) = \zeta_1\,\zeta_2\,\zeta_3 > 0.$$

As P_2 is unstable, at least one of its eigenvalues has positive real part. In fact, this eigenvalue is positive and real, which can be easily seen from the graph of the

characteristic polynomial of $J(P_2)$). Indeed, since

$$\chi_{P_2}(\zeta) = (\zeta-\zeta_1)(\zeta-\zeta_2)(\zeta-\zeta_3) = \zeta^3-(\zeta_1+\zeta_2+\zeta_3)\zeta^2+[\zeta_1\zeta_2+\zeta_3(\zeta_1+\zeta_2)]\zeta-\zeta_1\,\zeta_2\,\zeta_3,$$

it follows that $\chi_{P_2}(0) = -\zeta_1\,\zeta_2\,\zeta_3 < 0$ and thus the coefficient of ζ^3 being positive implies that at least one of the eigenvalues of $J(P_2)$, say ζ_1, is positive and real. Hence,

$$\zeta_1\,\zeta_2\,\zeta_3 > 0 \quad \Longrightarrow \quad \mathrm{Re}\,\zeta_2, \mathrm{Re}\,\zeta_3 \text{ have the same sign,}$$

while

$$\zeta_1 + \zeta_2 + \zeta_3 < 0 \quad \Longrightarrow \quad \mathrm{Re}\,\zeta_2, \mathrm{Re}\,\zeta_3 < 0.$$

Therefore, $\dim W^s_{loc}(P_2) = 2$. □

3.5 Backward Bifurcation

The local stability analysis in the preceding section indicates the existence of a backward bifurcation leading to a region of bi-stability under Assumptions (A1)–A4); that is, there is an open range of the parameter σ, namely $\sigma_0 < \sigma < \bar{\sigma}$, such that the infection-free equilibrium and an endemic, or chronic infection, equilibrium co-exist and are both locally asymptotically stable. The bifurcation diagram is shown in Figure 3.2. Backward bifurcation is known to occur in epidemic models with

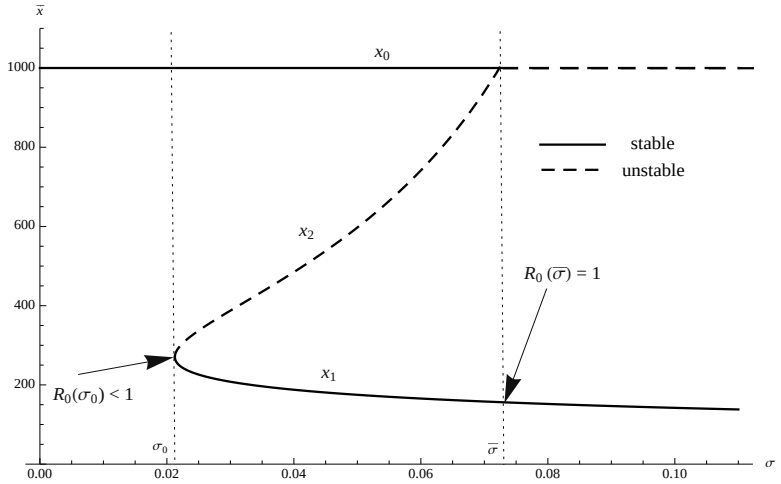

Figure 3.2: Backward bifurcation and bi-stability of equilibria with respect to the parameter σ. Parameter values are realistic for HTLV-I infection and are selected in biologically relevant ranges as in Table 5.1: $\lambda = 20$, $\beta = 0.001$, $\epsilon = 0.9$, $\tau = 0.01$, $r = 0.15$, $k = 1150$, $\mu_1 = 0.02$, $\mu_2 = 0.02$, $\mu_3 = 0.03$.

vaccination [1, 14]. Gómez and Li have also investigated backward bifurcation in a model for HTLV-I infection in [22], suggesting that such a phenomenon is intrinsic to the dynamics of HTLV-I. The biological implications of a backward bifurcation with respect to viral infection is discussed at the end of Chapter 4. Challenges to effective treatment strategies to HTLV-I infection arising from a backward bifurcation are examined in [22], and new insights for the treatment of HTLV-I infection arising from our model is discussed in Chapter 5.

Chapter 4

Global Dynamics

In this chapter, we examine more thoroughly the dynamics of model (2.3). Because of the high dimension of our model, along with the complicated phenomenon of a backward bifurcation, establishing the global behaviour of solutions is a non-trivial mathematical task. We begin by introducing several preliminary definitions and notation that will be used throughout this chapter. It will be shown that model (2.3) is cooperative in Γ. Roughly speaking, a cooperative system is one in which the generated flow preserves a partial ordering in forward time. We state important results from the theory of monotone dynamical systems and the theory of compound differential systems that will aid us in our pursuit. Following this, we present our main theoretical results, which completely characterize the global behaviour of solutions of our mathematical model both in the presence and absence of bi-stability.

Our methodology follows the geometric approach to global stability developed by Li and Muldowney [30], which has been applied to epidemiological models without backward bifurcation [28, 29, 31]. Due to the presence of bi-stability in our system of differential equations, however, we will need to adapt this approach. The main idea remains the same. It is to rule out the existence of simple, closed, rectifiable, invariant curves in $\bar{\Gamma}$ and to show that the ω-limit set of each trajectory consists of a single equilibrium.

4.1 Definitions and Notation

Here we present some notation and define several important notions of stability for equilibria and periodic trajectories that will be used in Sections 4.2 and 4.3.

Let $f : D \to \mathbb{R}^n$ be a continuously differentiable function defined on an open set

$D \subset \mathbb{R}^n$ and consider the autonomous system of ordinary differential equations

$$x' = f(x), \quad x \in D. \tag{4.1}$$

Denote by $\phi_t(x_0)$ the unique solution $x(t)$ of system (4.1) with initial value $x(0) = x_0 \in D$, $\gamma(x_0) = \{\phi_t(x_0) \in \mathbb{R}^n : t \in \mathbb{R}\}$ the orbit or trajectory through x_0, and $\omega(x_0) = \{\bar{x} \in \mathbb{R}^n : \exists$ a sequence $\{t_n\}, t_n \nearrow +\infty$ such that $\phi_{t_n}(x_0) \to \bar{x}\}$ the omega-limit set of x_0. If P is a hyperbolic equilibrium, use $W^s(P)$ and $W^u(P)$ to denote the respective stable and unstable manifolds of P.

An equilibrium point $\bar{x}$ of system (4.1) satisfies $f(\bar{x}) = 0$. The equilibrium $\bar{x}$ is said to be *stable* if for every $\epsilon > 0$, there exists $\delta = \delta(\epsilon) > 0$ such that for each x_0, $|x_0 - \bar{x}| < \delta$ implies $|\phi_t(x_0) - \bar{x}| < \epsilon$ for all $t > 0$. It is *asymptotically stable* if, in addition, $|\phi_t(x_0)| \to \bar{x}$ as $t \to \infty$.

Suppose system (4.1) has a periodic solution $p(t)$ with least period $\omega > 0$ and trajectory $\gamma = \{p(t) : 0 \le t \le \omega\}$. Then γ is said to be *orbitally stable* if for every $\epsilon > 0$, there exists $\delta > 0$ such that for each x_0, $|x_0 - p(0)| < \delta$ implies $d\big(\phi_t(x_0), \gamma\big) < \epsilon$ for all $t > 0$, where $d(x, \gamma) = \min_{y \in \gamma} |x - y|$ is the distance from the point x to the orbit γ. The trajectory γ is said to be *orbitally asymptotically stable (o. a. s.)* if, in addition, $d\big(\phi_t(x_0), \gamma\big) \to 0$ as $t \to \infty$. Lastly, γ is *orbitally asymptotically stable with asymptotic phase (o. a. s. w. a. p.)* if it is orbitally stable and there is a $\delta_0 > 0$ such that for each x_0 with $d(x_0, \gamma) \le \delta_0$, there exists $\tau(x_0)$, called the asymptotic phase of x_0, such that $|\phi_t(x_0) - p(t - \tau(x_0))| \to 0$ as $t \to \infty$.

4.2 Cooperative Systems

In this section, we present several important results from the theory of cooperative and competitive systems which will be used to study the global behaviour of our mathematical model (2.3).

An orthant K of $\mathbb{R}^n$,

$$K = \{x \in \mathbb{R}^n : (-1)^{m_i} x_i \ge 0, 1 \le i \le n\}, \quad \text{where} \quad m_i \in \{0, 1\},$$

generates a partial ordering $\le_K$ in $\mathbb{R}^n$ given by

$$x \le_K y \quad \text{iff} \quad y - x \in K, \quad \text{and} \quad x <_K y \quad \text{iff} \quad y - x \in \mathring{K}.$$

The flow of (4.1) is said to be K-*monotone* or to *preserve* $\le_K$ if for each $x, y \in D$ with $x \le_K y$, then $\phi_t(x) \le_K \phi_t(y)$ for all $t \ge 0$ for which both $\phi_t(x)$ and $\phi_t(y)$ are defined. A slightly stronger form of K-monotonicity may be satisfied by the

flow. Specifically, ϕ is called *strongly order preserving*, or *SOP* for short, if it is K-monotone and for each $x, y \in D$ with $x <_K y$, there exist open subsets U, V of D, where $x \in U$, $y \in V$, and $t_0 > 0$ such that $\phi_{t_0}(U) \leq_K \phi_{t_0}(V)$. Note that K-monotonicity implies in this case that $\phi_t(U) \leq_K \phi_t(V)$ for all $t \geq t_0$. In the case when the Jacobian matrix $\frac{\partial f}{\partial x}(x)$ of system (4.1) is irreducible, the flow ϕ is SOP [48, 49]. Recall that an $n \times n$ matrix is *irreducible* if it cannot be written in the form

$$\left[\begin{array}{c|c} A & B \\ \hline 0 & C \end{array}\right],$$

where A and C are square matrices, by any re-ordering of the standard basis in $\mathbb{R}^n$.

For $x \in D$, we say that x can be *approximated from below* if there is a sequence $\{x_n\}_{n=1}^{\infty}$ in D satisfying $x_n <_K x_{n+1} <_K x$ for $n \geq 1$, and $x_n \to x$ as $n \to \infty$. Similarly, x can be *approximated from above* if there is a sequence $\{x_n\}_{n=1}^{\infty}$ in D satisfying $x <_K x_{n+1} <_K x_n$ for $n \geq 1$, and $x_n \to x$ as $n \to \infty$.

If D is convex and the flow of system (4.1) preserves the partial ordering $\leq_K$ for $t \geq 0$, then system (4.1) is called *cooperative* or *type K-monotone*. It is called *competitive* if the partial ordering is preserved for $t \leq 0$. When the orthant K has been identified, it is customary to drop the subscript K in the partial order relations, e.g. one may write '$\leq$' instead of '$\leq_K$'. An equivalent characterization of cooperative and competitive systems in terms of the Jacobian matrix, $\frac{\partial f}{\partial x}(x)$, is given in Lemma 4.2.1 below. For small values of n, it provides a simple way to identify whether the system (4.1) is cooperative or competitive in a convex domain D. The proof may be found in [48].

Lemma 4.2.1 (Lemma 2.1, Smith (1988))**.** *Let $D \subset \mathbb{R}^n$ be convex. The autonomous system of ordinary differential equations (4.1) is* cooperative *in D if there exists a diagonal matrix $P = \mathrm{diag}(\alpha_1, \ldots, \alpha_n)$, where each $\alpha_i \in \{-1, 1\}$ for $i = 1, \ldots, n$, such that*

$$P\frac{\partial f_i}{\partial x_j}(x)P \geq 0, \quad \textit{for} \quad i \neq j, x \in D,$$

i.e. all off-diagonal entries of $P\frac{\partial f}{\partial x}(x)P$ are non-negative. It is competitive *in D if there exists a diagonal matrix $P = \mathrm{diag}(\alpha_1, \ldots, \alpha_n)$, where each $\alpha_i \in \{-1, 1\}$ for $i = 1, \ldots, n$, such that*

$$P\frac{\partial f_i}{\partial x_j}(x)P \leq 0, \quad \textit{for} \quad i \neq j, x \in D,$$

i.e. all off-diagonal entries of $P\frac{\partial f}{\partial x}(x)P$ are non-positive.

Remark 4.2.1. Informally, system (4.1) is cooperative if it generates a monotone semi-flow in forward time, while it is competitive if the time-reversed flow is cooperative. That is, a competitive system is one in which a monotone semi-flow is generated in backward time.

Proposition 4.2.1. *Model (2.3) is cooperative in* Γ *and irreducible in* $\mathring{\Gamma}$*. Therefore, in* $\mathring{\Gamma}$ *the flow is SOP.*

Proof. The Jacobian matrix for model (2.3) is

$$J(x,u,y) = \begin{bmatrix} -\beta y - \mu_1 & 0 & -\beta x \\ \left(\sigma\beta - \frac{\epsilon r}{k}\right) y & -\frac{\epsilon r}{k} y - \tau - \mu_2 & \sigma\beta x + \epsilon r\left(1 - \frac{x+u}{k}\right) \\ 0 & \tau & -\mu_3 \end{bmatrix}.$$

Choose $P = \mathrm{diag}(-1,1,1)$ and apply Lemma 4.2.1. Then it is readily seen that model (2.3) is cooperative in the convex region Γ with respect to the partial ordering defined by the orthant

$$K = \{(x,u,y) \in \mathbb{R}^3 : x \leq 0, u \geq 0, y \geq 0\}.$$

Moreover, the Jacobian is irreducible if $y > 0$, namely for (x,u,y) in $\mathring{\Gamma}$. Thus, the flow of model (2.3) is SOP in $\mathring{\Gamma}$. □

The following important results about cooperative and competitive systems will be useful. For a more complete discussion and a survey of results on cooperative and competitive systems, we refer the reader to [24], [48], and [49]. The first result resolves the issue of global convergence in the case where only one equilibrium exists in the region D. In the remainder of this section, we assume that the set D is convex, the flow on system (4.1) is SOP, and the following compactness condition holds.

(C1) For each $x_0 \in D$, the orbit $\gamma(x_0)$ has compact closure in D. Furthermore, if the sequence $\{x_n\}_{n\geq 1}$ approximates x_0 from below or from above, then $\cup_{n\geq 0}\omega(x_n)$ has compact closure contained in D.

Theorem 4.2.1 (Theorem 3.1, Smith (1995))**.** *Suppose that* D *contains exactly one equilibrium* e *and that every point of* $D \setminus e$ *can be approximated from above and from below in* D*. Then* $\omega(x) = e$ *for all* $x \in D$*.*

Theorem 4.2.2 (Theorem 2.1, Hirsch (1982); Theorem 2.2, Smith (1995))**.** *A cooperative system cannot have an attracting periodic orbit nor can any two points of a compact limit set be related by* $<_K$*.*

Remark 4.2.2. Observe that for two-dimensional cooperative systems, Theorem 4.2.2 precludes the existence of periodic orbits since any closed Jordan curve in $\mathbb{R}^2$ necessarily contains two points related by $<_K$.

Meanwhile, three-dimensional cooperative and competitive systems are known to possess the Poincaré-Bendixson property:

Theorem 4.2.3 (Theorem 4.1, Hirsch (1982); Theorem 4.1, Smith (1995))**.** *A compact limit set of a cooperative or competitive system in $\mathbb{R}^3$ that contains no equilibria is a periodic orbit.*

In particular, Theorem 4.2.2 and Theorem 4.2.3 imply that the ω-limit set of a trajectory of a cooperative system must either

i) contain a finite number of equilibrium points unrelated by $<_K$, or

ii) be an unstable (non-attracting) closed orbit.

One last required result for cooperative, or type K-monotone, systems concerns the existence of heteroclinic trajectories connecting equilibria in the case where an unstable steady state is present. The theorem states that, in general, a steady state of system (4.1) is either asymptotically stable, or it is a saddle and there exist two distinct asymptotically stable steady states that are each connected to the saddle by a monotone heteroclinic orbit of system (4.1) [48]. A proof of this result for smooth mappings on Banach spaces may be found in [47] and that of its translation to flows in [48].

Theorem 4.2.4 (Theorem 2.8, Smith (1988))**.** *Let $D \subset \mathbb{R}^n$ be convex, suppose system (4.1) is type K-monotone, and let f have a locally Lipschitzian derivative in D. Suppose $f(x_0) = 0$, $s_0 = s\Big(\frac{\partial f}{\partial x}(x_0)\Big) > 0$ is a simple eigenvalue of $\frac{\partial f}{\partial x}(x_0)$ with corresponding eigenvector $v \geq_K 0$, and $x_0 + K$ is contained in D. Then, there exists a unique C^1 function $y : [0, \infty) \to x_0 + K$ with the following properties:*

i) $y(r) = x_0 + rv + o(r)$ *as* $r \to 0$,

ii) $\phi_t(y(r)) = y\big(e^{s_0 t} r\big), t \in \mathbb{R}, r \geq 0$,

iii) $0 \leq r_1 \leq r_2$ *implies* $y(r_1) \leq_K y(r_2)$,

iv) Either $\lim_{r\to\infty} \|y(r)\| = \infty$ *or* $\lim_{r\to\infty} y(r) = x_1$, *where* $x_1 \geq_K x_0$ *and* $f(x_1) = 0$. *If* $x_1 >_K x_0$, *then* $s\Big(\frac{\partial f}{\partial x}(x_1)\Big) \leq 0$. *If* $\frac{\partial f}{\partial x}(x_1)$ *is irreducible and* $s_1 = s\Big(\frac{\partial f}{\partial x}(x_1)\Big)$ *with corresponding eigenvector* $w \geq_K 0$, *then* $\lim_{r\to\infty} \big(y'(r)/\|y'(r)\|\big) = w$.

v) If $\lim_{r\to\infty} \|y(r)\| = \infty$, *then* $\|\phi_t(x)\| \to \infty$ *as* $t \to \infty$ *for all* $x \geq_K x_0$, $x \neq x_0$. *If* $\lim_{r\to\infty} y(r) = x_1$, *then* $\phi_t(x) \to x_1$ *for all* x *with* $x_0 \leq_K x \leq_K x_1$, $x \neq x_0$.

4.3 Compound Systems and Stability

In this section, we define the so-called k-th compound system of the general non-linear autonomous system (4.1) and state an important theorem due to Muldowney [40] that describes the behaviour of closed orbits of system (4.1). This result will be applied to our three dimensional model (2.3) to rule out the existence of periodic trajectories in Γ.

Definition 4.3.1. The *k-th compound system* associated to the non-linear autonomous system of ordinary differential equations (4.1) is a system of linear equations

$$z' = \frac{\partial f}{\partial x}^{[2]} z, \tag{4.2}$$

where $\frac{\partial f}{\partial x}^{[2]}$ is the second additive compound matrix of the Jacobian matrix, $\frac{\partial f}{\partial x}$, of f (see Appendix B.1).

The following result, proved by Muldowney [40], describes a sufficient condition for non-constant periodic trajectories of the autonomous system (4.1) to be o. a. s. w. a. p.

Theorem 4.3.1 (Theorem 4.2, Muldowney (1990))**.** *A non-constant periodic solution $x = p(t)$ of system (4.1) is orbitally asymptotically stable with asymptotic phase if the linear second compound system*

$$z'(t) = \frac{\partial f}{\partial x}^{[2]} \big(p(t)\big) z(t)$$

is asymptotically stable.

As a consequence of the above theorem (see Corollary 4.3 from [40]), to show the asymptotic stability of the second compound matrix $\frac{\partial f}{\partial x}^{[2]}$ along a periodic solution $p(t)$ with least period $\omega > 0$, it is enough to show that for some Lozinskiĭ measure μ on $\binom{n}{2} \times \binom{n}{2}$ matrices,

$$\int_0^\omega \mu\left(\frac{\partial f}{\partial x}^{[2]} \big(p(t)\big)\right) dt < 0. \tag{4.3}$$

Condition (4.3) may be generalized to provide greater freedom in determining the stability of the second compound system (4.2) and leads to an alternative formulation of Theorem 4.3.1. In particular, let $A = A(x)$ be an invertible $\binom{n}{2} \times \binom{n}{2}$ matrix satisfying $|A(x)| \leq M$, $|A^{-1}(x)| \leq M$ for some $M > 0$, and consider

$w(t) = A\big(x(t)\big)z(t)$. By direct differentiation, one can show that $w(t)$ satisfies the differential equation

$$w'(t) = B(t)w(t) \tag{4.4}$$

where $B = A_f A^{-1} + A\frac{\partial f}{\partial x}^{[2]} A^{-1}$ and $A_f = (DA) \bullet f$ or equivalently, A_f denotes the matrix obtained by replacing each entry a_{ij} in A with its directional derivative in the direction of the vector field f. A similar argument shows that if

$$\int_0^\omega \mu\left(A_f A^{-1} + A\frac{\partial f}{\partial x}^{[2]} A^{-1} \right) dt < 0, \tag{4.5}$$

then $|w(t)| = \big|A\big(x(t)\big)z(t)\big| \to 0$ as $t \to \infty$. This implies that $|z(t)| \to 0$ as $t \to \infty$. Therefore, under the more flexible condition (4.5), we obtain the same result as in Theorem 4.3.1, namely, any non-constant periodic solution of the non-linear autonomous system (4.1) is orbitally asymptotically stable with asymptotic phase.

4.4 Theoretical Results

We now present our main theoretical results. The first result establishes the global asymptotic stability of the infection-free equilibrium P_0 when P_0 is the only equilibrium in $\bar{\Gamma}$ using the theory of monotone flows and cooperative systems.

Theorem 4.4.1 (Global Stability when P_0 is the only Equilibrium in Γ)**.** *When $0 < R_0 < R_0(\sigma_0)$ (equivalently, $0 < \sigma < \sigma_0$), the infection-free equilibrium P_0 is the only equilibrium in $\bar{\Gamma}$ and it is globally asymptotically stable.*

Proof. The set $\mathring{\Gamma} \cup \{P_0\}$ is convex and positively invariant, and contains a unique equilibrium P_0. Applying Proposition 4.2.1 and Theorem 4.2.1 in $\mathring{\Gamma} \cup \{P_0\}$ establishes the global stability of P_0 in the interior $\mathring{\Gamma}$ of Γ. On the boundary of Γ, the direction of the vector field for model (2.3) indicates that solutions starting on $\partial\Gamma$ either enter $\mathring{\Gamma}$ and subsequently converge to P_0, or remain on the positively invariant x-axis and converge to P_0 along the x-axis. This establishes the global stability of P_0 in the closure $\bar{\Gamma}$ of Γ. □

A similar argument may be used to establish the global asymptotic stability when a unique endemic, or chronic infection, equilibrium exists in the interior $\mathring{\Gamma}$ of Γ. Thus, we have the following result.

Theorem 4.4.2 (Global Stability of Unique Endemic Equilibrium when $R_0 > 1$)**.** *Assume $R_0 > 1$. Then, model (2.3) is uniformly persistent in Γ and there exists a unique endemic equilibrium P_1 that is globally asymptotically stable in $\mathring{\Gamma}$.*

Remark 4.4.1. It should be noted that if $R_0(\sigma_0) = 1$, backward bifurcation and bi-stability do not occur and the standard forward bifurcation is observed. In this case, Theorem 4.4.1 and Theorem 4.4.2 together establish the global behaviour of solutions to model (2.3), and the basic reproduction number for viral infection R_0 acts as a sharp threshold parameter completely characterizing the global dynamics of model (2.3).

Next, we establish the global dynamics when backward bifurcation occurs. Because of multi-stability, the proof for Theorems 4.4.1 and 4.4.2 does not apply. We demonstrate that every trajectory in Γ converges to a single equilibrium. Since model (2.3) is cooperative in Γ, it may admit unstable periodic trajectories when multiple equilibria exist in $\mathring{\Gamma}$. Using Theorem 4.3.1, it will be shown that under a mild biologically reasonable assumption, any non-constant periodic solution of model (2.3), if it exists, is orbitally asymptotically stable with asymptotic phase. Therefore, we conclude that model (2.3) cannot have non-constant periodic orbits in Γ.

Theorem 4.4.3 (Non-existence of Closed Orbits in Γ)**.** *There cannot exist any non-constant periodic solutions of model (2.3) in* Γ *provided*

$$\frac{\epsilon r}{k} < 2\sigma\beta. \tag{B1}$$

Remark 4.4.2. Assumptions (A2) and (B1) provide a range for σ for which bi-stability may occur. A biologically relevant interpretation of Assumption (B1) is that both infectious and mitotic transmission of HTLV-I are important for the infection and occur on the same order of magnitude.

Proof of Theorem 4.4.3. Assume condition (B1) holds. Let $p(t) = (x(t), u(t), y(t))$ be a non-constant periodic solution of model (2.3) with least period $\omega > 0$ and let $\gamma = \{p(t) : 0 \leq t < \omega\}$ be its orbit. Consider the 3×3 non-constant invertible matrix

$$A = A(x(t), u(t), y(t)) = \begin{bmatrix} 1 & 0 & 0 \\ 0 & \frac{u(t)}{y(t)} & 0 \\ 0 & 0 & \frac{1}{\sigma}\frac{u(t)}{y(t)} \end{bmatrix}.$$

Since $A = \operatorname{diag}\big(1, \frac{u}{y}, \frac{1}{\sigma}\frac{u}{y}\big)$, then $A^{-1} = \operatorname{diag}\big(1, \frac{y}{u}, \sigma\frac{y}{u}\big)$, hence

$$A_f A^{-1} = \begin{bmatrix} 0 & 0 & 0 \\ 0 & \frac{u}{y}\big(\frac{u'}{u} - \frac{y'}{y}\big) & 0 \\ 0 & 0 & \frac{1}{\sigma}\frac{u}{y}\big(\frac{u'}{u} - \frac{y'}{y}\big) \end{bmatrix} \begin{bmatrix} 1 & 0 & 0 \\ 0 & \frac{y}{u} & 0 \\ 0 & 0 & \sigma\frac{y}{u} \end{bmatrix} = \begin{bmatrix} 0 & 0 & 0 \\ 0 & \frac{u'}{u} - \frac{y'}{y} & 0 \\ 0 & 0 & \frac{u'}{u} - \frac{y'}{y} \end{bmatrix}.$$

Next, compute $AJ^{[2]}A^{-1}$. Note that this amounts to multiplying the second and third rows of $J^{[2]}$ by $\frac{u}{y}$, $\frac{1}{\sigma}\frac{u}{y}$, and the second and third columns by $\frac{y}{u}$, $\sigma\frac{y}{u}$, respectively. We obtain

$$AJ^{[2]}A^{-1} = \begin{bmatrix} -\beta y - \mu_1 - \frac{\epsilon r}{k}y - \tau - \mu_2 & \left[\sigma\beta x + \epsilon r\left(1 - \frac{x+u}{k}\right)\right]\frac{y}{u} & \sigma\beta\frac{xy}{u} \\ \tau\frac{u}{y} & -\beta y - \mu_1 - \mu_3 & 0 \\ 0 & \frac{1}{\sigma}\left(\sigma\beta - \frac{\epsilon r}{k}\right)y & -\frac{\epsilon r}{k}y - \tau - \mu_2 - \mu_3 \end{bmatrix}.$$

Let $B = A_f A^{-1} + AJ^{[2]}A^{-1}$. We write B as a block matrix

$$B = \left[\begin{array}{c|c} B_{11} & B_{12} \\ \hline B_{21} & B_{22} \end{array}\right],$$

where

$$\begin{aligned} B_{11} &= -\beta y - \mu_1 - \frac{\epsilon r}{k}y - \tau - \mu_2, \\ B_{12} &= \left[\left[\sigma\beta x + \epsilon r\left(1 - \tfrac{x+u}{k}\right)\right]\tfrac{y}{u} \quad \sigma\beta\tfrac{xy}{u}\right], \\ B_{21} &= \begin{bmatrix} \tau\frac{u}{y} \\ 0 \end{bmatrix}, \\ B_{22} &= \begin{bmatrix} \frac{u'}{u} - \frac{y'}{y} - \beta y - \mu_1 - \mu_3 & 0 \\ \frac{1}{\sigma}\left(\sigma\beta - \frac{\epsilon r}{k}\right)y & \frac{u'}{u} - \frac{y'}{y} - \frac{\epsilon r}{k}y - \tau - \mu_2 - \mu_3 \end{bmatrix}. \end{aligned}$$

Select a vector norm $|\cdot|$ on $\mathbb{R}^3 \cong \mathbb{R}^{\binom{3}{2}}$ as

$$|(v_1, v_2, v_3)| := \max\{|v_1|, |v_2| + |v_3|\}, \quad \text{for} \quad (v_1, v_2, v_3) \in \mathbb{R}^3, \tag{4.6}$$

i.e. Let $z = (v, w) = (v_1, (v_2, v_3)) \in \mathbb{R} \times \mathbb{R}^2$ and define $|z| := \max\{|v|_1, |w|_1\}$, where $|\cdot|_1$ denotes the standard ℓ_1-norm on Euclidean space.

Let $|\cdot|$ also denote the induced matrix norm and let $\mu(\cdot)$ denote the Lozinskiĭ measure associated to $|\cdot|$ (see Appendix B.2 for more details on the Lozinskiĭ measure, also known as the logarithmic norm). Then,

$$\mu(B) \leq \sup\{g_1, g_2\}, \tag{4.7}$$

where

$$g_1 = \mu_1(B_{11}) + |B_{12}| \quad \text{and} \quad g_2 = |B_{21}| + \mu_1(B_{22}). \tag{4.8}$$

For the full derivation of relation (4.7), see Appendix A.3. We determine

$$\begin{aligned}
\mu_1(B_{11}) &= -\beta y - \mu_1 - \frac{\epsilon r}{k} y - \tau - \mu_2 < 0,\\
|B_{12}| &= \left[\sigma\beta x + \epsilon r\left(1 - \frac{x+u}{k}\right)\right]\frac{y}{u} = \frac{u'}{u} + \tau + \mu_2,\\
|B_{21}| &= \tau\frac{u}{y} = \frac{y'}{y} + \mu_3,\\
\mu_1(B_{22}) &= \frac{u'}{u} - \frac{y'}{y} - \mu_3 + \max\left\{-\mu_1 - \frac{1}{\sigma}\Big(2\sigma\beta - \frac{\epsilon r}{k}\Big)y, -\frac{\epsilon r}{k}y - \tau - \mu_2\right\}.
\end{aligned}$$

Note that the quantity $\big(2\sigma\beta - \frac{\epsilon r}{k}\big) > 0$ under Assumption (B1). Then,

$$g_1 = \frac{u'}{u} - \beta y - \mu_1 - \frac{\epsilon r}{k} y \le \frac{u'}{u} - \mu_1,$$

and

$$\begin{aligned}
g_2 &= \frac{u'}{u} + \max\left\{-\mu_1 - \frac{1}{\sigma}\Big(2\sigma\beta - \frac{\epsilon r}{k}\Big)y, -\frac{\epsilon r}{k}y - \tau - \mu_2\right\}\\
&\le \frac{u'}{u} + \max\{-\mu_1, -\tau - \mu_2\}.
\end{aligned}$$

Hence,

$$\mu(B) = \mu\Big(A_f A^{-1} + A J^{[2]} A^{-1}\Big) \le \frac{u'}{u} - \bar{b},$$

where $\bar{b} = \min\{\mu_1, \tau + \mu_2\} > 0$.

Next, integrate $\mu(B)$ over one period ω to obtain

$$\begin{aligned}
\int_0^\omega \mu(B)\, ds &\le \int_0^\omega \left(\frac{u'(s)}{u(s)} - \bar{b}\right) ds\\
&= \log u(s)\Big|_{s=0}^{\omega} - \bar{b}s\Big|_{s=0}^{\omega}\\
&= \big[\log u(\omega) - \log u(0)\big] - \bar{b}(\omega - 0)\\
&= \log\frac{u(\omega)}{u(0)} - \bar{b}\omega\\
&= \log 1 - \bar{b}\omega, \qquad \text{since } u(\omega) = u(0),\\
&= -\bar{b}\omega\\
&< 0 \quad \text{for all } t > 0.
\end{aligned}$$

Thus, the second compound matrix $J^{[2]}\big(p(t)\big)$ is asymptotically stable. It follows from Theorem 4.3.1 that the non-constant periodic orbit $p(t)$ is orbitally asymptotically stable with asymptotic phase. Since model (2.3) is cooperative in Γ (by

Proposition 4.2.1), Theorem 4.2.2 states that any closed orbits must be unstable (non-attracting). This contradiction precludes the existence of periodic trajectories in the feasible region Γ provided Assumption (B1) holds. $\square$

To study the global behaviour of trajectories in the case when $R_0 < 1$ and bi-stability occurs, we require the so-called Butler-McGehee Lemma. A proof may be found in [16] or [20] and a generalization in [19]. For a general non-linear autonomous system of ordinary differential equations (4.1), recall that we use the following notation: Denote by $\gamma(x_0)$ the orbit through a point $x_0 \in D$ and $\omega(x_0)$ the omega limit set of the orbit $\gamma(x_0)$. If P is a hyperbolic equilibrium, then use $W^s(P)$ and $W^u(P)$ to denote the respective stable and unstable manifolds of P.

Lemma 4.4.1 (Butler-McGehee: Lemma A1, Freedman and Waltman (1984); Lemma 2.1, Butler and Waltman (1986))**.** *Let P be an isolated hyperbolic equilibrium of the non-linear autonomous system (4.1) and let $x_0 \in D$ be a point. Suppose $P \in \omega(x_0)$. Then, either*

i) $\omega(x_0) = P$, *or*

ii) $\exists$ *points* $Q_1, Q_2 \in \omega(x_0)$, *different from* P, *such that* $Q_1 \in W^s(P)$ *and* $Q_2 \in W^u(P)$.

Theorem 4.4.4 (Global Dynamics when Bi-stability Occurs)**.** *Assume (A1)–(A4) hold. When $R_0(\sigma_0) < R_0 < 1$ (equivalently, $\sigma_0 < \sigma < \bar{\sigma}$), there exist three equilibria in $\bar{\Gamma}$: the infection-free equilibrium P_0 on the boundary $\partial\Gamma$, along with two distinct endemic, or chronic infection, equilibria P_1 and P_2 in the interior $\mathring{\Gamma}$. Under condition (B1), both P_0 and P_1 are attractors whose basins of attraction are separated by the two-dimensional stable manifold of the saddle point P_2.*

Proof. We need to show that the ω-limit set of any trajectory in $\mathring{\Gamma}$ consists of a single equilibrium. Since model (2.3) is cooperative, there are only two possibilities for the structure of its ω-limit sets. In particular, for a trajectory starting from $y_0 \in \mathring{\Gamma}$, either (i) $\omega(y_0)$ contains an equilibrium, or (ii) $\omega(y_0)$ is a non-attracting periodic orbit. Due to the non-existence of closed orbits in Γ proved in Theorem 4.4.3, it follows that every compact ω-limit set must contain an equilibrium.

If $P_0 \in \omega(y_0)$, then $\omega(y_0) = \{P_0\}$ since P_0 is locally asymptotically stable. Similarly, $P_1 \in \omega(y_0)$ implies $\omega(y_0) = \{P_1\}$.

Suppose that $P_2 \in \omega(y_0)$ and $\omega(y_0) \neq \{P_2\}$. Then, by the Butler-McGehee Lemma (Lemma 4.4.1), $\omega(y_0)$ contains points on the unstable manifold $W^u(P_2)$ of P_2. Since $W^u(P_2)$ is 1-dimensional, it must be a heteroclinic orbit connecting P_2 with P_0 or P_1 (Theorem 4.2.4). Since $W^u(P_2)$ and $\omega(y_0)$ are invariant and $\omega(y_0)$ is

compact, $\overline{W^u(P_2)} \subset \omega(y_0)$, and thus $\omega(y_0)$ contains either P_0 or P_1, contradicting the asymptotic stability of P_0 or P_1. Therefore, $\omega(y_0) = \{P_2\}$. □

4.5 Summary and Significance of Theoretical Results

We conclude this chapter by summarizing the existence and stability of possible equilibria of our mathematical model for HTLV-I infection and providing intuitive biological interpretations of the results in terms of case studies of individuals. Our main theoretical results, which characterize the global behaviour of solutions to model (2.3) both in the absence and presence of bi-stability, are stated below.

Theorem 4.5.1 (Global Dynamics in the Absence of Bi-stability)**.** *Assume that* $R_0(\sigma_0) = 1$.

i) When $R_0 < 1$*, the infection-free equilibrium* P_0 *is globally asymptotically stable in* $\bar{\Gamma}$*;*

ii) When $R_0 > 1$*, there exists a unique endemic equilibrium* P_1 *that is globally asymptotically stable in* $\mathring{\Gamma}$*.*

Theorem 4.5.2 (Global Dynamics in the Presence of Bi-stability)**.** *Assume (A1)–(A4) are satisfied.*

i) When $0 < R_0 < R_0(\sigma_0)$*, the infection-free equilibrium* P_0 *is globally asymptotically stable in* $\bar{\Gamma}$*;*

ii) When $R_0(\sigma_0) < R_0 < R_0(\bar{\sigma}) = 1$*, backward bifurcation and bi-stability occur: both* P_0 *and the endemic equilibrium* P_1 *are attractors in* $\bar{\Gamma}$*. A second endemic equilibrium* P_2 *exists and is a saddle whose stable manifold has dimension 2.*

Under the additional assumption (B1), every trajectory in $\mathring{\Gamma}$ *converges to a single equilibrium and the two-dimensional stable manifold of* P_2 *separates the basins of attraction of* P_0 *and* P_1 *in* $\mathring{\Gamma}$*;*

iii) When $R_0 > 1$*, a unique endemic equilibrium* P_1 *exists and is globally asymptotically stable in* $\mathring{\Gamma}$*.*

The simulations in Figures 4.1 and 4.2 are meant to illustrate the main theoretical results stated above and are accompanied by relevant biological interpretations for each of the cases in Theorem 4.5.2. We remark that the two cases in Theorem 4.5.1 correspond respectively to the first and third cases of Theorem 4.5.2. These demonstrations agree with the observations of HTLV-I infection by Gómez-Acevedo and Li [22]. The graphs plot $CD4^+$ helper T-cell counts in units of cells per mm^3 for

each compartment of model (2.3) on the vertical axis against time t in days on the horizontal axis for a given individual with a specified R_0. The basic reproduction number R_0 depends on parameters whose values are influenced by intrinsic factors that are unique to each individual (see Section 5.2). The level of healthy target cells $x(t)$ is shown in blue, that of latently infected target cells $u(t)$ in green, and actively infected target cells $y(t)$ in red. Parameter values are realistic for HTLV-I infection and are chosen from Table 5.1 in Chapter 5. Note that the normal $CD4^+$ helper T-cell count in a healthy individual is approximately 1000 cells per mm^3, although normal cell counts may vary from 500 to 1600 cells per mm^3 of peripheral blood.[1] The normal $CD4^+$ helper T-cell count is precisely the level of healthy $CD4^+$ T-cells in an individual in the absence of infection, which we have denoted by x_0. The initial viral dosage at the onset of infection will be given in terms of a percentage of this average. For example, if the initial viral dosage is stated to be 5% $CD4^+$, then it means at the beginning of the infection, 5% $\times$ (1000 cells per mm^3) = 50 cells per mm^3 are infected and introduced into the peripheral blood.

4.5.1 Strong Immune System Clears Infection

Suppose that Person A is an individual whose value of R_0 satisfies $0 < R_0 < R_0(\sigma_0)$ so that the first case of Theorem 4.5.2 holds. This corresponds to Case (i) of Theorem 4.5.1 when $R_0 < 1$ and bi-stability does not occur. An interpretation of the result is that Person A elicits a strong immune response against the specific virus strain that has invaded him or her. As shown in Figure 4.1(a), the number of healthy target cells initially drops down to a low level, but recovers to the normal $CD4^+$ helper T-cell count of 1000 cells per mm^3. Meanwhile, the levels of latently and actively infected cells increase in the initial stage of infection, but rapidly decline to zero soon after. Even with a high initial viral dosage of 10% $CD4^+$, Person A is still able to completely clear the infection.

4.5.2 Weak Immune System Succumbs to Infection

Suppose now that an individual, Person B, has a value of R_0 greater than 1. The outcome of the HTLV-I infection is thus governed by the third case of Theorem 4.5.2. This corresponds to Case (ii) of Theorem 4.5.1 when $R_0 > 1$. An interpretation of this situation is that Person B elicits a weak immune response against the virus. Such a scenario occurs, for example, in individuals whose circulating CTLs or antibodies have poor recognition of HTLV-I epitotes, or those who are immuno-compromised.

[1] According to the US Centres for Disease Control and Prevention. For reference, Acquired Immune Deficiency Syndrome (AIDS) is generally characterized by a $CD4^+$ helper T-cell count below 200 cells per mm^3.

Looking at Figure 4.1(b), it is seen that after the initial infection, the level of healthy target cells drops rapidly and remains at a low level as time progresses. Once the system settles at the chronic infection equilibrium, both latently and actively infected cells are present in the peripheral blood and make up a significant proportion of the total target cell population. Even with a tiny initial viral dosage of 0.1% $CD4^+$, Person B will become chronically infected at an equilibrium state in less than five years. Notice that at the equilibrium state, the number of latently infected cells outnumber the number of actively infected cells. This observation is consistent with the hypothesis that the majority of the proviral load of HTLV-I-infected individuals resides in latently infected cells. At the same time, it is also seen that the number of actively infected cells at equilibrium is positive, reinforcing the idea that persistent expression of the viral protein Tax and infected target cell activation, rather than complete latency, is a key factor in the dynamics of HTLV-I. We will re-visit these ideas about HTLV-I infection in Chapter 5.

4.5.3 Dependence on Initial Viral Dosage

Next, we take a look at what happens in the second case of Theorem 4.5.2 when backward bifurcation and bi-stability occur. Consider Person C, whose value of R_0 satisfies $R_0(\sigma_0) < R_0 < 1$. To illustrate the consequence of a backward bifurcation with respect to infection, we provide the following intuitive biological interpretation. Person C elicits a moderate immune response against the virus. Referring to Figure 4.2, we observe that at the beginning of the infection, if the initial viral dosage is low, say 1% $CD4^+$, the level of healthy target cells eventually converges to the infection-free steady state; Person C clears the infection (Figure 4.2(a)). However, if the initial viral dosage is slightly higher, for instance 2.5% $CD4^+$, the populations of target cells converge instead to the stable endemic equilibrium, and Person C becomes chronically infected in fewer than five years (Figure 4.2(b)). Thus, in this range of R_0 where bi-stability is present, the outcome of the infection, whether it is cleared or it becomes chronic, displays sensitive dependence on the initial viral dosage at the onset of the infection.

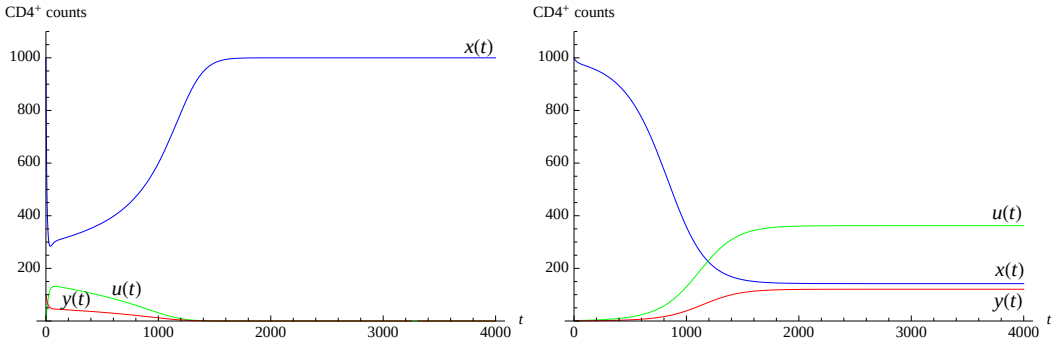

(a) Person A - initial viral dosage 10% $CD4^+$.

(b) Person B - initial viral dosage 0.1% $CD4^+$.

Figure 4.1: Time series simulations illustrating the first and third cases of Theorem 4.5.2. (a) shows the first case when there is global convergence to the infection-free equilibrium, and (b) shows the third case when there is global convergence to an endemic, or chronic infection, equilibrium. The level of healthy target cells $x(t)$ in blue, latently infected target cells $u(t)$ in green, and actively infected target cells $y(t)$ in red are shown over the course of approximately 11 years from the initial infection. The value of σ is 0.01 in (a) and 0.1 in (b). The remaining parameter values are the same: $\lambda = 20$, $\beta = 0.001$, $\epsilon = 0.9$, $\tau = 0.01$, $r = 0.15$, $k = 1150$, $\mu_1 = 0.02$, $\mu_2 = 0.02$, $\mu_3 = 0.03$.

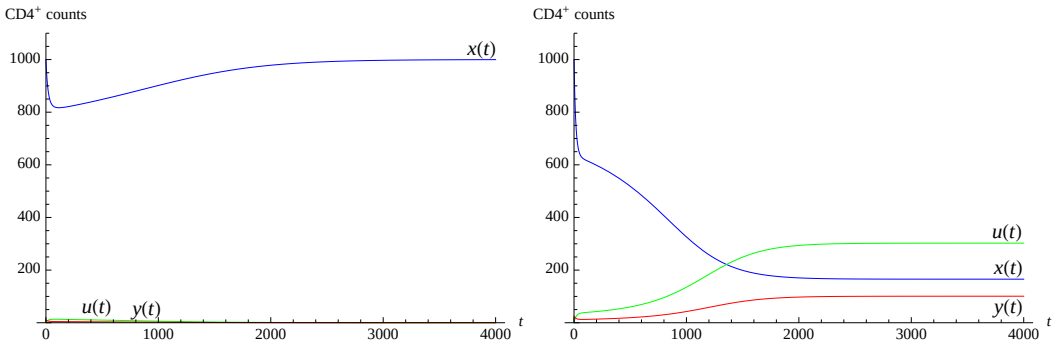

(a) Person C - initial viral dosage 1% $CD4^+$.

(b) Person C - initial viral dosage 2.5% $CD4^+$.

Figure 4.2: Time series simulations illustrating the second case of Theorem 4.5.2. In the presence of bi-stability, the initial viral dosage is a significant determining factor for the outcome of the infection. The level of healthy target cells $x(t)$ in blue, latently infected target cells $u(t)$ in green, and actively infected target cells $y(t)$ in red are shown over the course of approximately 11 years from the initial infection. The value of σ is 0.06. The remaining parameter values are the same as in Figure 4.1: $\lambda = 20$, $\beta = 0.001$, $\epsilon = 0.9$, $\tau = 0.01$, $r = 0.15$, $k = 1150$, $\mu_1 = 0.02$, $\mu_2 = 0.02$, $\mu_3 = 0.03$.

Chapter 5

Numerical Investigation

The primary focus in this chapter is to investigate numerically new aspects of HTLV-I infection considered in our model (2.3), especially the role of transcriptional latency of proviral cells and the spontaneous re-activation of latently infected target cells, under biologically reasonable parameters. Key observations arise that challenge conventional ways of thinking about viral infection and provide useful insights to the dynamics of HTLV-I *in vivo*.

5.1 Parameters

5.1.1 Range of Parameter Values

Parameter values have been estimated using both experimental and theoretical methods in studies of $CD4^+$ lymphocyte kinetics by Kirschner and Webb [27], Nelson, Murray, and Perelson [41], and Asquith et al. [7]. A biologically reasonable range is obtained for each parameter value based on estimates in the literature. The rate of production λ of healthy $CD4^+$ helper T-cells from the bone marrow falls in the range of 15–25 cells/mm^3/day [27]. As infection by HTLV-I only causes minor detriment to T-cell functionality [3], it is expected that all three populations of target cells considered in our model display natural death rates similar to that of healthy target cells, between 0.01–0.05 day^{-1} [27, 41]. The rate of rapid Tax-driven selective mitosis r lies in the range 0.04–0.4 day^{-1}, which is in the same order of magnitude as the one proposed in [27]. In the absence of infection, the normal $CD4^+$ helper T-cell count averages 1000 cells/mm^3, and we consider a target cell carrying capacity of 1150 cells/mm^3. Using Perelson's scaling relation [43], $\beta k \approx 1$ day^{-1}, we determine values for the coefficient of infectious transmissibility β to be in the order of 10^{-3} mm^3/cell/day. Asquith et al. [7] have quantified the rate of expression of Tax τ in proviral cells to be between 0.03–3% per day. The biological

meaning of the parameters as well as the relevant ranges in which the parameters lie are summarized in Table 5.1.

It is easily verified that when parameter values are selected from biologically relevant ranges, the assumptions and theoretical results observed in Chapters 3 and 4 are valid, thus the behaviour of solutions to model (2.3) is realistic for HTLV-I infection.

Parameter	Range or Value	Biological Meaning
λ	15–25 cells/mm^3/day	rate of production of target cells ($CD4^+$ helper T-cells)
β	0.0005–0.003 mm^3/cell/day	infectious transmissibility coefficient
r	0.04–0.4 day^{-1}	rate of Tax-driven selective proliferation of actively infected target cells
k	1150 cells/mm^3	carrying capacity of target cells
σ	0–1	surviving fraction of proviral cells from infectious transmission
ϵ	0–1	surviving fraction of proviral cells from mitotic transmission
τ	0.0003–0.03 day-1	rate of spontaneous Tax expression
μ_1	0.01–0.05 day^{-1}	natural death rate of healthy cells
μ_2	0.01–0.05 day^{-1}	natural death rate of latently infected cells
μ_3	0.01–0.05 day^{-1}	natural death rate of actively infected cells

Table 5.1: Biologically relevant parameter values.

5.2 Parameter Values are Influenced by Intrinsic Factors

Intrinsic factors such as host genetics and host-virus interactions are unique to each individual and influence parameter values. As we will see, these factors in turn play integral roles in the mechanisms and the outcomes of HTLV-I infection.

5.2.1 Role of Host Genetics

As mentioned in Section 4.5 in Chapter 4, the level $x_0 = \frac{\lambda}{\mu_1}$ of healthy target cells in the absence of HTLV-I infection coincides with the normal $CD4^+$ helper T-cell count in a healthy individual, which is typically 1000 cells per mm^3 of blood but may vary quite significantly among healthy persons, ranging from 500 to 1600 cells per mm^3. Slight variations in the rate of production of new $CD4^+$ helper T-cells λ from the bone marrow and the natural death rate of these healthy target cells μ_1 depend

entirely on the individual in question and affect the value of x_0. For example, an individual whose lymphocytes undergo faster differentiation in the bone marrow and have a long natural lifespan in the periphery is likely to have a higher than average normal $CD4^+$ helper T-cell count.

It is seen that R_0, the basic reproduction number for viral infection for our model (2.3), is a decreasing function of x_0 due to Assumption (A2):

$$\frac{\partial R_0}{\partial x_0} = \frac{\tau}{\mu_3(\tau+\mu_2)}\Big(\sigma\beta - \frac{\epsilon r}{k}\Big) < 0.$$

This observation is in contrast with the common occurrence in epidemiological and immunological models in which the basic reproduction number has a positive correlation with the initial population size [15, 23, 52]. In particular, it implies that a healthy individual whose normal $CD4^+$ helper T-cell count at equilibrium x_0 is lower than average would have a naturally higher value of R_0, given that all other parameters are fixed, and a subsequently higher chance of lying in the basin of attraction of the stable endemic, or chronic infection, equilibrium upon initial infection. This idea may appear at first to be counter-intuitive as one would expect that a smaller population of susceptible healthy cells would provide fewer opportunities for cell-to-cell transmission of HTLV-I-infected cells to occur, resulting in a lower chance for the provirus to establish itself in the target cell population. However, it is known that $CD4^+$ helper T-cells exhibit considerable immune functionality such as the release of various cytokines and growth factors that activate and regulate other immune cells involved in both innate and adaptive immunity including macrophages, dendritic cells, NK-cells, B-cells, and CTLs. We hypothesize that in response to a given initial viral dosage, an individual with a smaller x_0 mounts an anti-HTLV-I immune response that is not necessarily weaker in terms of antigen specificity, but rather less directed, e.g. immune cells may be more spread out instead of aggregating at the site of infection due to a lower concentration of cytokines since there are fewer $CD4^+$ T-cells. This is especially critical in the early stages of infection whereby failure to eliminate the invading pathogen effectively allows HTLV-I to establish itself in a latent compartment and successfully evade destruction (see Subsection 5.3.2 below). The situation is illustrated in Figure 5.1.

5.2.2 Role of Host-Virus Interactions

It is natural to expect that properties of specific strains of HTLV-I affect parameters such as β, the coefficient of infectious transmissibility, r, the rate of selective proliferation of Tax^+ target cells, and τ, the rate of spontaneous Tax expression. Aside from these, there are several aspects of the host-virus interaction that impact

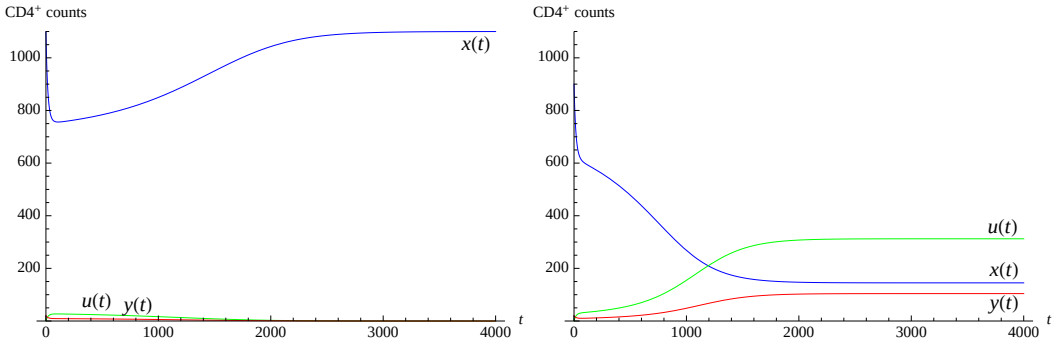

(a) Person D - initial viral dosage 2% $CD4^+$. (b) Person E - initial viral dosage 2% $CD4^+$.

Figure 5.1: Time series simulations demonstrating the effect of differences in x_0 after exposure to an initial infection. The level of healthy target cells $x(t)$ are shown in blue, that of latently infected target cells $u(t)$ in green, and actively infected target cells $y(t)$ are shown in red. Time is shown in days. (a) Person D has a slightly higher than average normal $CD4^+$ T-cell count of $x_0 = 1100$ cells per mm^3. Here $R_0 = 0.80$. Person D is infected with HTLV-I, but is able to clear the infection. (b) Person E has a slightly lower than average normal T-cell count of $x_0 = 900$ cells per mm^3. The value of R_0 is increased, namely $R_0 = 0.92$. After being infected by the same initial viral dosage, Person E is unable to control the virus and becomes chronically infected in fewer than five years. The value of λ is 22 cells per mm^3 per day in (a) and 18 cells per mm^3 per day in (b). All remaining parameter values are the same: $\beta = 0.001$, $\sigma = 0.06$, $\epsilon = 0.9$, $\tau = 0.01$, $r = 0.15$, $k = 1150$, $\mu_1 = 0.02$, $\mu_2 = 0.02$, $\mu_3 = 0.03$.

parameter values. For instance, the parameters σ and ϵ, representing the surviving fractions of newly infected cells from infectious and mitotic transmission, respectively, greatly depend inversely on the efficiency of host immune responses to virally infected target cells: stronger immune responses correspond to lower values of σ, ϵ; weaker immune responses correspond to higher values of σ, ϵ.

Next, as mentioned in Section 2.2 in Chapter 2, the HTLV-I genome is overall genetically stable with low sequence variability. Moreover, the frequently observed high proviral load in an infected individual is comprised of large populations of infected T-cell clones, rather than a genetically diverse pool of infected target cells. Since infectious transmission is highly error-prone and would result in the latter, we infer that the vast majority of newly infected target cells from infectious transmission are eliminated before silencing Tax expression, so that the surviving proportion is substantially smaller; that is, $\sigma \ll 1$. On-going replication of the provirus thus occurs primarily through mitotic transmission and must involve rapid selective mitotic division of Tax-expressing infected target cells as normal homeostatic T-cell proliferation is insufficient for maintaining such a high proviral load. At the same

time, efficient lysis of proviral cells that continue to express viral proteins leads us to conclude that a significant proportion of newly infected target cells from mitotic transmission rapidly hide Tax expression before detection by the immune system, so that $\epsilon \approx 1$.

5.3 Observations and Insights

In this section, we examine in more detail the dynamic interaction between infected target cell activation and latency that forms the basis of our mathematical model. Our findings validate the proposed hypothesis of HTLV-I infection *in vivo* by demonstrating that experimental observations do indeed follow from our model. By selecting realistic parameter values, we offer important insights on the infection and persistence of HTLV-I.

5.3.1 Establishment of Proviral Load in Infected Individuals

The proviral load of a chronically infected individual at equilibrium, $\bar{v} = \bar{u} + \bar{y}$, depends on the values of the parameters and is commonly expressed as a proportion or percentage of the total number of $CD4^+$ helper T-cells. Specifically,

$$\text{Proportion of Proviral Cells} = \frac{\text{number of infected cells}}{\text{total number of cells}} = \frac{\bar{v}}{\bar{x} + \bar{v}}. \tag{5.1}$$

Using parameter values that are realistic for HTLV-I infection, it is seen that numerical simulations for our model agree with the common experimental observation that an HTLV-I-infected person may harbour an abnormally high proviral load. For example, the proviral load at equilibrium for Person B in Figure 4.1 is 77% $CD4^+$, and that of Person E in Figure 5.1 is 74% $CD4^+$. As shown in Figure 5.2, the establishment of the proviral load during chronic HTLV-I infection requires both infectious and mitotic transmission: below certain thresholds for either β or r, endemic equilibria may not exist. Cross-sections of the bifurcation surface to illustrate the role of one of the parameters under investigation, either β or r, for fixed values of the other parameter is shown in Figure 5.3. Notice that backward bifurcation and bi-stability, which we have seen with respect to the parameter σ in Chapter 3, may occur with respect to β for large enough values of r, and also with respect to r when β is below a certain value. It is easily verified from the definition of the basic reproduction number for viral infection R_0 that R_0 is an increasing function of both parameters, β and r, as expected. That is, both higher infectious transmissibility as well as faster rate of Tax^+ infected T-cell proliferation drive the system to chronic infection. Interestingly, we observe that regardless of the rate of selec-

tive proliferation r, the coefficient of infectious transmissibility β is not a significant determinant of proviral load (Figures 5.3(a)–(b)), whereas r contributes substantially to the proviral load whenever endemic equilibria exist (Figures 5.3(c)–(d)). These observations agree with the proposed mechanism regarding HTLV-I infection described in Chapter 2 along with the assumptions made in Chapter 3. We will see shortly in Subsection 5.3.4 below that the rate of Tax expression also plays a major role in determining the proviral load during chronic HTLV-I infection.

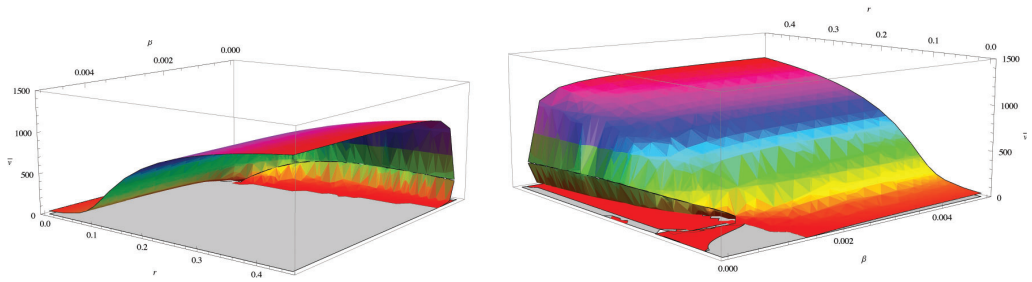

(a) (b)

Figure 5.2: Two-parameter bifurcation surface displaying the effects of both routes of viral transmission, infectious (β) and mitotic (r), on the equilibrium proviral load $\bar{v}$. Two views are shown. Parameter values are: $\lambda = 20$, $\sigma = 0.06$, $\epsilon = 0.9$, $\tau = 0.01$, $k = 1150$, $\mu_1 = 0.02$, $\mu_2 = 0.02$, $\mu_3 = 0.03$.

5.3.2 Viral Persistence in Latently Infected Cells

From Section 3.3 in Chapter 3, it was observed that when an infected individual has settled at an endemic steady state, the equilibrium levels of latently infected and actively infected target cells are related by Equation (3.6), specifically,

$$\bar{u} = \frac{\mu_3}{\tau}\bar{y}.$$

Asquith et al. [7] determined that, among HTLV-I-infected individuals, the rate of spontaneous Tax expression *in vivo* mainly falls in the range of 0.03–3% per day in both ACs and HAM/TSP patients, indicating that only a very small proportion of latently infected cells become activated each day. The average life span of a $CD4^+$ helper T-cell is approximately 30 days, so that one may expect the estimated turnover rate to be roughly $1/30$ day^{-1} $\approxeq 0.033$ day^{-1}. As significant impairment is not observed in proviral cells, we expect the natural death rates of HTLV-I-infected target cells to be in the same order of magnitude as that of healthy cells, with actively infected cells experiencing slightly higher elimination due to minor detriment to T-cell functionality. Hence, it is seen that in general, $\tau < \mu_3$, re-

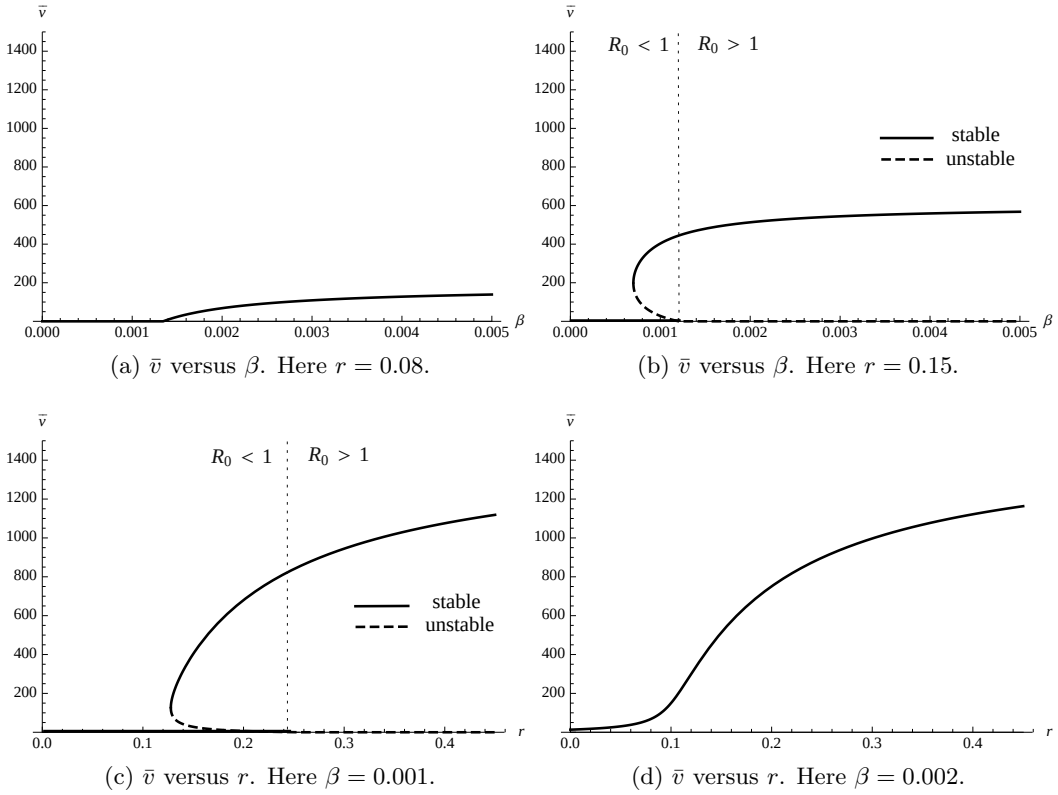

(a) $\bar{v}$ versus β. Here $r = 0.08$.

(b) $\bar{v}$ versus β. Here $r = 0.15$.

(c) $\bar{v}$ versus r. Here $\beta = 0.001$.

(d) $\bar{v}$ versus r. Here $\beta = 0.002$.

Figure 5.3: Cross-sections of the surface in Figure 5.2 with respect to β for a given rate of selective mitotic division r, shown in (a)–(b), and r for a given coefficient of infectious transmissibility β, shown in (c)–(d). Aside from β and r, the remaining parameters are fixed: $\lambda = 20$, $\sigma = 0.06$, $\epsilon = 0.9$, $\tau = 0.01$, $k = 1150$, $\mu_1 = 0.02$, $\mu_2 = 0.02$, $\mu_3 = 0.03$.

affirming the hypothesis that the provirus persists in latently infected cells during chronic HTLV-I infection.

The proportions of infected cells that are either latent or active in an infected individual only depend on the parameters τ and μ_3, regardless of proviral load, and are unaffected by the initial viral dosage. Using the relationship between $\bar{u}$ and $\bar{y}$ at equilibrium, these fractions are

$$\begin{aligned} \text{Proportion of Latently Infected Cells} &= \frac{\text{number of Tax}^- \text{ infected cells}}{\text{total number of infected cells}} \\ &= \frac{\bar{u}}{\bar{u}+\bar{y}} = \frac{\mu_3}{\tau+\mu_3}, \end{aligned} \tag{5.2}$$

and

$$\text{Proportion of Actively Infected Cells} = \frac{\text{number of Tax}^+ \text{ infected cells}}{\text{total number of infected cells}} = \frac{\bar{y}}{\bar{u}+\bar{y}} = \frac{\tau}{\tau+\mu_3}. \quad (5.3)$$

As observed previously, the proportion of proviral cells that are latent may be rather high. For instance from Figure 5.1, we see that 75% of Person E's proviral load is comprised of latently infected cells.

5.3.3 Tax Expression Drives Chronic Infection and Promotes Bistability

We have hypothesized that HTLV-I-infected target cells are able to evade host immune responses by silencing the viral protein Tax and hiding in a pool of latently infected cells, becoming essentially 'invisible'. If this is the case, then one would expect the optimal viral strategy to be complete passivity. However, consider R_0, the basic reproduction number for viral infection defined in Chapter 3. Although the rate τ of spontaneous Tax expression is generally quite low (0.03–3% of Tax^- CD4^+ T-cells become Tax^+ each day), if $\tau \approx 0$ then

$$R_0 \approx \frac{\tau}{\mu_2\mu_3}\Big(\sigma\beta x_0 + \epsilon r\Big(1-\frac{x_0}{k}\Big)\Big),$$

which may be made arbitrarily small as $\tau \to 0$. For example, R_0 may be reduced below the threshold for which endemic equilibria exist and chronic infection is not possible (e.g. in Figures 5.7(a)–(c)), corresponding to the interpretation that a pool of proviral cells that is almost exclusively latent cannot maintain its numbers without the benefit of rapid selective proliferation incurred by active viral transcription in Tax-expressing infected cells. This observation suggests that HTLV-I does not propagate in host target cells through complete viral latency; rather, the mechanism by which HTLV-I persists *in vivo* is more dynamic in nature and involves a delicate balance between viral latency and activation.

Next, we make two additional observations regarding the effect of Tax expression in determining whether the infection becomes chronic or dies out. First, it is seen that a simple computation yields

$$\frac{\partial R_0}{\partial \tau} = \frac{\mu_2}{\mu_3(\tau+\mu_2)^2}\Big(\sigma\beta x_0 + \epsilon r\Big(1-\frac{x_0}{k}\Big)\Big) > 0;$$

that is, an increase in τ increases the value of R_0 (see Figure 5.4). Second, numerical simulations indicate that increasing τ also increases the range for which backward

bifurcation and bi-stability occur, as illustrated in Figure 5.5. Here we use σ as the bifurcation parameter for fixed values of τ and view its impact on the equilibrium proviral load $\bar{v}$. As a side observation, note that for a fixed value of σ, comparison of Figures 5.5(a)–(c) suggests that increased Tax expression not only widens the range of bi-stability, it also appears to increase the proviral load. This observation, upon which we will elaborate in Subsection 5.3.4, may initially seem counter-intuitive as expression of viral proteins should be expected to promote elimination by Tax-specific immune responses and lower, instead of raise, the proviral load. Following our discussion of the implications of bi-stability at the end of Chapter 4, we remark that a broader range for the presence of a backward bifurcation means that (i) newly infected individuals would have a higher probability of lying in the basin of attraction of the stable endemic equilibrium, thus being more likely to become chronically infected, and (ii) the initial viral dosage would play a more crucial role on the outcome of infection as the basin of attraction of the stable endemic equilibrium becomes larger. An increased rate of Tax expression is therefore seen to be a factor that drives the system towards chronic infection.

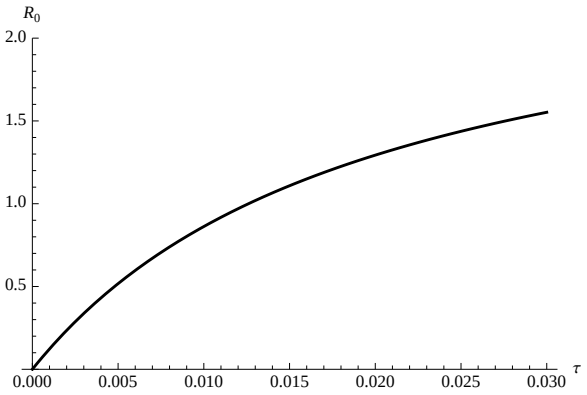

Figure 5.4: The basic reproduction number for viral infection R_0 is an increasing function of τ, the rate of spontaneous expression of the viral protein Tax. Parameter values are: $\lambda = 20$, $\beta = 0.001$, $\sigma = 0.06$, $\epsilon = 0.9$, $r = 0.15$, $k = 1150$, $\mu_1 = 0.02$, $\mu_2 = 0.02$, $\mu_3 = 0.03$.

A serious consequence arises from the second observation which is shown in Figure 5.5(c). In particular, when τ is large enough, the loop of the backward bifurcation curve falls behind the vertical axis $\sigma = 0$, so that bi-stability is always present when $\sigma < \bar{\sigma}$, or equivalently when $R_0 < 1$. Note that Assumption (A3(ii)) no longer holds and the first case of our main theoretical result, Theorem 4.5.2 from Chapter 4, does not appear. In this scenario, global stability of the infection-free equilibrium is never possible, and an increased magnitude of initial infection strongly favours convergence to the stable chronic infection steady state.

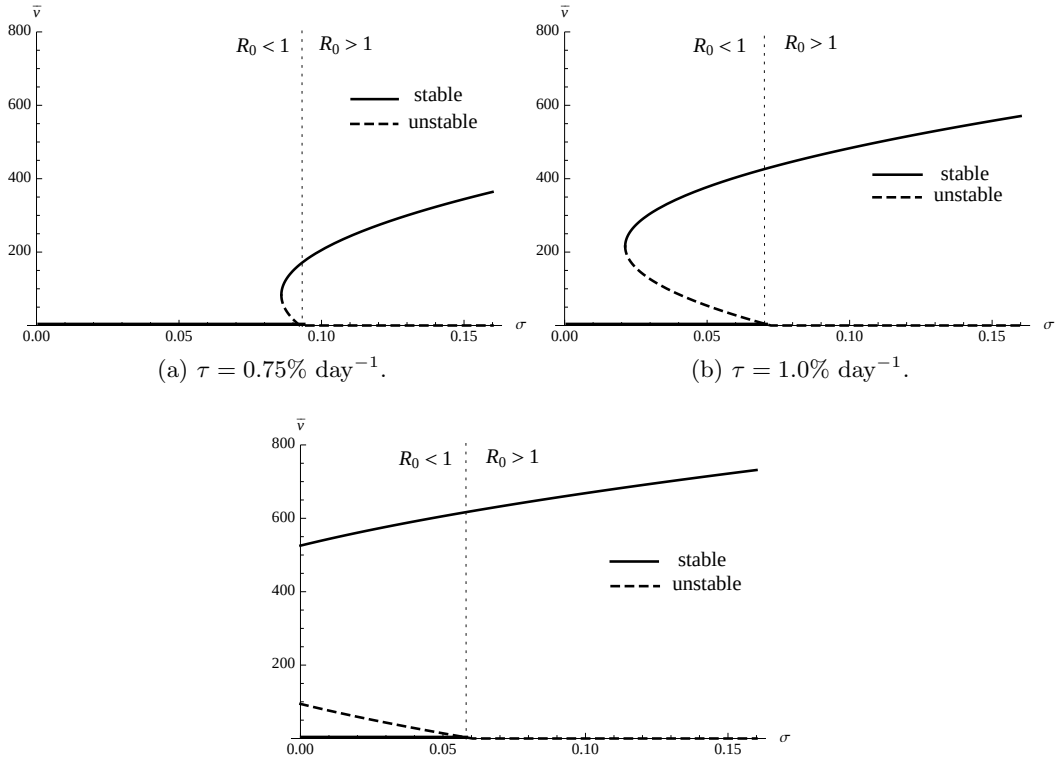

(a) $\tau = 0.75\%$ day^{-1}.

(b) $\tau = 1.0\%$ day^{-1}.

(c) $\tau = 1.25\%$ day^{-1}.

Figure 5.5: Tax expression increases the range for which backward bifurcation and bi-stability occur. The bifurcation diagram for the parameter σ is plotted against the equilibrium proviral load $\bar{v}$ for increasing values of τ, the rate of spontaneous Tax expression. Parameter values are: $\lambda = 20$, $\beta = 0.001$, $\epsilon = 0.9$, $r = 0.15$, $k = 1150$, $\mu_1 = 0.02$, $\mu_2 = 0.02$, $\mu_3 = 0.03$.

5.3.4 Increased Tax Expression Increases Proviral Load

The rate of spontaneous Tax expression τ is a significant determinant of the equilibrium proviral load, $\bar{v} = \bar{u} + \bar{y}$, of an individual who is chronically infected by HTLV-I. Two-parameter surface plots illustrating the effects of infectious transmissibility β and rate of Tax expression τ on proviral load $\bar{v}$, and the relationship between the rapid rate of selective Tax-driven proliferation r, the rate of Tax expression τ, and proviral load $\bar{v}$ are shown in Figure 5.6. Upon examination of a few cross-sections of each surface for fixed values of β and r as in Figure 5.7, we notice unexpectedly that Tax expression and proviral load are positively, rather than negatively, correlated. We point out a few interesting observations. Backward bifurcation and bi-stability may occur with respect to τ for both low and high values of r (Figures 5.7(a), (c)), but may not be present if the infectious transmissibility β is high enough (Figure 5.7(b)). There are two branches representing equilibrium proviral

load when $R_0 < 1$ and multiple chronic infection steady states exist, one stable and the other unstable. When $R_0 > 1$, the unstable branch vanishes whilst the stable branch remains. The lower unstable branch coincides with the intuitive notion that increased expression of viral proteins exposes infected cells to immune surveillance and results in a decrease in proviral load. Of much greater significance is the upper stable branch, which displays a definite positive correlation between proviral load and rate of viral activation. Although this observation may at first run counter to intuition by indicating that the net effect of increased Tax expression is to increase rather than decrease the proviral load, we argue that the benefits conferred by T-cell activation, such as infectious transmission and rapid mitotic transmission, allow the provirus to replicate faster than it is being destroyed. The proviral load should then be expected to increase as the surviving proportion of newly infected cells, either through horizontal or vertical transmission, subsequently hide viral proteins and become latent. Several time series plots of $CD4^+$ T-cell levels illustrating the impact of minor changes in τ on $\bar{v}$ are depicted in Figure 5.8.

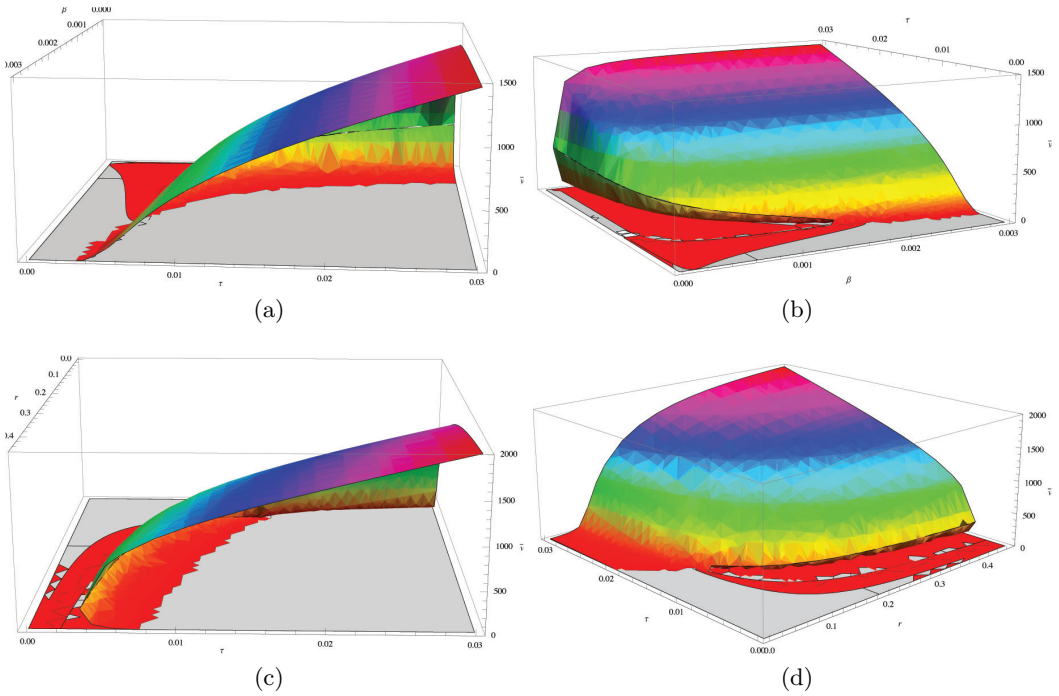

Figure 5.6: Two-parameter bifurcation surfaces demonstrating how equilibrium proviral load $\bar{v}$ is affected by (a)–(b): β and τ, with $r = 0.15$ fixed, and (c)–(d): r and τ, with $\beta = 0.001$ fixed. Two views of each of the two surfaces are shown. Parameter values are: $\lambda = 20$, $\sigma = 0.06$, $\epsilon = 0.9$, $k = 1150$, $\mu_1 = 0.02$, $\mu_2 = 0.02$, $\mu_3 = 0.03$.

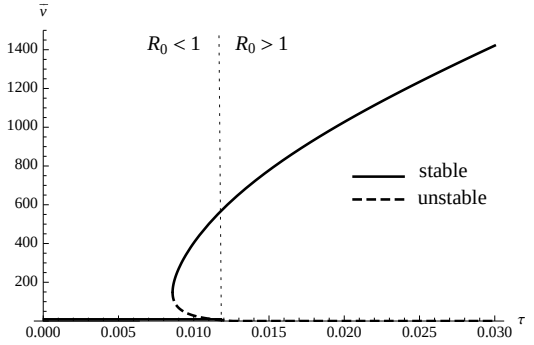

(a) $\beta = 0.001$ cells/mm^3/day, $r = 0.15$ day^{-1}.

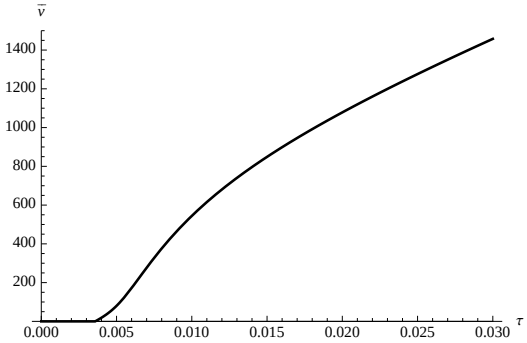

(b) $\beta = 0.003$ cells/mm^3/day, $r = 0.15$ day^{-1}.

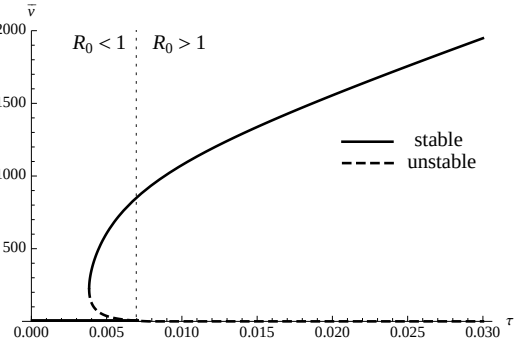

(c) $\beta = 0.001$ cells/mm^3/day, $r = 0.40$ day^{-1}.

Figure 5.7: The effect of the rate of viral protein expression τ on equilibrium proviral load $\bar{v}$ during chronic infection for several fixed values of β and r. Note that for small values of τ, chronic infection is not possible as endemic equilibria do not exist. Remaining parameter values are: $\lambda = 20$, $\sigma = 0.06$, $\epsilon = 0.9$, $k = 1150$, $\mu_1 = 0.02$, $\mu_2 = 0.02$, $\mu_3 = 0.03$.

5.3.5 Tax Expression Affects Time to Reach Equilibrium

Not only does the rate of expression of viral proteins in proviral cells increase the proviral load at equilibrium, it also has a strong impact on the length of time it takes an individual to reach equilibrium, whether it be the infection-free steady state or a chronic infection steady state. Time series plots for an individual, Person G, demonstrating the possible situations are shown in Figure 5.9. In Figures 5.9(a)–(b), Person G is given an initial viral dosage of 10% CD4$^+$ proviral cells that have relatively low rates of Tax expression, and lies in the basin of attraction of the infection-free steady state. A slight increase in Tax expression significantly increases the time for complete clearance of the virus and for the level of healthy CD4$^+$ helper T-cells to return to normal. During this extended period of time, a lower CD4$^+$ helper T-cell count could reduce overall immune functionality and leave Person G

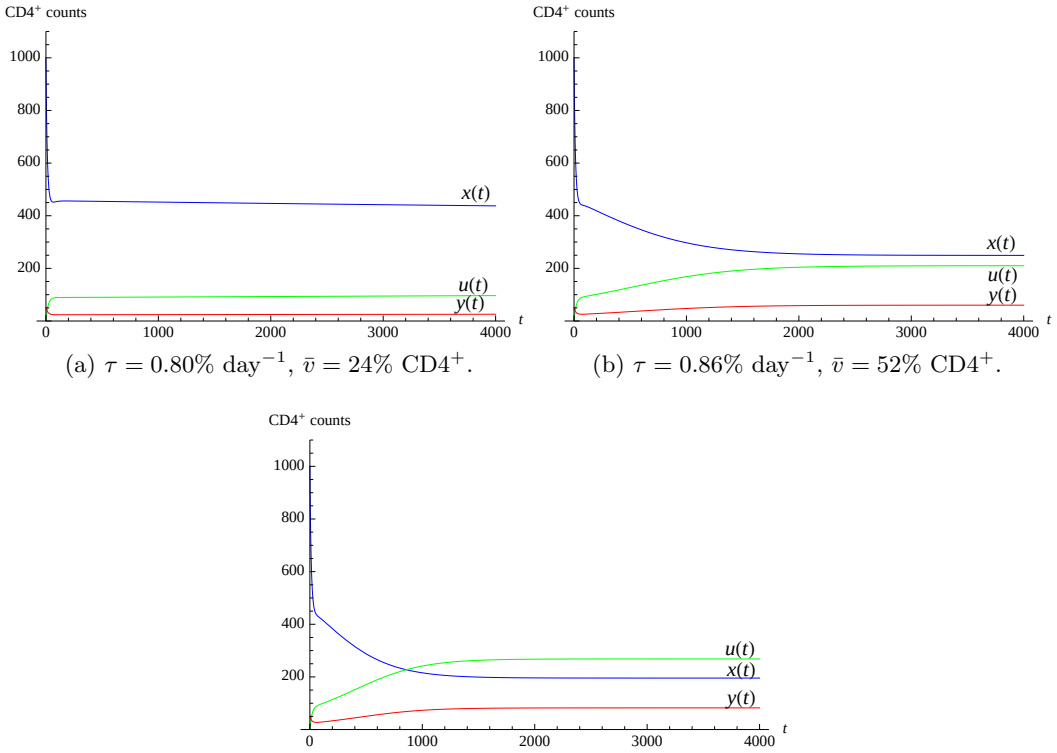

(a) $\tau = 0.80\%$ day^{-1}, $\bar{v} = 24\%$ CD4$^+$. (b) $\tau = 0.86\%$ day^{-1}, $\bar{v} = 52\%$ CD4$^+$.

(c) $\tau = 0.92\%$ day^{-1}, $\bar{v} = 64\%$ CD4$^+$.

Figure 5.8: Time series simulations showing that the rate of spontaneous Tax expression τ has a significant impact on equilibrium proviral load $\bar{v}$ during chronic infection. Person F, given an initial viral dosage of 5% CD4$^+$, is chronically infected by HTLV-I. The levels of healthy target cells $x(t)$ in blue, latently infected target cells $u(t)$ in green, and actively infected target cells $y(t)$ in red are plotted against time. Parameter values for Person F are: $\lambda = 20$, $\beta = 0.001$, $\sigma = 0.075$, $\epsilon = 0.9$, $r = 0.15$, $k = 1150$, $\mu_1 = 0.02$, $\mu_2 = 0.02$, $\mu_3 = 0.03$.

more susceptible to invading pathogens including bacterial or other viral infections. In Figures 5.9(c)–(d), Person G is initially infected by 1.5% CD4$^+$ proviral cells whose rates of Tax expression are relatively high, and lies in the basin of attraction of the stable chronic infection equilibrium. A small increase in Tax expression not only increases the proviral load at equilibrium, it also reduces considerably the length of time required for Person G to reach the chronic infection steady state. It is possible that the sudden sharp decline in healthy CD4$^+$ helper T-cell counts in chronically infected individuals induced by a high continuous rate of viral protein expression is a crucial factor in the pathogenesis of the inflammatory disease HAM/TSP.

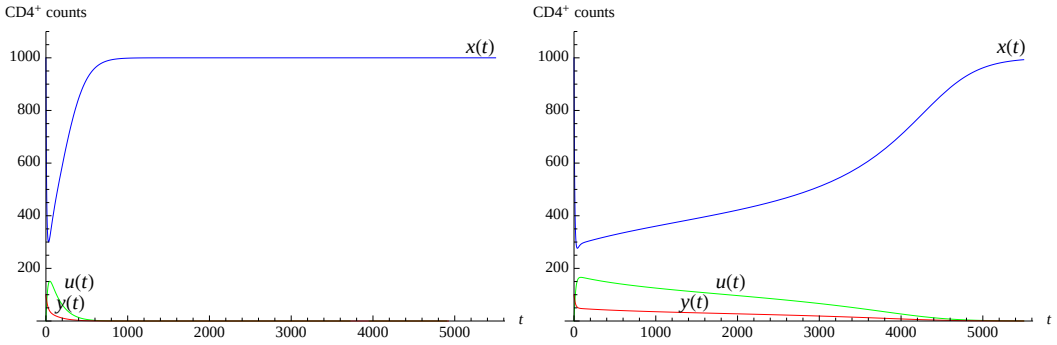

(a) $\tau = 0.42\%$ day^{-1}. Clears infection in about 2 years.

(b) $\tau = 0.84\%$ day^{-1}. Takes approximately 15 years to clear infection.

(c) $\tau = 1.00\%$ day^{-1}, $\bar{v} = 71\%$ CD4$^+$. Takes over 12 years to reach chronic infection steady state.

(d) $\tau = 1.42\%$ day^{-1}, $\bar{v} = 90\%$ CD4$^+$. Submits to infection in less than 2 years with increased proviral load.

Figure 5.9: Time series simulations demonstrating the impact of Tax expression on the duration of time required for Person G to settle at equilibrium. The levels of healthy cells $x(t)$ are shown in blue, that of latently infected cells $u(t)$ in green, and of actively infected cells $y(t)$ in red over the course of 15 years. (a)–(b): Initial viral dosage is 10% CD4$^+$ with relatively low rates of Tax expression. Increasing the value of τ increases the time needed to clear HTLV-I. (c)–(d): Initial viral dosage is 1.5% CD4$^+$ with relatively high rates of Tax expression. The result of increased Tax expression is a decreased time to settle at chronic infection steady state. Parameter values for Person G are: $\lambda = 20$, $\beta = 0.001$, $\sigma = 0.06$, $\epsilon = 0.9$, $r = 0.15$, $k = 1150$, $\mu_1 = 0.02$, $\mu_2 = 0.02$, $\mu_3 = 0.03$.

5.3.6 Tax Expression as a Risk Factor to HAM/TSP Development

Arising from investigation of our mathematical model, we speculate that the rate of spontaneous Tax expression τ is a plausible risk factor to the pathogenesis of HAM/TSP. As discussed in Subsection 5.3.2, the proportion of the equilibrium proviral load consisting of actively infected target cells depends only on the rate of Tax expression τ and the natural death rate of Tax$^+$ proviral cells μ_3, and is equal

to $\frac{\tau}{\tau+\mu_3}$. Direct calculation shows that

$$\frac{\partial}{\partial\tau}\Big(\frac{\tau}{\tau+\mu_3}\Big) = \frac{\mu_3}{(\tau+\mu_3)^2} > 0;$$

that is, a faster continual rate of viral protein expression results in a higher fraction of the proviral load consisting of actively infected, instead of latently infected, target cells once equilibrium is reach (see Figure 5.10). We hypothesize that perhaps it is the relative proportion of proviral cells actively expressing Tax rather than the absolute magnitude of the proviral load that predisposes a chronically infected individual to the development of HTLV-I-associated diseases. This alternative explanation suggests that the rate of spontaneous Tax expression, which directly influences this proportion, may be crucial to assessing the risk of HAM/TSP: a high rate of Tax expression corresponds to a high actively infected proportion of the proviral load and a greater chance of developing HAM/TSP.

Our conjecture helps to rectify the conflicting argument that the proviral load should play an important part in determining disease status yet its magnitude is neither necessary nor sufficient to cause HAM/TSP. It is also consistent with the suggestion that HTLV-I-specific immune responses are responsible for the tissue damage leading to HTLV-I-associated pathologies as increased Tax expression leading to subsequent increase in the proportion of Tax^+ proviral cells would provide additional antigenic stimulation for CTL proliferation and account for the presence of a persistent cellular immune response observed during chronic HTLV-I infection in both ACs and HAM/TSP patients. The identification of Tax expression as a possible important risk factor to HAM/TSP development may help to resolve the unanswered question as to why only a small percentage of chronically infected individuals acquire the disorder whilst the vast majority remains as lifelong asymptomatic carriers, and motivates the creation of appropriate treatment regimes targeting the rate of Tax expression to prevent the progression of HAM/TSP.

5.3.7 Treatment Strategies Should Target Rate of Tax Expression

We have seen from Section 4.5 in Chapter 4 that the outcome of HTLV-I infection may depend on the initial viral dosage at the time of infection due to the existence of a backward bifurcation and bi-stability in our model. The phenomenon of a backward bifurcation also presents serious challenges to effective elimination of HTLV-I in already infected individuals.

In the literature of compartmental models, it is known that viral clearance may be achieved by reducing the value of R_0, the basic reproduction number for viral infection, below one [15, 23, 36, 42]. Current treatment regimes for chronic HTLV-I

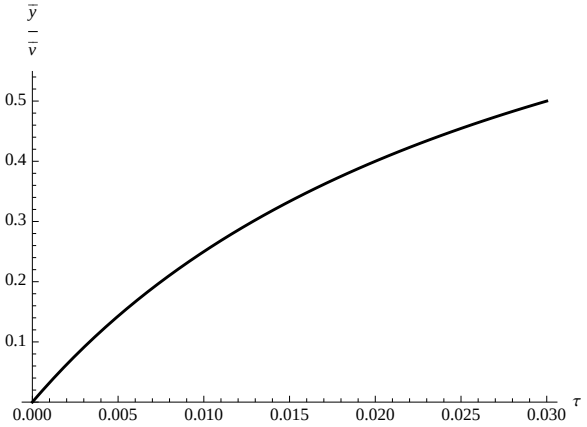

Figure 5.10: A positive correlation between the rate of spontaneous Tax expression and the Tax^+ proportion of the proviral load at equilibrium suggests an alternative explanation for the development of HAM/TSP. Parameter values are: $\lambda = 20$, $\beta = 0.001$, $\sigma = 0.075$, $\epsilon = 0.9$, $r = 0.15$, $k = 1150$, $\mu_1 = 0.02$, $\mu_2 = 0.02$, $\mu_3 = 0.03$.

infection administer drugs such as zidovudine (AZT) and lamivudine (3TC) that inhibit viral replication by blocking the action of the viral enzyme reverse transcriptase [8, 34, 35, 50], resulting in a reduction of the ratio $\frac{\beta}{\mu_3}$ and subsequently R_0. However, due to the existence of a backward bifurcation, it is possible for individuals with a value of R_0 less than one to become chronically infected by HTLV-I if the initial viral dosage is high enough, as described in Section 4.5. An unfortunate consequence is that even for a chronically infected individual whose value of R_0 is initially greater than one, the usual treatment strategy may still fail; lowering R_0 below one may be insufficient to eliminate the infection.

Following our discussions regarding proviral load, transmissibility, and especially Tax expression above, it can be inferred that not only is the current treatment method of lowering the value of $\frac{\beta}{\mu_3}$ insufficient to clear HTLV-I infection, it is also ineffective at controlling the proviral load. We suggest that a better treatment strategy is to instead reduce τ, the rate of spontaneous expression of the viral protein Tax. As illustrated in Figure 5.11, even if chronic infection remains, a more substantial decrease in proviral load can be attained given the same value of R_0. Further, if our hypothesis from Subsection 5.3.6 is correct, lowering the rate of Tax expression may be an important measure in the prevention of HAM/TSP pathogenesis. Lastly, it is seen in Figure 5.11(d) that a combination of the two treatment regimes may even be effective at achieving complete viral clearance.

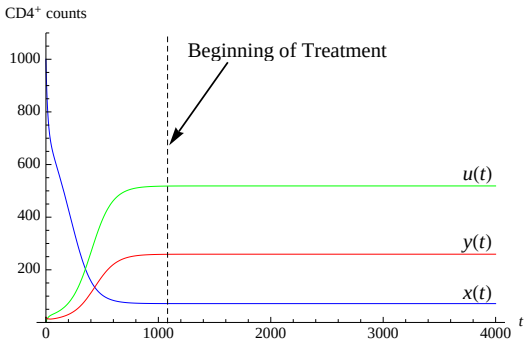

(a) Infection without treatment. $R_0 = 1.11$, $\bar{v} = 92\%$ CD4$^+$.

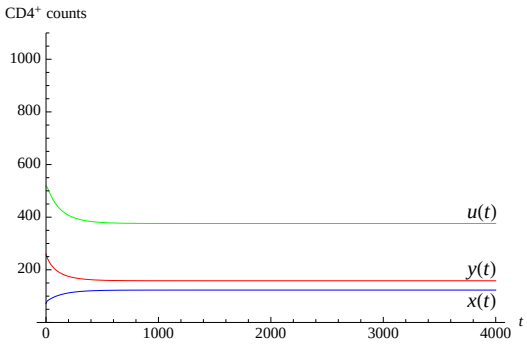

(b) Treatment by AZT. $R_0 = 0.86$, $\bar{v} = 81\%$ CD4$^+$.

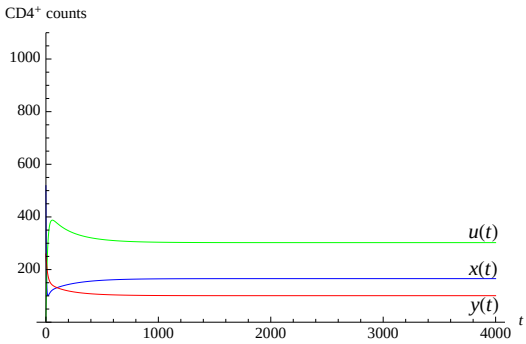

(c) Treatment by lowering Tax expression by 0.5%. $R_0 = 0.86$, $\bar{v} = 71\%$ CD4$^+$.

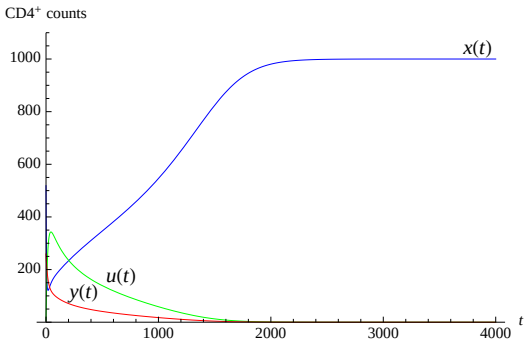

(d) Combination therapy eliminates virus. $R_0 = 0.67$.

Figure 5.11: Time series simulations showing the effects of treatment regimes on Person H, an individual with chronic HTLV-I infection. The levels of healthy cells $x(t)$ are shown in blue, that of latently infected cells $u(t)$ in green, and of actively infected cells $y(t)$ in red. (a): Person H is chronically infected by HTLV-I, initial viral dosage is 1% CD4$^+$. (b)–(c): The effect of two possible treatment regimes administered to Person H three years after initial infection. (d): Combination of both treatment regimes results in complete clearance of the virus approximately five years after treatment is administered. (a) Parameter values for Person H are: $\lambda = 20$, $\beta = 0.001$, $\sigma = 0.06$, $\epsilon = 0.9$, $\tau = 0.015$, $r = 0.15$, $k = 1150$, $\mu_1 = 0.02$, $\mu_2 = 0.02$, $\mu_3 = 0.03$. (b) Treatment by AZT: $\beta = 0.0009$, $\mu_3 = 0.0356$, with all other parameters fixed. (c) All parameters are as in (a), with the exception of τ, which is lowered to $\tau = 0.010$. (d) Combined treatment of AZT and reduced Tax expression: $\beta = 0.0009$, $\mu_3 = 0.0356$, $\tau = 0.010$, with all other parameters as in (a).

Chapter 6

Conclusions and Future Directions

In this thesis, a mathematical model based on a new hypothesis for the infection of HTLV-I focussing on viral infection and persistence *in vivo* is developed. The proposed mechanism of viral infection considers a highly dynamic interaction among three compartments of target cells of the virus: healthy, latently infected, and actively infected $CD4^+$ helper T-cells. The differentiation between two pools of infected target cells and the relationship between them are key features of our model and represent important aspects of realistic HTLV-I infection. Mathematical and numerical investigations give rise to significant mathematical and biological consequences. Our findings indicate that HTLV-I, by entertaining a dynamic interaction with the host immune system rather than a passive one, is effective in its goal of long-term viral persistence *in vivo*.

6.1 Conclusions

From the study of our mathematical model for HTLV-I infection arises the following conclusions.

- ▷ **Backward bifurcation and bi-stability are inherent to HTLV-I infection.**

  Local stability analysis of solutions near each equilibrium point reveals the existence of the complicated phenomenon of a backward bifurcation and bi-stability: it is possible for a stable infection-free equilibrium and a stable chronic infection equilibrium to co-exist. Bi-stability in our model helps to explain the role of initial viral dosage on the outcome of infection and the challenges encountered against effective elimination of the virus by current

treatment regimes. Numerical investigations show the appearances of backward bifurcation and bi-stability with respect to multiple parameters, suggesting that bi-stability is an inherent characteristic of HTLV-I infection.

▷ **Establishing the global dynamics of our model raises non-trivial mathematical issues and is a necessary step to investigating the finer aspects of the model unambiguously.**

Compartmentalization of infected proviral cells into two separate classes, latently infected and actively infected, substantially increases the mathematical difficulty in characterizing the global behaviour of solutions analytically due to the resulting high dimension of our system combined with the presence of bi-stability. We require the use of advanced mathematical theories, including the theory of monotone dynamical systems and the theory of compound differential systems, in order to establish the global dynamics. We determine that simple, closed, rectifiable, invariant curves such as homoclinic loops, heteroclinic trajectories, and non-constant periodic orbits cannot exist, and that the ω-limit set of each solution consists of exactly one equilibrium point. A complete understanding of the global dynamical behaviour of solutions both in the presence and absence of bi-stability allows us to study thoroughly other aspects of our model, such as the role of parameters on the outcome of infection.

▷ **A balance between transcriptional latency and activation of proviral cells offers opportunities for HTLV-I to evade destruction by human immune responses whilst establishing high proviral loads.**

The dynamic interaction between infected target cell latency and activation helps to explain the puzzling experimental observation that chronically infected individuals may harbour unusually high proviral loads despite strong positive selection by HTLV-I-specific immune responses. Infected target cell latency is accompanied by suppression of the viral protein Tax and provides a way in which infected target cells may evade detection by the immune system, allowing accumulation of the proviral load. Meanwhile, infected target cell activation is associated with spontaneous expression of Tax, which induces rapid selective proliferation and simultaneous exposure to immune surveillance. A delicate balance between the two compartments of proviral cells demonstrates the way in which HTLV-I persists during chronic infection.

▷ **The rate τ of spontaneous expression of the viral protein Tax has a substantial impact on HTLV-I infection.**

Spontaneous Tax expression, which has not been before considered in mathematical models for HTLV-I, promotes the presence of backward bifurcation and bi-stability and is shown to be a major driving force towards chronic infection, significantly affecting the time to reach steady state after initial infection and playing a critical role in the determination of both the equilibrium proviral load and the proportion of the proviral load that actively expresses Tax. The latter is hypothesized to be an important risk factor to the development of HAM/TSP, implying that it is the relative proportion of Tax^+ proviral cells rather than the absolute magnitude of the proviral load that is the ultimate cause of HAM/TSP pathogenesis.

▷ **Treatment strategies should target Tax expression.**

The identification of the rate of spontaneous Tax expression as a determinant of the outcome of HTLV-I infection suggests that alternative treatment regimes that aim to reduce Tax expression, rather than current therapies that focus on lowering infectious transmissibility, may be more effective in decreasing the burden of chronic HTLV-I infection both by controlling the proviral load as well as reducing the risk of disease progression, and may even hold the key to complete viral elimination.

6.2 Further Questions

Study of our mathematical model has provided invaluable insights to HTLV-I infection *in vivo*. Still, there arise several questions of interest that require further investigation.

6.2.1 Explicit Incorporation of the HTLV-I-specific CTL Response

In our mathematical model, we have examined the role of HTLV-I-specific immune responses implicitly by considering surviving fractions of infected target cells from infectious transmission (σ), and from mitotic transmission (ϵ). It is widely accepted that anti-HTLV-I cytotoxic T-lymphocytes (CTLs) have a large impact on both proviral load and disease status [3, 12, 39, 51]. The next step to our modelling effort would be to incorporate the CTL response by explicitly including a compartment of HTLV-I-specific $CD8^+$ CTLs. Due to the higher dimension of the resulting system, we would expect to see complicated dynamical behaviour, which may yield unexpected mathematical and biological phenomena which do not appear in our model.

Compartmentalization of the CTL response in mathematical models of HTLV-I has previously been considered in [23, 54]. Wodarz, Nowak, and Bangham [54] include the effects of mitotic division of target cells and conduct extensive numerical investigation, while the approach of Gómez-Acevedo, Li, and Jacobson in [23] demonstrates important analytical methods used in the mathematical modelling of HTLV-I infection and focusses more on the specific role played by CTLs.

6.2.2 Mitotis of All Target Cells

The mathematical model we have developed concentrates on the rapid selective mitosis of actively infected target cells driven by expression of the viral protein Tax. The mitotic division of healthy and latently infected target cells occurs at a substantially slower rate and has been ignored in our study. However, proliferation of healthy cells increases the number of potential target cells of HTLV-I and may help to propagate infection. Alternatively, an increase in $CD4^+$ helper T-cells plays a protective role by increasing the efficiency of immune responses to the virus. At the same time, proliferation of latently infected cells increases the pool of target cells that make up the vast majority of the proviral load. Consideration of mitotis in healthy and latently infected cell compartments may be an important aspect of HTLV-I infection and persistence.

6.2.3 HTLV-I Infection in Tissue

We have considered the dynamics of HTLV-I in the peripheral blood, where the interaction between the pools of infected and uninfected target cells is assumed to be homogeneous. However, $CD4^+$ helper T-cells circulate in and out of all bodily tissues and it is known, for example, that lymphoid organs are major reservoirs for HTLV-I [37, 38]. It is therefore reasonable to examine HTLV-I infection when it is localized in tissue. An interesting observation arises in this scenario that would need to be addressed in the mathematical model. As mentioned in Chapter 5, $CD4^+$ helper T-cells exhibit immune functionality such as the release of cytokines and growth factors that regulate and direct immune cells, including other $CD4^+$ helper T-cells. The recruitment of $CD4^+$ helper T-cells to the site of infection results in aggregation or clumping of potential target cells of the virus. It is natural to surmise that a higher concentration of target cells gathered in the infected tissue would result in a higher rate of contact between healthy and actively infected cells. Hence, the infectious transmissibility coefficient β should be expected to change over time. It is uncertain if the proviral load would be positively or negatively impacted. On the one hand, aggregation of $CD4^+$ helper T-cells would increase the rate of infectious transmission, raising the proviral load. On the other hand, T-cell

signalling of other immune cells, such as $CD8^+$ cytotoxic T-lymphocytes (CTLs) to the site of infection would be expected to induce lysis of infected target cells, thereby lowering the proviral load. The balance between these two opposing forces appears to play an important role in determining the outcome of HTLV-I infection in tissue.

6.2.4 Natural Selection for Specific T-cell Clones During Different Stages of Infection

The previous question brings to light the idea that in general parameter values are not constant; rather, they change as the infection progresses. The notion of natural selection comes into play, whereby the infected T-cell clone best suited to persist in the host during different stages of the infection is the one that undergoes rapid clonal expansion. For example, it has been suggested that HTLV-I infection *in vivo* follows a two-stage process [37, 38]. In the early stage, infected T-cells clones that display high infectious transmissibility along with continuous expression of viral proteins are selected for clonal expansion. There is no formation of a latent reservoir of infected target cells during this stage. It is only after the establishment of HTLV-I-specific immune responses that viral protein expression is silenced, and selection for infected T-cell clones that undergo mitosis at a rapid rate occurs. Thus, infectious transmission is a transient phase that ceases to contribute to the infection in the later stage. Mortreux et al. [37, 38] indicate that such a two-stage process for HTLV-I carries important consequences for treatment: reverse transcriptase inhibitors are suitable during the early stage of infection, but become ineffective during the later stage, whereby inhibiting T-cell proliferation is necessary.

Appendix A

Derivations

In this appendix, we present the derivations of several quantities and assumptions that appear in Chapter 3.

A.1 Derivation of the Basic Reproduction Number R_0

Here we derive the *basic reproduction number for viral infection* using three different methods.

A.1.1 Method I. Using the Next Generation Operator

View the Jacobian matrix at the infection-free equilibrium $J(P_0)$ as a block matrix

$$J(P_0) = \left[\begin{array}{c|cc} -\mu_1 & 0 & -\beta x_0 \\ \hline 0 & -\tau - \mu_2 & \sigma\beta x_0 + \epsilon r\left(1 - \frac{x_0}{k}\right) \\ 0 & \tau & -\mu_3 \end{array}\right].$$

The upper-left block has a negative eigenvalue, which is given by its single entry. Write the lower-right block in the following way:

$$\begin{aligned} J_{2\times 2}(P_0) &= \begin{bmatrix} -\tau - \mu_2 & \sigma\beta x_0 + \epsilon r\left(1 - \frac{x_0}{k}\right) \\ \tau & -\mu_3 \end{bmatrix} \\ &= \begin{bmatrix} 0 & \sigma\beta x_0 + \epsilon r\left(1 - \frac{x_0}{k}\right) \\ 0 & 0 \end{bmatrix} - \begin{bmatrix} \tau + \mu_2 & 0 \\ -\tau & \mu_3 \end{bmatrix}. \end{aligned}$$

Let

$$F = \begin{bmatrix} 0 & \sigma\beta x_0 + \epsilon r\left(1 - \frac{x_0}{k}\right) \\ 0 & 0 \end{bmatrix} \quad \text{and} \quad V = \begin{bmatrix} \tau + \mu_2 & 0 \\ -\tau & \mu_3 \end{bmatrix},$$

so that

$$V^{-1} = \frac{1}{\mu_3(\tau+\mu_2)}\begin{bmatrix}\mu_3 & 0\\ \tau & \tau+\mu_2\end{bmatrix} = \begin{bmatrix}\frac{1}{\tau+\mu_2} & 0\\ \frac{\tau}{\mu_3(\tau+\mu_2)} & \frac{1}{\mu_3}\end{bmatrix}.$$

Then,

$$FV^{-1} = \begin{bmatrix}\frac{\tau}{\mu_3(\tau+\mu_2)}\big(\sigma\beta x_0 + \epsilon r\left(1-\frac{x_0}{k}\right)\big) & \frac{1}{\mu_3}\big(\sigma\beta x_0 + \epsilon r\left(1-\frac{x_0}{k}\right)\big)\\ 0 & 0\end{bmatrix}.$$

The spectral radius is precisely R_0:

$$R_0 = \rho\big(FV^{-1}\big) = \frac{\tau}{\mu_3(\tau+\mu_2)}\Big(\sigma\beta x_0 + \epsilon r\left(1-\frac{x_0}{k}\right)\Big).$$

A.1.2 Method II. Using the Stability Condition for P_0

Here we use the condition that the infection-free equilibrium P_0 is unstable if and only if $R_0 > 1$. Again, look at the lower-right 2×2 block of $J(P_0)$,

$$J_{2\times 2}(P_0) = \begin{bmatrix}-\tau-\mu_2 & \sigma\beta x_0 + \epsilon r\left(1-\frac{x_0}{k}\right)\\ \tau & -\mu_3\end{bmatrix}.$$

Using the well-known Routh-Hurwitz criterion for 2×2 matrices, since $\operatorname{tr}\big(J_{2\times 2}(P_0)\big) < 0$, it follows that $J_{2\times 2}(P_0)$ is stable if and only if $\det\big(J_{2\times 2}(P_0)\big) > 0$. Hence, for instability, we require

$$\begin{aligned}
&\det\big(J_{2\times 2}(P_0)\big) = \mu_3(\tau+\mu_2) - \tau\Big(\sigma\beta x_0 + \epsilon r\left(1-\frac{x_0}{k}\right)\Big) < 0\\
\iff\ &\frac{\tau}{\mu_3(\tau+\mu_2)}\Big(\sigma\beta x_0 + \epsilon r\left(1-\frac{x_0}{k}\right)\Big) > 0\\
\iff\ &R_0 > 1.
\end{aligned}$$

Setting $R_0 = \frac{\tau}{\mu_3(\tau+\mu_2)}\Big(\sigma\beta x_0 + \epsilon r\left(1-\frac{x_0}{k}\right)\Big)$ yields the expression for the basic reproduction number.

A.1.3 Method III. Using the Biological Interpretation

Biologically, the basic reproduction number may be expressed in the following way:

$$R_0 = I_T \cdot C_e = I_T \cdot C \cdot e,$$

where I_T is the mean infectious period and C_e, the infection rate or effective contact rate, is the product of two quantities, the contact rate C, and the effective rate e.

In model (2.3), the rate at which a cell leaves the actively infected cell compartment is μ_3. One may think of the mean infectious period (i.e. the average duration in the y compartment) as the reciprocal of this rate, so $I_T = \frac{1}{\mu_3}$. It is observed that a fraction $\frac{\tau}{\tau+\mu_2}$ goes from the u-compartment to the y-compartment, representing the proportion of latently infected cells that begin to express the viral Tax protein and become actively infected. Thus, $e = \frac{\tau}{\tau+\mu_2}$. Lastly, the contact rate (which is a somewhat misleading name as it involves a rate due to mitosis) is given by the sum of the contribution of proviral cells from both infectious and mitotic transmission routes; that is, $C = \sigma\beta x_0 + \epsilon r\left(1 - \frac{x_0}{k}\right)$.

Therefore, we have derived

$$R_0 = I_T \cdot C \cdot e = \frac{\tau}{\mu_3(\tau+\mu_2)}\Big(\sigma\beta x_0 + \epsilon r\left(1 - \frac{x_0}{k}\right)\Big).$$

R_0 may be thought of as representing the average number of secondary infected cells resulting from a single actively infected cell introduced into a completely susceptible population of healthy cells over its lifetime (the mean infectious period).

A.2 Derivation of Assumption (A3(i)) and Discussion of Assumption (A3(ii))

Assumption (A3(i)) implies that for a fixed value of $0 < \sigma_0 < 1$, the height of the vertex of the parabola $f_2(x)$ at the point $\tilde{x}$ lies above the corresponding height of the straight line $f_1(x)$ at the same point. Furthermore, Assumption (A3(ii)) implies that when $\sigma = 0$ and with all other parameters fixed, the graph of $f_2(x)$ lies underneath the graph of $f_1(x)$. Thus, when $R_0 = R_0(\sigma) < 1$ (equivalently, $\sigma < \bar{\sigma}$), as the value of σ increases, there will first be no endemic equilibria when $\sigma = 0$, and two endemic equilibria when $\sigma_0 < \sigma < \bar{\sigma}$. These provide sufficient conditions for the existence of a backward bifurcation resulting in a region of bi-stability in the feasible region Γ.

Remark A.2.1 (Derivation of Assumption (A3(i)))**.**

$$\begin{aligned}
&f_2(\tilde{x}) > f_1(\tilde{x})\\
&\iff \frac{k\beta\tau}{\epsilon r\mu_3}\tilde{x}\Big[\Big(\sigma\beta - \frac{\epsilon r}{k}\Big)\tilde{x} + \epsilon r - \frac{\mu_3}{\tau}(\tau+\mu_2)\Big] > \lambda - \mu_1\tilde{x},\\
&\iff \frac{k\beta\tau}{\epsilon r\mu_3}\tilde{x}\Big[\Big(\sigma\beta - \frac{\epsilon r}{k}\Big)\tilde{x} + \epsilon r - \frac{\mu_3}{\tau}(\tau+\mu_2)\Big] + \mu_1\tilde{x} > \lambda, \quad \text{divide by } \mu_1,\\
&\iff \left[\frac{\beta\tau}{\mu_1\mu_3}\cdot\frac{\epsilon r - \frac{\mu_3}{\tau}(\tau+\mu_2)}{2\frac{\epsilon r}{k}} + 1\right]\tilde{x}(\sigma) > \frac{\lambda}{\mu_1} = x_0.
\end{aligned}$$

In particular,

$$\left[\frac{\beta\tau}{\mu_1\mu_3}\tilde{x}_{\sigma=0}+1\right]\tilde{x}(\sigma)>x_0.$$

Isolating σ yields the equivalent inequality

$$\sigma>\sigma_0.$$

In the above derivation, we have used the expression

$$\tilde{x}(\sigma)=\frac{\epsilon r-\frac{\mu_3}{\tau}(\tau+\mu_2)}{2\left(\frac{\epsilon r}{k}-\sigma\beta\right)},\quad \text{which implies}\quad \left(\frac{\epsilon r}{k}-\sigma\beta\right)\tilde{x}=\frac{1}{2}\left(\epsilon r-\frac{\mu_3}{\tau}(\tau+\mu_2)\right).$$

Remark A.2.2 (Discussion of Assumption (A3(ii)))**.** Setting $\sigma=0$ in the expression for $\tilde{x}(\sigma)$, it is immediately seen that $\tilde{x}(\sigma)>\tilde{x}_{\sigma=0}$. This yields the inequality

$$\left[\frac{\beta\tau}{\mu_1\mu_3}\tilde{x}_{\sigma=0}+1\right]\tilde{x}(\sigma)>\left[\frac{\beta\tau}{\mu_1\mu_3}\tilde{x}_{\sigma=0}+1\right]\tilde{x}_{\sigma=0}.$$

Thus, for no endemic equilibria to exist when $\sigma=0$, we may assume that

$$\left[\frac{\beta\tau}{\mu_1\mu_3}\tilde{x}_{\sigma=0}+1\right]\tilde{x}_{\sigma=0}<x_0.$$

Observe that under this assumption,

$$\begin{aligned}\sigma_0&=\frac{\epsilon r}{k\beta}-\frac{\epsilon r-\frac{\mu_3}{\tau}(\tau+\mu_2)}{2\beta x_0}\left[\frac{k\beta\tau(\epsilon r-\frac{\mu_3}{\tau}(\tau+\mu_2))}{2\epsilon r\mu_1\mu_3}+1\right]\\&=\frac{\epsilon r}{k\beta}-\frac{\epsilon r}{k\beta x_0}\tilde{x}_{\sigma=0}\left[\frac{\beta\tau}{\mu_1\mu_3}\tilde{x}_{\sigma=0}+1\right]\\&>0.\end{aligned}$$

A.3 Derivation of Relation (4.7) in the Proof of Theorem 4.4.3

Consider a 3×3 matrix $B=[b_{ij}]$. Let $z=(v,w)\in\mathbb{R}\times\mathbb{R}^2$, where $v=v_1\in\mathbb{R}$, $w=(v_2,v_3)\in\mathbb{R}^2$. Define a vector norm $|\cdot|_{B_{vec}}$ on $\mathbb{R}^3\cong\mathbb{R}^{\binom{3}{2}}$ as

$$|x|_{B_{vec}}:=\max\{|v|_1,|w|_1\},$$

where $|\cdot|_1$ stands for the standard ℓ_1-norm of a vector. Next, write $B : \mathbb{R} \times \mathbb{R}^2 \to \mathbb{R} \times \mathbb{R}^2$ as a 2×2 block matrix

$$B = \left[\begin{array}{c|c} B_{11} & B_{12} \\ \hline B_{21} & B_{22} \end{array}\right] = \left[\begin{array}{c|cc} b_{11} & b_{12} & b_{13} \\ \hline b_{21} & b_{22} & b_{23} \\ b_{31} & b_{32} & b_{33} \end{array}\right], \quad \text{with} \quad \begin{array}{cc} B_{11} : \mathbb{R} \to \mathbb{R} & B_{12} : \mathbb{R}^2 \to \mathbb{R}, \\ B_{21} : \mathbb{R} \to \mathbb{R}^2 & B_{22} : \mathbb{R}^2 \to \mathbb{R}^2. \end{array}$$

It is known that the induced ℓ_1-matrix norms for the diagonal block matrices are

$$|B_{11}|_1 = |b_{11}| \quad \text{and} \quad |B_{22}|_1 = \max\{|b_{22}| + |b_{32}|, |b_{23}| + |b_{33}|\} \quad \text{(i.e. column sum)}.$$

For the off-diagonal block matrices, we define

$$|B_{12}|_{21} = \sup_{w\neq 0, w\in\mathbb{R}^2} \frac{|B_{12}w|_1}{|w|_1} \quad \text{and} \quad |B_{21}|_{12} = \sup_{v\neq 0, v\in\mathbb{R}} \frac{|B_{21}v|_1}{|v|_1}.$$

Then,

$$|B_{12}|_{21} = \sup_{v_2, v_3\neq 0} \frac{|b_{12}v_2 + b_{13}v_3|}{|v_2| + |v_3|} \leq \sup_{v_2, v_3\neq 0} \max\{|b_{12}|, |b_{13}|\},$$

so that

$$|B_{12}|_{21} \leq \max\{|b_{12}|, |b_{13}|\}.$$

Conversely, pick $w_0 = (1, 0)^T$ if $|b_{12}| \geq |b_{13}|$ or $w_0 = (0, 1)^T$ if $|b_{13}| \geq |b_{12}|$. Then the maximum is attained, i.e.

$$|B_{12}|_{21} \geq \frac{|B_{12}w_0|_1}{|w_0|_1} = \max\{|b_{12}|, |b_{13}|\}.$$

Similarly,

$$|B_{21}|_{12} = \sup_{v_1\neq 0} \frac{|b_{21}v_1 + b_{31}v_1|}{|v_1|} \leq \sup_{v_1\neq 0} \max\{|b_{21}|, |b_{31}|\},$$

implying

$$|B_{21}|_{12} \leq |b_{21}| + |b_{31}|.$$

Conversely, pick $v_0 = 1$. Then the maximum value is attained, i.e.

$$|B_{21}|_{12} \geq |B_{21}|_1 = |b_{21}| + |b_{31}|.$$

Thus,

$$|B_{12}|_{21} = \max\{|b_{12}|, |b_{13}|\} \quad \text{and} \quad |B_{21}|_{12} = |b_{21}| + |b_{31}|.$$

In the following, let I denote the 2×2 identity matrix, $I_{2\times2}$. Compute

$$(I + hB)z = \begin{bmatrix} 1 + hB_{11} & hB_{12} \\ hB_{21} & 1 + hB_{22} \end{bmatrix} \begin{bmatrix} v \\ w \end{bmatrix} = \begin{bmatrix} (1 + hB_{11})v + hB_{12}w \\ hB_{21}v + (I + hB_{22})w \end{bmatrix},$$

and consider

$$\begin{aligned} &|(I + hB)z|_{B_{vec}} \\ &= \max\{|(1 + hB_{11})v + hB_{12}w|_1, |hB_{21}v + (I + hB_{22})w|_1\} \\ &\le \max\{|1 + hB_{11}|_1|v|_1 + h|B_{12}|_{21}|w|_1, h|B_{21}|_{12}|v|_1 + |I + hB_{22}|_1|w|_1\} \\ &\le \max\{|1 + hB_{11}|_1 + h|B_{12}|_{21}, h|B_{21}|_{12} + |I + hB_{22}|_1\} \cdot \underbrace{\max\{|v|_1, |w|_1\}}_{=|z|_{B_{vec}}}. \end{aligned}$$

So,

$$\|I + hB\| \le \max\{|1 + hB_{11}|_1 + h|B_{12}|_{21}, |I + hB_{22}|_1 + h|B_{21}|_{12}\},$$

and

$$\frac{\|I + hB\| - 1}{h} \le \max\left\{\frac{|1 + hB_{11}|_1 - 1}{h} + |B_{12}|_{21}, \frac{|I + hB_{22}|_1 - 1}{h} + |B_{21}|_{12}\right\}.$$

Letting $h \to 0^+$, we obtain

$$\mu(B) \le \max\{\mu_1(B_{11}) + |B_{12}|_{21}, \mu_1(B_{22}) + |B_{21}|_{12}\} = \max\{g_1, g_2\},$$

where $\mu_1(B_{11}) = \operatorname{Re} b_{11}$ and $\mu_1(B_{22}) = \max\{\operatorname{Re} b_{22} + |b_{32}|, \operatorname{Re} b_{33} + |b_{23}|\}$ are the Lozinskiĭ measures of the diagonal block matrices of B induced by the ℓ_1-norm.

Appendix B

Second Additive Compound and Lozinskiĭ Measure

In this appendix, we define the second additive compound matrix and the Lozinskiĭ measure, or logarithmic norm.

B.1 Second Additive Compound Matrix

Let A denote a linear operator on $\mathbb{R}^n$ as well as its matrix representation with respect to the standard canonical basis of $\mathbb{R}^n$. Denote by $\bigwedge^2 \mathbb{R}^n$ the exterior product of $\mathbb{R}^n$ consisting of exterior products $v_1 \wedge v_2$ of two vectors v_1, v_2 in $\mathbb{R}^n$. The linear operator A, along with its standard basis of $\mathbb{R}^n$, induces a linear operator $A^{[2]}$ with corresponding canonical basis of $\bigwedge^2 \mathbb{R}^n$. Its matrix representation with respect to the canonical basis in $\bigwedge^2 \mathbb{R}^n$ is called the *second additive compound matrix of* A (see [18, 40]). It satisfies the property $(A+B)^{[2]} = A^{[2]} + B^{[2]}$ for any two $n \times n$ matrices A and B. The second additive compound matrix of $A = [a_{ij}]$ when $n = 3$ is given below by

$$A^{[2]} = \begin{bmatrix} a_{11} + a_{22} & a_{23} & -a_{13} \\ a_{32} & a_{11} + a_{33} & a_{12} \\ -a_{31} & a_{21} & a_{22} + a_{33} \end{bmatrix}. \tag{B.1}$$

B.2 The Lozinskiĭ Measure or Logarithmic Norm

Definition B.2.1. Denote by $|\cdot|$ any vector norm in $\mathbb{R}^n$ and the matrix norm it induces, and let $A \in \boldsymbol{M_n}(\mathbb{R})$. The *Lozinskiĭ measure*, also called the *logarithmic*

norm, of the $n \times n$ matrix A with respect to $|\cdot|$ is defined by

$$\mu(A) := \lim_{h \to 0^+} \frac{|I + hA| - 1}{h} = \frac{d}{dt}^{+} |I + hA|_{h=0}. \tag{B.2}$$

As an example, the Lozinskiĭ measures of $A = (a_{ij})$ with respect to the three common norms $|x|_\infty = \sup_i |x_i|$, $|x|_1 = \sum_i |x_i|$, and $|x|_2 = (\sum_i |x_i|^2)^{\frac{1}{2}}$ are, respectively,

$$\begin{aligned} \mu_\infty(A) &= \sup_i \Big(\mathrm{Re} a_{ii} + \sum_{j \neq i} |a_{ij}| \Big), \\ \mu_1(A) &= \sup_j \Big(\mathrm{Re} a_{jj} + \sum_{i \neq j} |a_{ij}| \Big), \quad \text{and} \\ \mu_2(A) &= \rho \left(\frac{A + A^*}{2} \right), \end{aligned} \tag{B.3}$$

where ρ is the spectral radius and A^* denotes the Hermitian adjoint (or conjugate transpose) of A. For further details about the Lozinskiĭ measure, we refer the reader to [17, 40].

Remark B.2.1. It can be shown that any Lozinskiĭ measure $\mu(A)$ dominates the stability modulus of A, which is the eigenvalue of A with the largest real part. As a result, an alternative characterization of the second compound matrix $A^{[2]}$ being stable, as stated in the first condition of Theorem 3.4.1, is that there is some Lozinskiĭ measure μ on $\boldsymbol{M_N}(\mathbb{R})$, where $N = \binom{n}{2}$, for which $\mu\big(A^{[2]}\big) < 0$. This condition can be interpreted as $a_{ii} < 0$ for $i = 1, \ldots, n$, and $A^{[2]}$ is diagonally dominant in rows.

Bibliography

[1] Julien Arino, C. Connell McCluskey, and Pauline van den Driessche. Global Results for an Epidemic Model with Vaccination that Exhibits Backward Bifurcation. *SIAM Journal on Applied Mathematics*, 64(1):260–276, 2003.

[2] Becca Asquith and Charles R.M. Bangham. The Role of Cytotoxic T Lymphocytes in Human T-cell Lymphotropic Virus Type 1 Infection. *Journal of Theoretical Biology*, 207(1):65–79, 2000.

[3] Becca Asquith and Charles R.M. Bangham. Quantifying HTLV-I dynamics. *Immunology and Cell Biology*, 85:280–286, 2007.

[4] Becca Asquith and Charles R.M. Bangham. How does HTLV-I persist despite a strong cell-mediated immune response? *Trends in Immunology*, 29(1):4–11, 2008.

[5] Becca Asquith, Angelina J. Mosley, Anna Barfield, Sara E.F. Marshall, Adrian Heaps, Peter Goon, Emmanuel Hanon, Yuetsu Tanaka, Graham Taylor, and Charles R.M. Bangham. A functional $CD8^+$ cell assay reveals individual variation in $CD8^+$ cell antiviral efficacy and explains differences in human T-lymphotropic virus type 1 proviral load. *Journal of General Virology*, 86:1515–1523, 2005.

[6] Becca Asquith, Angelina J. Mosley, Adrian Heaps, Yuetsu Tanaka, Graham Taylor, Angela R. McLean, and Charles R.M. Bangham. Quantification of the virus-host interaction in human T lymphotropic virus type I infection. *Retrovirology*, 2(1):75–83, 2005.

[7] Becca Asquith, Yan Zhang, Angelina J. Mosley, Catherine M. de Lara, Diana L. Wallace, Andrew Worth, Lambrini Kaftantzi, Kiran Meekings, George E. Griffin, Yuetsu Tanaka, David F. Tough, Peter C. Beverly, Graham P. Taylor, Derek Macallan, and Charles R. M. Bangham. *In vivo* T lymphocyte dynamics in humans and the impact of human T-lymphotropic virus 1 infection. *PNAS*, 104(19):8035–8040, 2007.

[8] Emanuela Balestrieri, Giancarlo Forte, Claudia Matteucci, Antonio Mastino, and Beatrice Macchi. Effect of Lamivudine on Transmission of Human T-Cell Lymphotropic Virus Type 1 to Adult Peripheral Blood Mononuclear Cells In Vitro. *Antimicrobial Agents and Chemotherapy*, 46(9):3080–3083, 2002.

[9] Charles R. M. Bangham, Allan G. Kermode, Sarah E. Hall, and Susan Daenke. The cytotoxic T-lymphocyte response to HTLV-I: the main determinant of disease? *Seminars in Virology*, 7(1):41–48, 1996.

[10] Charles R.M. Bangham. HTLV-1 infections. *Journal of Clinical Pathology*, 53(8):581–586, 2000.

[11] Charles R.M. Bangham, Sarah E. Hall, Katie J.M. Jeffery, Alison M. Vine, Aviva Witkover, Martin A. Nowak, Dominik Wodarz, Koichiro Usuku, and Mitsuhiro Osame. Genetic control and dynamics of the cellular immune response to the human T-cell leukaemia virus, HTLV-I. *Philosophical Transactions: Biological Sciences*, 354(1384):691–700, 1999.

[12] Charles R.M. Bangham, Kiran Meekings, Frederic Toulza, Mohamed Nejmeddine, Endre Majorovits, Becca Asquith, and Graham Taylor. The immune control of HTLV-I infection: selection forces and dynamics. *Frontiers in Bioscience*, 14:2889–2903, 2009.

[13] Charles R.M. Bangham and Mitsuhiro Osame. Cellular immune response to HTLV-1. *Oncogene*, 24:6035–6046, 2005.

[14] Fred Brauer. Backward bifurcations in simple vaccination models. *Journal of Mathematical Analysis and Applications*, 298(2):418–431, 2004.

[15] Fred Brauer, Pauline van den Driessche, Jianhong Wu, Linda J. S. Allen, and Chris T. Bauch. *Mathematical Epidemiology*. Lecture Notes in Mathematics / Mathematical Biosciences Subseries. Springer-Verlag New York, LLC, 2008. Issue 1945.

[16] Geoffrey Butler and Paul Waltman. Persistence in dynamical systems. *Journal of Differential Equations*, 63(2):255–263, 1986.

[17] W.A. Coppel. *Stability and Asymptotic Behaviour of Differential Equations*. D.C. Heath, Boston, 1965.

[18] Miroslav Fiedler. Additive compound matrices and an inequality for eigenvalues of symmetric stochastic matrices. *Czechoslovak Mathematical Journal*, 24(3):392–402, 1974.

[19] H. I. Freedman, Shigui Ruan, and Moxun Tang. Uniform Persistence and Flows Near a Closed Positively Invariant Set. *Journal of Dynamics and Differential Equations*, 6(4):583–600, 1994.

[20] H. I. Freedman and Paul Waltman. Persistence in models of three interacting predator-prey populations. *Mathematical Biosciences*, 68(2):213–231, 1984.

[21] Robert C. Gallo. The discovery of the first human retrovirus: HTLV-1 and HTLV-2. *Retrovirology*, 2(1):17–23, 2005.

[22] Horacio Gómez-Acevedo and Michael Y. Li. Backward bifurcation in a model for HTLV-I infection of $CD4^+$ T cells. *Bulletin of Mathematical Biology*, 67(1):101–114, 2005.

[23] Horacio Gómez-Acevedo, Michael Y. Li, and Steven Jacobson. Multistability in a Model for CTL Response to HTLV-I Infection and Its Implications to HAM/TSP Development and Prevention. *Bulletin of Mathematical Biology*, 72(3):681–696, 2010.

[24] Morris W. Hirsch. Systems of Differential Equations Which Are Competitive or Cooperative. I: Limit Sets. *SIAM Journal on Mathematical Analysis*, 13(2):167–179, 1982.

[25] Katie J.M. Jeffery, Asna A. Siddiqui, Mike Bunce, Alun L. Lloyd, Alison M. Vine, Aviva D. Witkover, Shuji Izumo, Koichiro Usuku, Kenneth I. Welsh, Mitsuhiro Osame, and Charles R.M. Bangham. The Influence of HLA Class I Alleles and Heterozygosity on the Outcome of Human T Cell Lymphotropic Virus Type I Infection. *Journal of Immunology*, 165(12):7278–7284, 2000.

[26] Katie J.M. Jeffery, Koichiro Usuku, Sarah E. Hall, Wataru Matsumoto, Graham P. Taylor, Jeanette Procter, Mike Bunce, Graham S. Ogg, Kenneth I. Welsh, Jonathan N. Weber, Alun L. Lloyd, Martin A. Nowak, Masahiro Nagai, Daisuke Kodama, Shuji Izumo, Mitsuhiro Osame, and Charles R.M. Bangham. HLA alleles determine human T-lymphotropic virus-I (HTLV-I) proviral load and the risk of HTLV-I-associated myelopathy. *Proceedings of the National Academy of Sciences of the United States of America*, 96(7):3848–3853, 1999.

[27] Denise Kirschner and Glenn F. Webb. A Model for Treatment Strategy in the Chemotherapy of AIDS. *Bulletin of Mathematical Biology*, 58(2):367–390, 1996.

[28] Michael Y. Li, John R. Graef, Liancheng Wang, and János Karsai. Global dynamics of a SEIR model with varying total population size. *Mathematical Biosciences*, 160(2):191–213, 1999.

[29] Michael Y. Li and James S. Muldowney. Global stability for the SEIR model in epidemiology. *Mathematical Biosciences*, 125(2):155–164, 1995.

[30] Michael Y. Li and James S. Muldowney. A Geometric Approach to Global-Stability Problems. *SIAM Journal on Mathematical Analysis*, 27(4):1070–1083, 1996.

[31] Michael Y. Li, Hal L. Smith, and Liancheng Wang. Global Dynamics of an SEIR Epidemic Model with Vertical Transmission. *SIAM Journal on Applied Mathematics*, 62(1):58–69, 2001.

[32] Michael Y. Li and Liancheng Wang. A Criterion for Stability of Matrices. *Journal of Mathematical Analysis and Applications*, 225(1):249–264, 1998.

[33] Yi Li and James S. Muldowney. On Bendixson's Criterion. *Journal of Differential Equations*, 106(1):27–39, 1993.

[34] Beatrice Macchi, Emanuela Balestrieri, and Antonio Mastino. Effects of nucleoside-based antiretroviral chemotherapy on human T cell

leukaemia/lymphotropic virus type 1 (HTLV-1) infection in vitro. *Journal of Antimicrobial Chemotherapy*, 51:1327–1330, 2003.

[35] Beatrice Macchi, Isabella Faraoni, Jing Zhang, Sandro Grelli, Cartesio Favalli, Antonio Mastino, and Enzo Bonmassar. AZT inhibits the transmission of human T cell leukaemia/lymphoma virus type I to adult peripheral blood mononuclear cells in vitro. *Journal of General Virology*, 78:1007–1016, 1997.

[36] C. Connell McCluskey and Pauline van den Driessche. Global Analysis of Two Tuberculosis Models. *Journal of Dynamics and Differential Equations*, 16(1):139–166, 2004.

[37] Franck Mortreux, Anne-Sophie Gabet, and Eric Wattel. Molecular and cellular aspects of HTLV-I associated leukemogenesis *in vivo*. *Leukemia*, 17(1):26–38, 2003.

[38] Franck Mortreux, Mirdad Kazanji, Anne-Sophie Gabet, Benoit de Thoisy, and Eric Wattel. Two-Step Nature of Human T-Cell Leukemia Virus Type 1 Replication in Experimentally Infected Squirrel Monkeys (Saimiri sciureus). *Journal of Virology*, 75(2):1083–1089, 2001.

[39] Angelina J. Mosley and Charles R.M. Bangham. A new hypothesis for the pathogenesis of Human T-lymphotropic virus type 1 associated myelopathy/tropical spastic paraparesis. *Bioscience Hypotheses*, 2(3):118–124, 2009.

[40] James S. Muldowney. Compound matrices and ordinary differential equation. *Rocky Mountain Journal of Mathematics*, 20(4):857–872, 1990.

[41] Patrick W. Nelson, James D. Murray, and Alan S. Perelson. A model of HIV-1 pathogenesis that includes an intracellular delay. *Mathematical Biosciences*, 163(2):201–215, 2000.

[42] Martin A. Nowak. *Evolutionary Dynamics: Exploring the Equations of Life*. Harvard University Press, 2006.

[43] Alan S. Perelson. Modeling the interaction of the immune system with HIV. pages 350–370, 1989.

[44] Alan S. Perelson. Modelling viral and immune system dynamics. *Nature Reviews Immunology*, 2:28–36, 2002.

[45] Fernando A. Proietti, Anna Bárbara F. Carneiro-Proietti, Bernadette C. Catalan-Soares, and Edward L. Murphy. Global epidemiology of HTLV-I infection and associated diseases. *Oncogene*, 24:6058–6068, 2005.

[46] Hiroshi Shiraki, Yasuko Sagara, and Yukiko Inoue. *Cell-to-cell transmission of HTLV-I*, pages 303–316. Japan Scientific Societies Press, 2003. in Two Decades of Adult T-cell Leukemia and HTLV-I Research.

[47] Hal L. Smith. Invariant Curves for Mappings. *SIAM Journal on Mathematical Analysis*, 17(5):1053–1067, 1986.

[48] Hal L. Smith. Systems of Ordinary Differential Equations Which Generate an Order Preserving Flow. A Survey of Results. *SIAM Review*, 30(1):87–113, 1988.

[49] Hal L. Smith. *Monotone Dynamical Systems: An Introduction to the Theory of Competitive and Cooperative Systems*, volume 41 of *Mathematical Surveys and Monographs*. American Mathematical Society, 1995.

[50] Graham P. Taylor, Sarah E. Hall, S. Navarrete, Colin A. Michie, R. Davis, Aviva D. Witkover, Martin Rossor, Martin A. Nowak, Peter Rudge, Estella Matutes, Charles R. M. Bangham, and Jonathan N. Weber. Effect of Lamivudine on Human T-Cell Leukemia Virus Type 1 (HTLV-1) DNA Copy Number, T-Cell Phenotype, and Anti-Tax Cytotoxic T-Cell Frequency in Patients with HTLV-1-Associated Myelopathy. *Journal of Virology*, 73(12):10289–10295, 1999.

[51] Utano Tomaru, Yoshihisa Yamano, and Steven Jacobson. *HTLV-I infection and the nervous system*, chapter 23, pages 285–299. Oxford University Press, second edition, 2005. in Clinical Neuroimmunology 2nd Edition.

[52] Liancheng Wang and Michael Y. Li. Mathematical analysis of the global dynamics of a model for HIV infection of $CD4^+$ T cells. *Mathematical Biosciences*, 200(1):44–57, 2006.

[53] Eric Wattel, Marielle Cavrois, Antoine Gessain, and Simon Wain-Hobson. Clonal Expansion of Infected Cells: A Way of Life for HTLV-I. *Journal of Acquired Immune Deficiency Syndromes and Human Retrovirology*, 13:S92–S99, 1996.

[54] Dominik Wodarz, Martin A. Nowak, and Charles R. M. Bangham. The dynamics of HTLV-I and the CTL response. *Immunology Today*, 20(5):220–227, 1999.